# 4th session

Objekttyp: **Group**

Zeitschrift: **IABSE reports of the working commissions = Rapports des commissions de travail AIPC = IVBH Berichte der Arbeitskommissionen**

Band (Jahr): **23 (1975)**

PDF erstellt am: **10.08.2024**

COLUMN BUCKLING CURVE OF WELDED STEEL TUBE

Ben Kato
Professor of Structural Engineering
Faculty of Engineering
University of Tokyo
Japon

ABSTRACT

This paper presents the results of experimental research regarding the buckling strength of centrally loaded welded steel tubular columns.

The specific contents of this paper are:

(1) Effect of thermal residual stress and locked-in stress induced by cold forming on the tangent modulus in elasto-plastic range.

(2) Effect of supporting fixtures.

(3) Formulation of column buckling curve and comparison with test results.

## 1. INTRODUCTION

The column curve for steel tubular struts adopted by Commission 8 of the European Convention of Constructional Steelwork seems to be derived from the knowledge of the performance of seamless tube which is almost free from residual stress, and it was ranked with the superior class(a) of the eventually settled three curves. For the use of structural members, however, welded steel tubes produced by cold forming and high frequency induction welding are much more popular than seamless tubes because of their excellent productivity and of versatility of sizes. Mechanical properties of welded steel tube as a whole are somewhat different from that of seamless steel tube mainly by the influences of welding thermal residual stress and of locked in stress induced by cold forming. Hence the column buckling behavior of welded steel tube in inelastic region may also differ from that of seamless tube.

A series of buckling test of welded steel tubular columns were carried out under pin-ended centrally loaded condition. Test results are compared with the theoretical prediction based on the mechanical properties obtained from the stub-column tests. They are also compared with design loads allowed by the current Japanese specification.

## 2. TANGENT MODULUS AND CRITICAL STRESS OF WELDED STEEL TUBE

In a welded tube, three types of stress may be introduced during its producing process;
1) Elastic and plastic bending stress of tube wall along the circumferential direction as shown in Fig.1(a). Combined with the applied compressive axial load, this causes the biaxial state of stress and thus affects the yielding of a column. On this problem, a study on the basis of mathematical plasticity had been made (1).
2) When a steel strip is bent to tubular shape by cold forming,it will warp upward as shown in Fig.1(b). This is forced to straighten up in the course of cold rolling process. Thus bending stress of wall in longitudinal direction is induced. Several examples of measurement of the distribution of this bending stress(2) are shown in Fig.2(b).
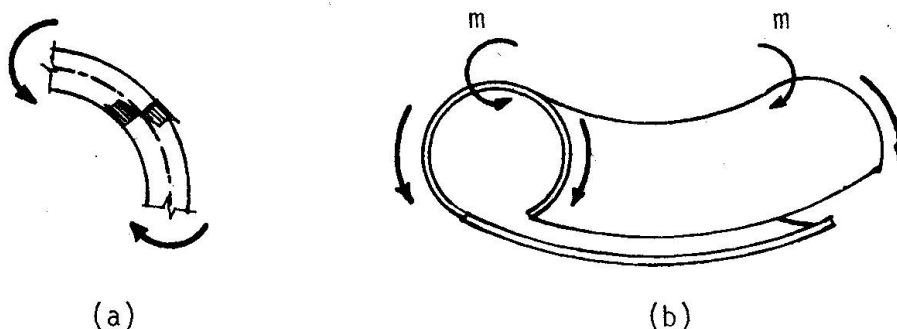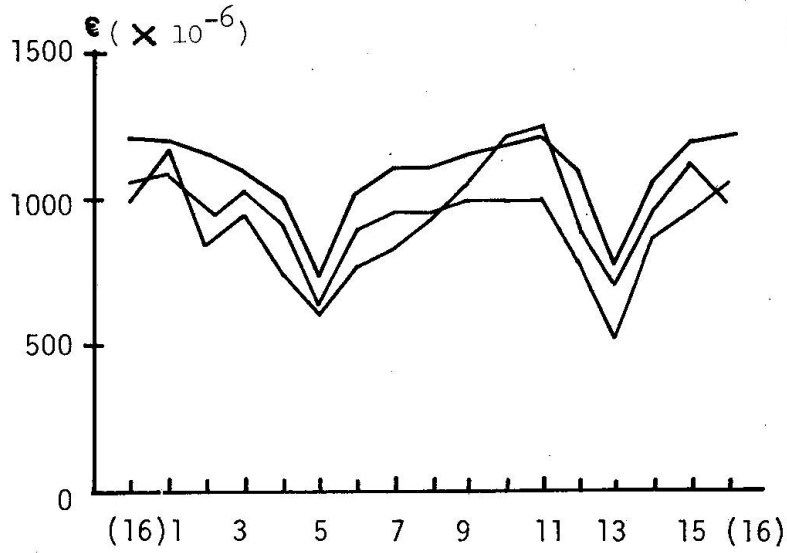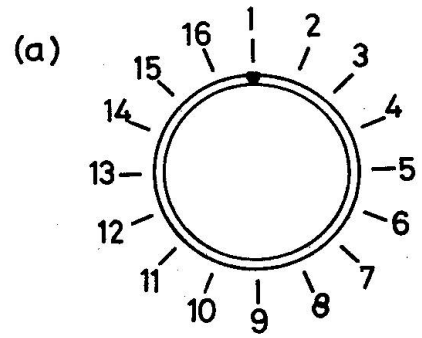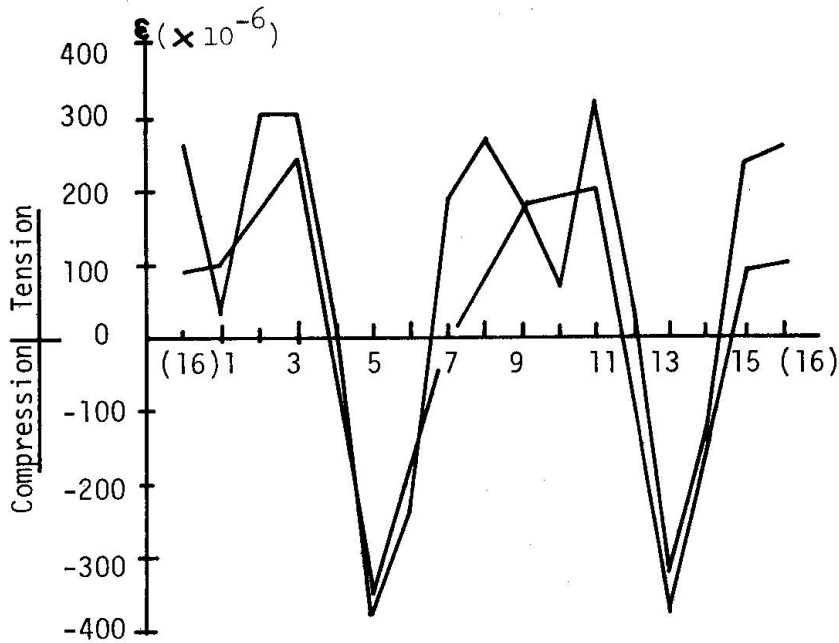


(a)                    (b)

Fig.1    Cold Forming of Steel Tube

Fig.2 Locked in Stress of
Welded Tube


(a)



(b) Bending Stress due to Cold Forming



(c) Thermal Residual Stress due to Welding

3) Thermal residual stress due to welding. Examples of the distribution of this residual stress(2) are shown in Fig.2(c).

Yielding of the column subject to axial compression is affected by these locked in stresses,and the average stress-strain relationship obtained from stub-column test shows so called round house shape as is shown in Fig.3. In case of seamless tube which is almost free from residual stress, it shows rather clear yield point(Fig.3).

To obtain the general expression of stress-strain relationship of this round house type,stub-column tubes with different yield points and diameter-to-thickness ratios were tested. As shown in Fig.4, $\sigma_p/\sigma_y$ ratios can be roughly
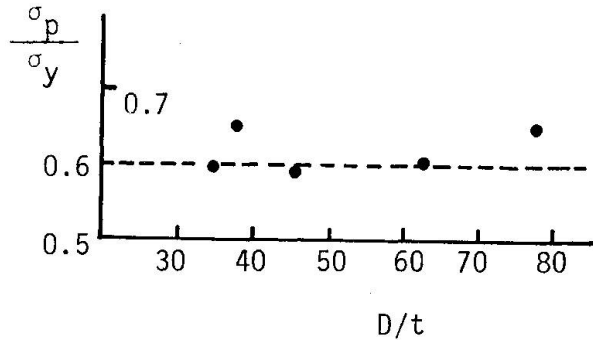


Fig.4　$\sigma_p/\sigma_y$ ratios
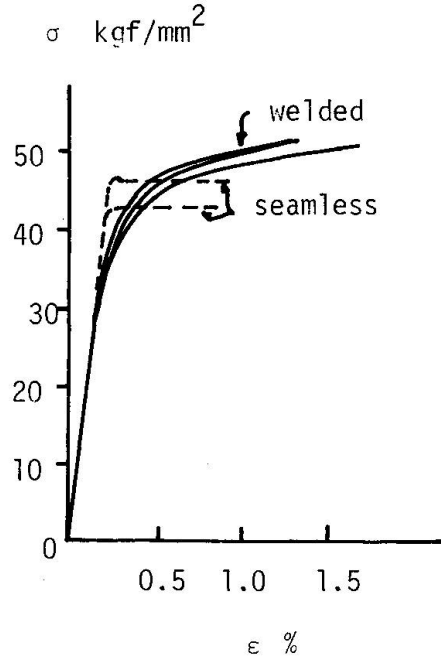


Fig.3　$\sigma - \varepsilon$ curve from stub-column tests

estimated as 0.6 through all tests, where $\sigma_p$ is the proportional limit and $\sigma_y$ is the yield strength defined by 0.2% offset basis. Assuming that $\sigma_p = 0.6\ \sigma_y$ , it was found that $\sigma$-$\varepsilon$ relation could be well approximated as

$$\sigma = \alpha(80\alpha + 1.0)E - \frac{\alpha^2\ (80\alpha + 0.4)^2 E}{\varepsilon + \alpha\ (80\alpha - 0.2)} \tag{1}$$

where　$\alpha = \sigma_y/E$

　　　　$E$ = Young's modulus

From eq.(1), tangent modulus $E_t$ can be expressed as

$$E_t = \frac{d\ \sigma}{d\ \varepsilon} = \frac{[\ \alpha(80\alpha + 1.0)E - \sigma\ ]^2}{\alpha^2(80\alpha + 0.4)^2\ E} \tag{2}$$

Then the critical stress in inelastic region is

$$\sigma_{cr} = \frac{\pi^2 E_t}{\lambda^2} = \frac{\pi^2}{\lambda^2} \frac{[\alpha(80\alpha + 1.0)E - \sigma_{cr}]^2}{\alpha^2(80\alpha + 0.4)^2 E} \qquad (3)$$

Eq. (3) can be written in nondimensional form as

$$\frac{\sigma_{cr}}{\sigma_y} = \frac{1}{\bar{\lambda}^2} [\frac{80\alpha + (1.0 - \sigma_{cr}/\sigma_y)}{80\alpha + 0.4}]^2$$

where

$$\bar{\lambda} = \lambda \sqrt{\frac{\sigma_y}{\pi^2 E}}$$

$$\lambda = \ell/r = \text{slenderness}$$

## 3. EFFECT OF SUPPORTING FIXTURES

It has been reported that it is very difficult to realize the ideal pin-end condition in column testing(3)(4). Knife edges and conventional spherical seats were reported to be unsatisfactory because of their inevitable friction. Shown in Fig.5 are hydraulically-supported spherically seated compression testing machine platens invented by R.L.Templin(5), which seems to be one of the best devices. Two series of test results of tubular columns are shown in Fig.6. Templin type platens were used in one
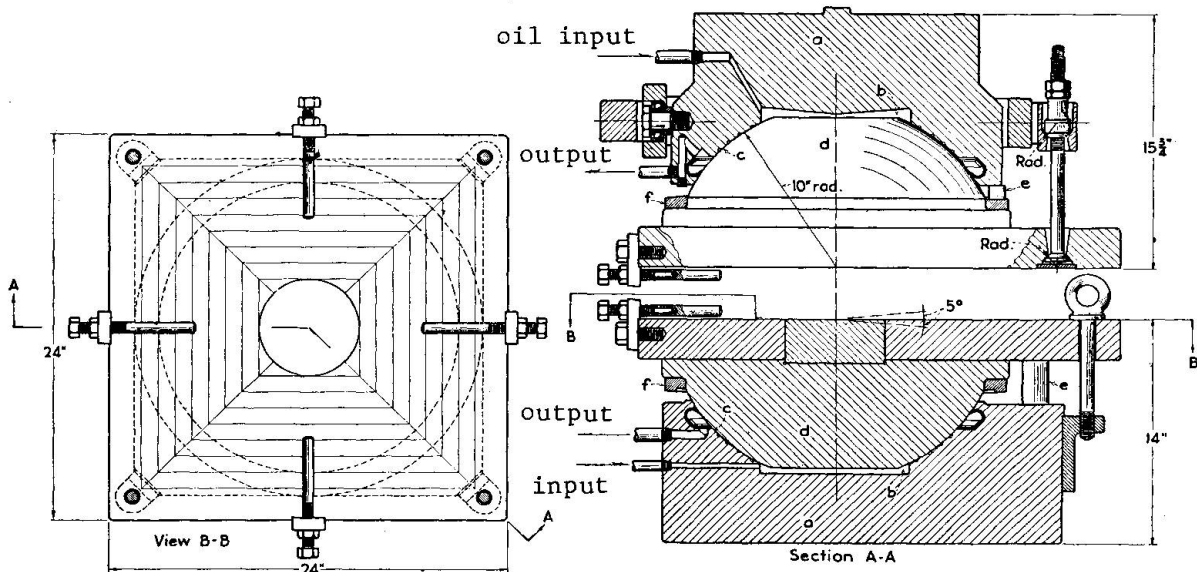


Fig.5  Templin Type End Fixture

test, while conventional spherical seats were used in the other(6). The latter test resulted in higher values up to 40% than theoretical prediction. Hence,test results of tubular columns refered in this report are limited to those obtained by using Templin type platens.

## 4. TEST RESULTS

Available test results of welded tubular columns are shown in Fig.7 and in Table 1.(7)(8)(9). Test results are compared with eq.(4). Deviation from theoretical prediction becomes large in elastic-to-plastic transitive region. Many test results are higher than Eular value in elastic region, which means that even the Templin's device would be not ideal.

In Fig.7, test results of seamless tubes are also plotted by open circles(6)(8). The column curve after DIN4114 is shown by dashed line in the same figure, which is described as

$$\sigma_{cr} = \frac{\pi^2 E \tau}{\lambda^2}$$

$$\tau = 1 - (\frac{\sigma_{cr} - \sigma_p}{\sigma_y - \sigma_p})^2 , \quad \sigma_p = 0.6 \sigma_y \tag{5}$$

This can be written in nondimensional form as

$$\frac{\sigma_{cr}}{\sigma_y} = \frac{1}{\bar{\lambda}^2} [ 1 - ( \frac{\sigma_{cr}/\sigma_y - 0.6}{0.4} )^2 ] \tag{6}$$

$$\bar{\lambda} = \lambda \sqrt{\frac{\sigma_y}{\pi^2 E}}$$

Test results on seamless tubes which are almost free from residual stress seem to show better correlation with eq.(6) than with eq.(4). Substantial difference can be seen between the buckling strength of welded tubes and of seamless tubes.

## 5. COMPARISON WITH JAPANESE COLUMN FORMULA

Column formulae specified by Japan Architectural Institute(A.I.J.)(10) are as follows;

$$f_c = [ 1 - 0.4 (\frac{\lambda}{\Lambda})^2 ] \sigma_y/\nu \qquad \text{for } \lambda \leqq \Lambda$$

$$f_c = \frac{0.6\sigma_y}{\nu(\frac{\lambda}{\Lambda})^2} \qquad \text{for } \lambda > \Lambda \tag{7}$$

where $\quad f_c$ = allowable compressive stress

$$\Lambda = \sqrt{\frac{\pi^2 E}{0.6\sigma_y}}$$

$$\nu = \frac{3}{2} + \frac{2}{3} (\frac{\lambda}{\Lambda})^2 \qquad \text{for } \lambda \leqq \Lambda$$

$$= 2.17 \qquad \text{for } \lambda > \Lambda \tag{8}$$

Above formulae can be written in nondimensional form as

$$\frac{f_c}{\sigma_y} = \frac{1 - 0.31 \lambda\sqrt{\frac{\sigma_y}{\pi^2 E}}}{1.5 + 0.4(\lambda\sqrt{\frac{\sigma_y}{\pi^2 E}})^2} \qquad \text{for } \lambda\sqrt{\frac{\sigma_y}{\pi^2 E}} \leqq 1.29$$

$\sigma$ •-----Templin Type Platen(ref.7)

O-----Conventional Spherical Seat(ref.5)
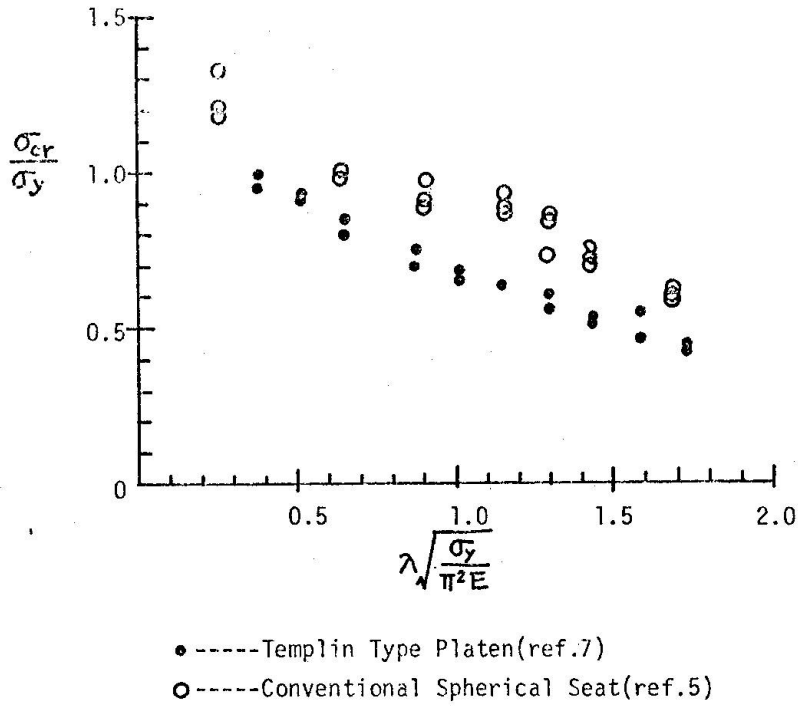
Fig.6 Effect of End Support Fixture
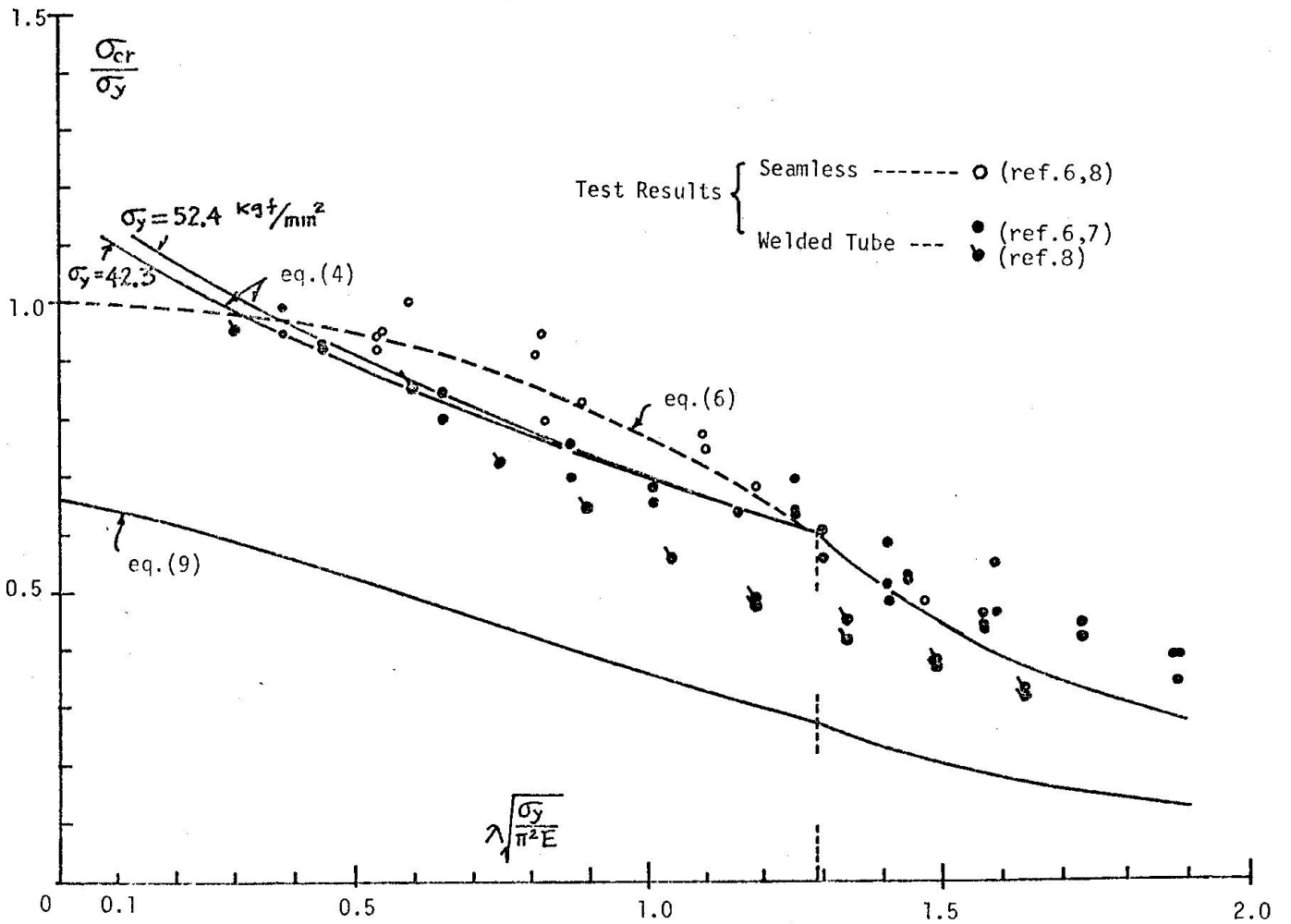


Fig.7 Test Results,Theoretical Curve & Design Formula

$$\frac{f_c}{\sigma_y} = \frac{1}{2.17} \quad \frac{1}{(\lambda\sqrt{\frac{\sigma_y}{\pi^2 E}})^2} \qquad \text{for} \quad \lambda\sqrt{\frac{\sigma_y}{\pi^2 E}} > 1.29$$

$$\text{------------------(9)}$$

The column curve expressed by eq.(9) is depicted in Fig.7 to compare with test results.
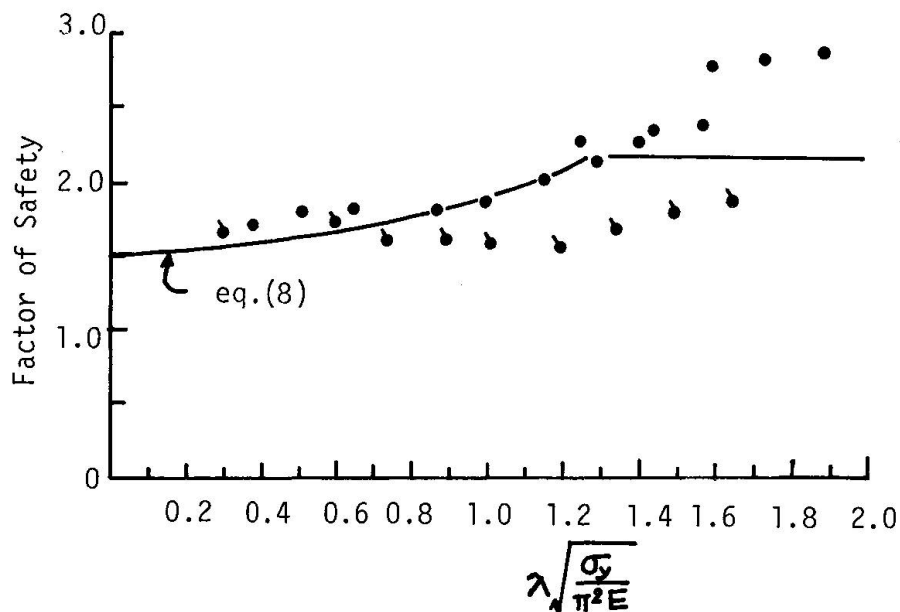


Fig.8 Factor of Safety

Each average of test results which have identical slenderness ratio are divided by corresponding nondimensional allowable stress comes from eq.(9), and is plotted in Fig.8. Nominal factor of safety specified by A.I.J. standard (eq.(8)) is also shown in the figure. In inelastic region, specified factor of safety increases paraborically starting from 1.5, while it is constantly designated as 2.17 throughout elastic region as seen in eq.(8). Safety factor of 1.5 is the one which is designated for the tension member. Test results of reference(8) show rather lower value. This might be caused by some imperfections(initial curvature,eccentricity) or unfavorable locked in stress for which no information is available from reference(8). Anyhow, as far as available test results are concerned, factor of safety of 1.5 is secured through the whole range.

## Table 1. TEST RESULTS

### Test A. Reference(6), Welded Tube, Grade of Steel:STK 50, $\sigma_y$=52.4 kgf/mm²

| size $\phi \times t$.mm | length mm | slenderness $\lambda = l/r$ | $\sigma_{max}(\sigma_{cr})$ kgf/mm² | $\sigma_{max}/\sigma_y$ | $\lambda \sqrt{\dfrac{\sigma_y}{\pi^2 E}}$ |
|---|---|---|---|---|---|
| 60.5×2.9 | 1,600 | 79.1 | 36.4 | 0.695 | 1.255 |
| | | 79.1 | 33.4 | 0.638 | 1.255 |
| | | 79.1 | 33.0 | 0.630 | 1.255 |
| | 1,800 | 88.9 | 25.1 | 0.480 | 1.413 |
| | | 88.7 | 26.8 | 0.511 | 1.410 |
| | | 88.9 | 30.6 | 0.585 | 1.413 |
| | 2,000 | 98.7 | 23.2 | 0.443 | 1.570 |
| | | 98.9 | 23.4 | 0.446 | 1.571 |
| | | 98.9 | 24.0 | 0.458 | 1.571 |
| | 2,400 | 118.5 | 18.1 | 0.346 | 1.885 |
| | | 118.7 | 20.1 | 0.384 | 1.890 |
| | | 118.4 | 20.2 | 0.386 | 1.885 |

### Test B. Reference(7), Welded Tube, Grade of Steel:STK 50,
$\sigma_y$=42.3 kgf/mm² for 139.8$\phi$×4.5mm    $\sigma_y$=43.8 kgf/mm² for 60.5$\phi$×3.2mm

| size | length | slenderness | $\sigma_{max}$ | $\sigma_{max}/\sigma_y$ | $\lambda\sqrt{\sigma_y/\pi^2 E}$ |
|---|---|---|---|---|---|
| 139.8×4.5 | 1,410 | 26.7 | 42.0 | 0.993 | 0.382 |
| | 1,409 | 26.7 | 40.0 | 0.945 | 0.382 |
| | 1,910 | 36.2 | 39.0 | 0.921 | 0.517 |
| | 1,910 | 36.2 | 39.2 | 0.926 | 0.517 |
| | 2,412 | 45.6 | 33.8 | 0.799 | 0.651 |
| | 2,413 | 45.6 | 35.9 | 0.850 | 0.651 |
| 60.5×3.2 | 1,210 | 59.7 | 33.2 | 0.758 | 0.871 |
| | 1,211 | 59.7 | 30.5 | 0.696 | 0.871 |
| | 1,411 | 69.5 | 28.5 | 0.651 | 1.010 |
| | 1,411 | 69.5 | 29.7 | 0.678 | 1.010 |
| | 1,610 | 79.4 | — | — | 1.155 |
| | 1,612 | 79.4 | 27.8 | 0.635 | 1.155 |
| | 1,812 | 89.2 | 24.6 | 0.561 | 1.299 |
| | 1,812 | 89.2 | 26.7 | 0.610 | 1.299 |
| | 2,012 | 99.1 | 23.1 | 0.527 | 1.440 |
| | 2,013 | 99.1 | 22.9 | 0.523 | 1.440 |
| | 2,213 | 109.1 | 20.3 | 0.464 | 1.590 |
| | 2,213 | 109.1 | 24.2 | 0.552 | 1.590 |
| | 2,412 | 118.9 | 18.6 | 0.425 | 1.730 |
| | 2,412 | 118.9 | 19.5 | 0.445 | 1.730 |

Test C. Reference(8), Welded Tube, Grade of Steel:STK 50, $\sigma_y$=46.3 kgf/mm$^2$

| size $\phi \times t$.mm | length mm | slenderness $\lambda = l/r$ | $\sigma_{max}(\sigma_{cr})$ kgf/mm$^2$ | $\sigma_{max}/\sigma_y$ | $\lambda\sqrt{\dfrac{\sigma_y}{\pi^2 E}}$ |
|---|---|---|---|---|---|
| | 3,840 | 110.0 | 14.6 | 0.316 | 1.640 |
| | 3,840 | 110.0 | 15.1 | 0.326 | 1.640 |
| | 3,491 | 100.0 | 17.4 | 0.377 | 1.490 |
| | 3,491 | 100.0 | 16.9 | 0.365 | 1.490 |
| | 3,142 | 90.0 | 19.1 | 0.411 | 1.340 |
| | 3,142 | 90.0 | 20.8 | 0.448 | 1.340 |
| 101.6×2.9 | 2,793 | 80.0 | 21.7 | 0.468 | 1.193 |
| | 2,793 | 80.0 | 22.2 | 0.478 | 1.193 |
| | 2,444 | 70.0 | 25.6 | 0.552 | 1.043 |
| | 2,095 | 60.0 | 29.7 | 0.643 | 0.895 |
| | 1,746 | 50.0 | 33.5 | 0.725 | 0.745 |
| | 1,396 | 40.0 | 39.5 | 0.852 | 0.597 |
| | 698 | 20.0 | 44.0 | 0.952 | 0.299 |

Test D. Reference(6), Seamless Tube, $\sigma_y$=52.0 kgf/mm$^2$ for 60.5$\phi$×2.9mm.
$\sigma_y$=37.6 kgf/mm$^2$ for 89.1$\phi$×3.5mm, 101.6$\phi$×3.5mm, 114.3$\phi$×4.5mm.

| | | | | | |
|---|---|---|---|---|---|
| 60.5×2.9 | 1,400 | 68.8 | 40.3 | 0.770 | 1.095 |
| | 1,400 | 69.0 | 39.2 | 0.749 | 1.100 |
| 89.1×3.5 | 1,200 | 39.9 | 35.4 | 0.940 | 0.535 |
| | 1,800 | 60.0 | 34.2 | 0.910 | 0.807 |
| 101.6×3.5 | 1,400 | 40.8 | 35.8 | 0.950 | 0.550 |
| | 2,100 | 60.8 | 35.6 | 0.945 | 0.818 |
| 114.3×4.5 | 1,550 | 39.9 | 34.7 | 0.920 | 0.537 |
| | 2,300 | 59.1 | 31.0 | 0.824 | 0.795 |

Test E. Reference(8), Seamless Tube, $\sigma_y$=46.1 kgf/mm$^2$

| | | | | | |
|---|---|---|---|---|---|
| | 3,442 | 99.0 | 22.26 | 0.482 | 1.470 |
| 101.6×2.9 | 2,793 | 80.0 | 31.31 | 0.680 | 1.192 |
| | 2,095 | 60.0 | 38.30 | 0.832 | 0.895 |
| | 1,396 | 40.0 | 46.45 | 1.020 | 0.596 |

234

REFERENCES

(1) Ben Kato & H. Aoki, Effects of Cold Forming on the Mechanical Properties of Welded Steel Tube, Trans. Architectural Institute of Japan, extra issue, Aug. 1969.
(2) Wakabayashi, M. et.al., Residual Stress in Welded Steel Tube, Proc. Annual Meeting of Kinki Branch of A.I.J., April, 1967.
(3) Progress Report of the Special Committee on Steel Column Research, Trans. A.S.C.E., vol. 89.
(4) Barlow, H.W., A Fixture for Obtaining Pin-end Conditions in Column Testing, Journal of Aeronautical Sciences, vol. 7, No.2, Dec. 1939.
(5) Templin, R.L., Hydraulically-supported Spherically-seated Compression Testing Machine Platens, Proc. of the 45th Annual Meeting, vol. 1. 42, A.S.T.M., 1942.
(6) Suzuki, T. & Fujimoto, M., NKK Design Manual of Tubular Structure, Nippon Kokan K.K.,
(7) Kato Ben et.al., Column Buckling Test on High Tensile Steel Tubes, Trans. Architectural Institute of Japan, No.63, Oct. 1959.
(8) Kato Ben et.al., Column Buckling Test on High Tensile Steel Tubes, Proc. Annual Meeting of Kanto Branch of A.I.J., No.35, June, 1965.
(9) Wakabayashi, M. et.al., Column Buckling Test on Welded Steel Tubes, Trans. Architectural Institute of Japan, Oct. 1968.
(10) Design Specification of Structural Steel for Buildings, Architectural Institute of Japan, 1968.

Bg. 16 A K 23

# CENTRALLY COMPRESSED BUILT-UP STRUTS

G. Ballio,L. Finzi,C. Urbano
Istituto di Scienza e Tecnica delle Costruzioni
Politecnico di Milano-Italy

## ABSTRACT

This paper presents the results of both an experimental and theoretical research on built-up compact struts.

Channels and unequal angles back to back are considered with different slendernesses and type of connectors.

The experimental results are compared with the ones obtained using the C.E.C.M.buckling curves for:

1)    welded connectors
2)    tightened bolted connections
3)    untightened bolted connections
4)    hotgalvanized or painted elements.

A numerical approach allowing for elastic unloading processes is finally presented.

## 1. Introductory Remarks

So far as the authors know, built-up struts are still designed with the theory of elastic equilibrium bifurcation for the fasterners as well as the whole strut (fig.1).

It is normally assumed that subjected to the critical load the equilibrium configuration and, in particular, the deflection $f_{gc}$ that characterises overall collapse, will be indeterminate. In this case, the fasteners (e.g. batten plates) are designed (fig.2) for a deflection $f_{1c}$ that will provoke the local failure of the most compressed of the chords. This means that initial out-of streightness in the axis and the load eccentricities will have no influence, nor will the transversally distributed loads (dead load, wind etc).

For simple struts, however, this concept was given up about twenty years ago, and replaced by another, which follows the behaviour of the strut step by step as the loads increase, taking into account realistic values of the geometrical and mechanical imperfections as well as real transversal loads.



FIG.1



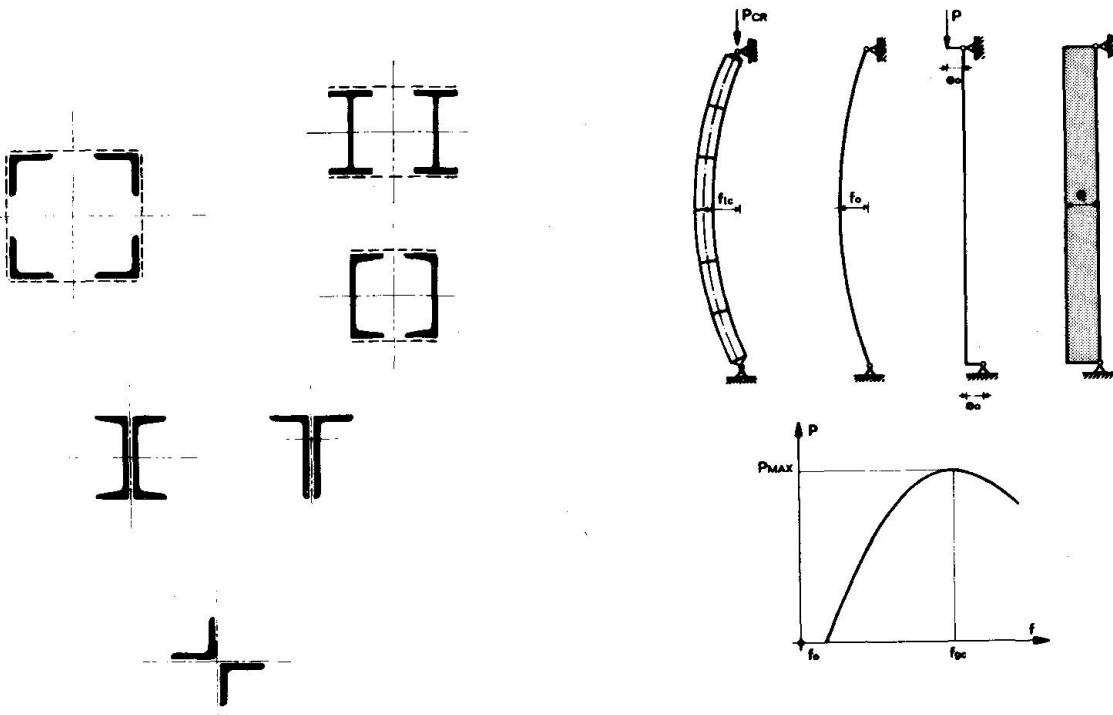FIG.2

This leads to a curve $P=P$ (f) which is characterised by a well defined maximum, and therefore by a value $f_{gc}$ of the deflection which characterises overall collapse for that maximum.

Both $P_{MAX}$ and $f_{gc}$ are greatly influenced by a number of factors that are present during loading. They are: mechanical characteristics (residual stresses $\sigma_o$) geometrical imperfections

(the initial out-of-straightness of the axis $f_o$ and load eccentricity $e_o$) loads $q$ distributed along the axis of the strut (forces linked to the volume or the surface - dead weight,wind, dynamic forces).

So it may be said that:

$$f_{gc} = f_{gc}\left(P_{MAX}, \sigma_o, e_o, f_o, q, \bar{\sigma}\right)$$

where $\sigma_o$, $f_o$, $e_o$ and $q$ must be worked out beforehand, on a statistical basis as well as the yield point $\bar{\sigma}$.

The load $P_{MAX}$ is less than that calculated without $\sigma_o$, $f_o$, $e_o$ and $q$ but being much more realistic, a safety factor may be adopted for these axially loaded struts that is the same as for tensioned bars. To sum up this new concept, then overall collapse deflection is no longer indeterminate, and can in fact be worked out quantitatively by a clear calculation process.

This kind of approach, when applied to simple struts of different cross section has lead to the definition of the European Curves $\sigma = \sigma(\lambda)$. If reference is now made in particular to built-up struts it will be seen that there need be no guarantee that the fasteners along the strut remain efficient until, between one fastener and the next, the failure of one of the component struts. All that is required now is that neither of the following conditions arises separately:

a) failure of a component strut between one fastener and the next when $f < f_{gc}$ ,

b) failure of a fastener along the strut when $f < f_{gc}$ .

This represents a different way of looking at the situation. The design of the fastener no longer depends on the local design of the component strut,but both depend on the overall behaviour of the structure.

This overall behaviour has only been studied within the limits of the theory of bifurcation.

Other more worthwile approaches are being looked into, but this, of course, is not easy.

It is particularly unrealistic to use calculation methods that do not take into account the unloading processes during lateral buckling of the strut. The component strut furthest from the original line of the axis may even become tensioned rather than compressed.

## 2. Experimental Results

The behaviour of one particular class of built-up compact struts was studied with back to back separators.

Two sets of experiments have so far been carried out. The first (see figs.3 and 4) used back to back 140UNP channels 15
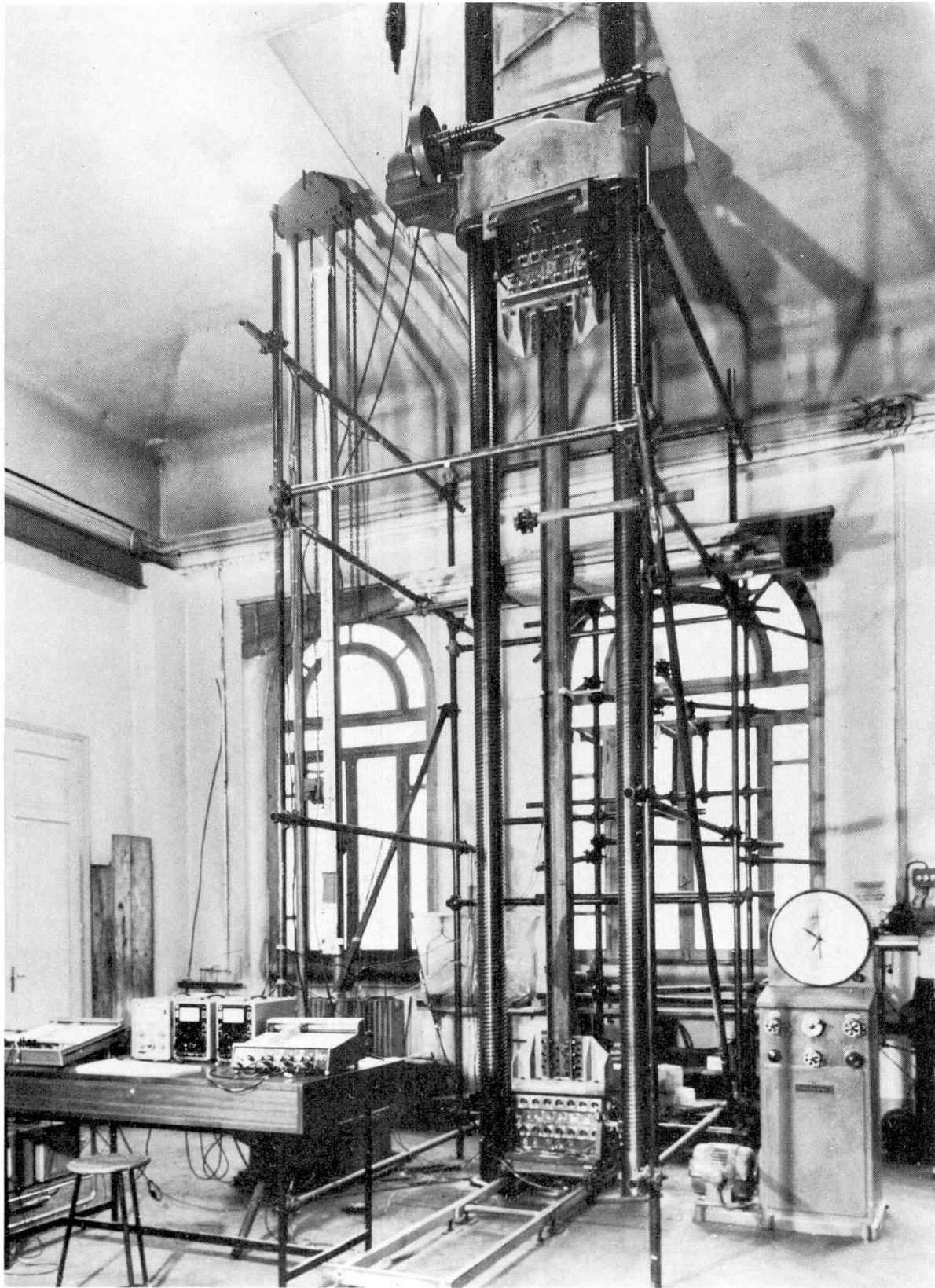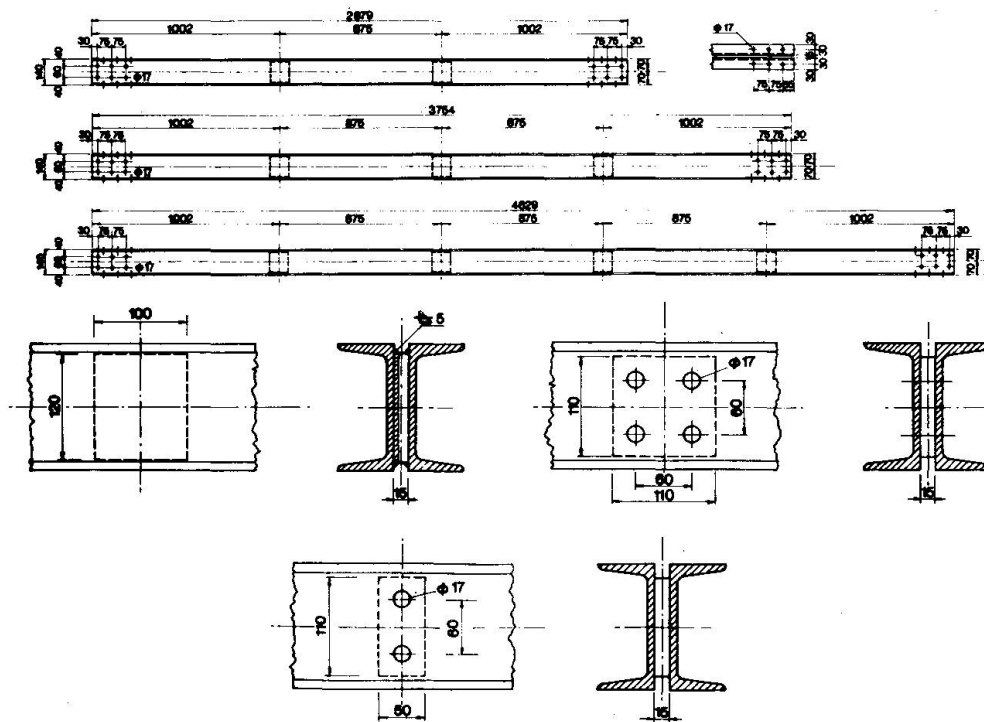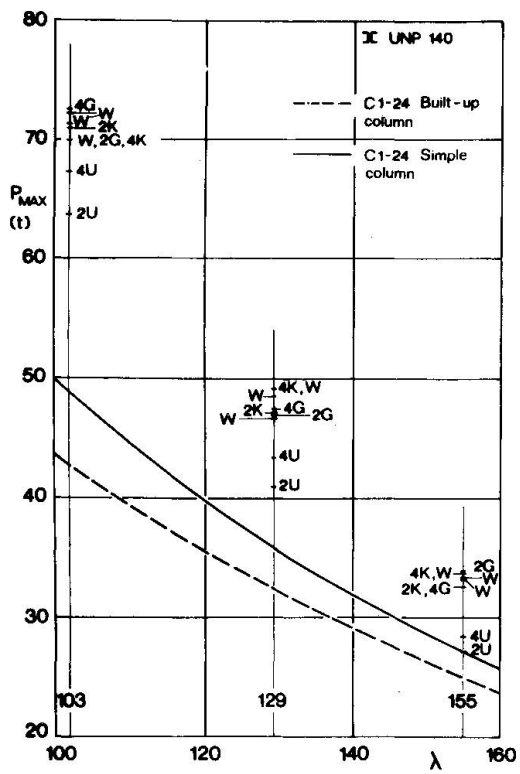
FIG.3

FIG.4



FIG.5

240

mm apart, fastened at 2,3 or 4 intermediate points with solid washers or packings. The specified yield point was $\bar{\sigma}$ =24Kg/mm$^2$. The total slenderness ratios, depending on the number of fasteners, were 103,129, and 155, while the local ratio (between packings) was 50. The end fasteners (24 shear resistent sections with $\emptyset$16 bolts of type 10 K) were all the same and designed for the ultimate load of the struts at zero slenderness.The intermediate fasteners were of the following kinds:

| Connections | | | | | Symbol |
|---|---|---|---|---|---|
| welds | | | | | W |

|  | 4 | $\emptyset$ 16 of type 10 K, | tightened | 4K |
|---|---|---|---|---|
|  | 2 | " "     " 10 K, | " | 2K |
| bolts | 4 | " "     " 8 G, | " | 4G |
|  | 2 | " "     " 8 G, | " | 2G |
|  | 4 | " "     " 10 K, | untightened | 4U |
|  | 2 | " "     " 10 K, | " | 2U |

The experimental results are given in fig.5 and are compared with the curve $P_{MAX} \cdot P_{MAX}(\lambda)$(maximum load depending on the slenderness of the simple strut) deduced from the European Curve C1-24.

The struts with untightened fasteners (in which the settlement of the bolt in its hole becomes significant) were the least successful.It also became clear that the European curve C1-24 for simple struts, at least for high slendernesses was not safe enough while the dashed curve referring to an ideal

slenderness $\lambda_{id} = \sqrt{(\lambda^2 + \lambda_1^2)}$ certainly is.

The second set of experiments was on (fig.6) unequal angles $5'' \times 3'' \times 5/16''$ with 2,3 and 4 intermediate fasteners.

The specified yield point was $\bar{\sigma}$ =36 K/mm$^2$. The total slendernesses, depending on the number of fasteners, were 97,117 and 137, while the local slenderness was 50.

The end connections were this time designed for the real capacities of the strut and were made of the same kind of bolts used for the intermediate fasteners.These latter were of the following kinds:

| Connections | | | | | Symbol |
|---|---|---|---|---|---|
| welds | | | | | W |

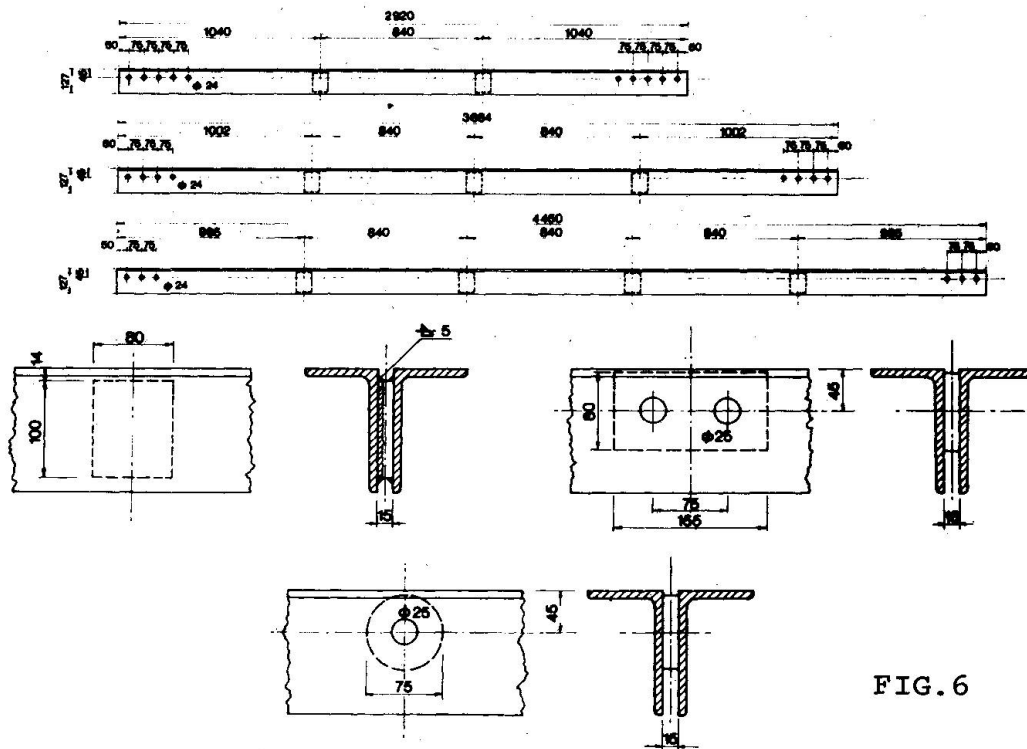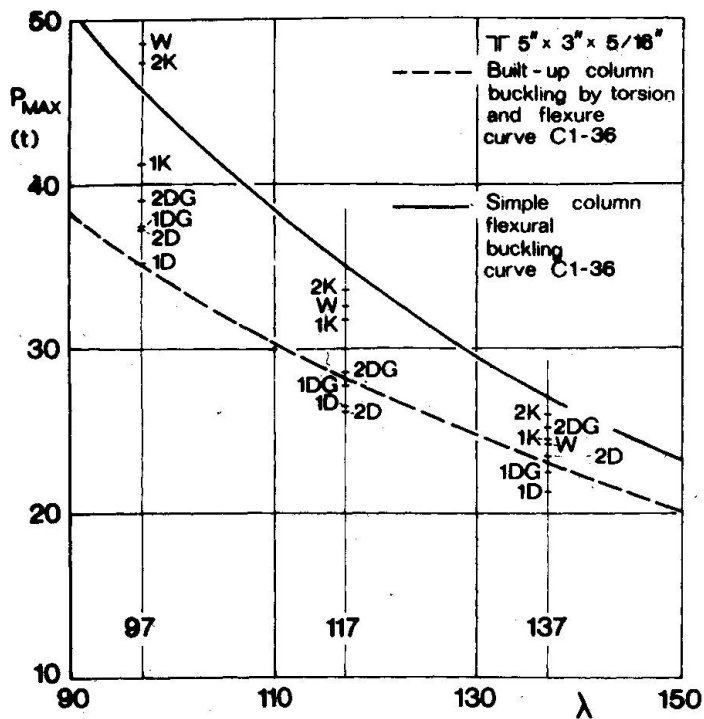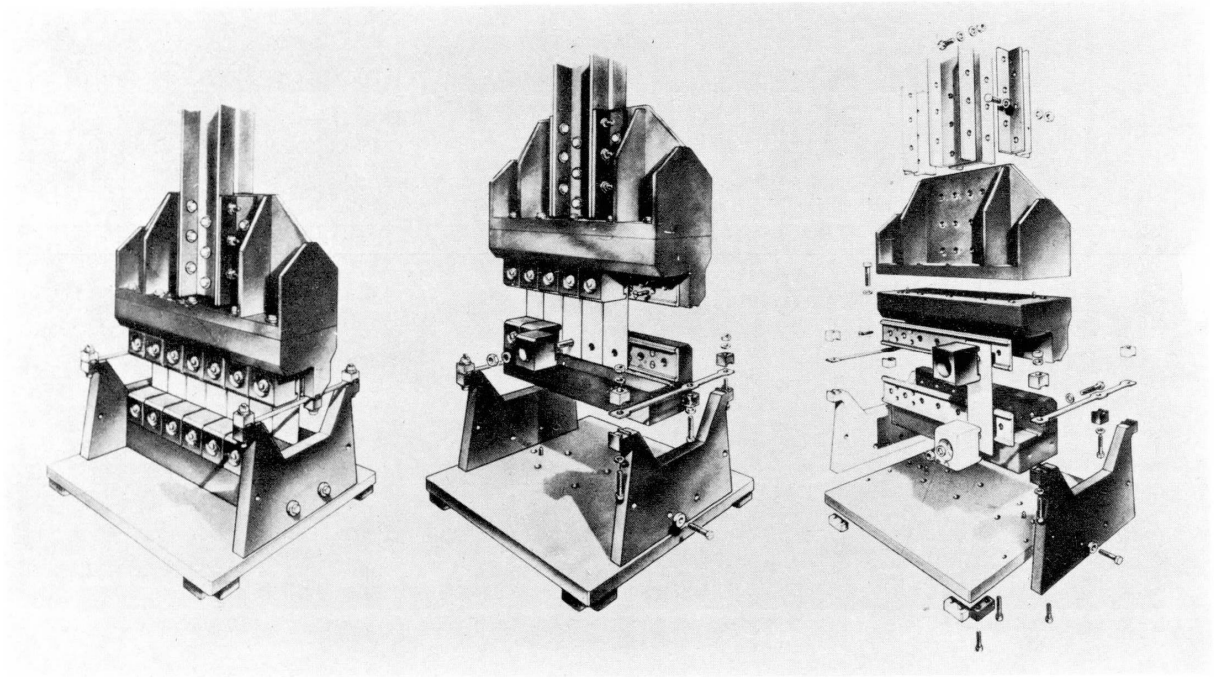|  | 2 | $\emptyset$ 24 of type 10 K, | tightened | 2K |
|---|---|---|---|---|
| bolts | 1 | " "     " 70 K | " | 1K |
|  | 2 | " "     " 5 D | " | 2D |
|  | 1 | " "     " 5 D | " | 1D |

FIG.6



FIG.7

242

FIG.9

The fasteners shown by the letter G were for hot galvanized struts and bolts.

The experimental results are given in fig.7 and are compared to the curve $P_{MAX} = P_{MAX}(\lambda)$ deduced from the European Curve C1-36. Clearly the curve cannot be used for our purposes. Here two dif ferent effects come together, the first being the unfavourable influence of flexural-torsional instability the second being the greater or lesser stiffness of the intermediate fasteners. Even reference to the dashed curve, which corrects the slender- ness by taking into account the above mentioned effects in the elastic range, does not guarantee safety in all situations. The authors consider that if normal safety margins are to be respect ed, welded joints or high strength friction type bolts are essen tial.

To sum up:

a) B uilt-up struts with washers or packings can only be consi- dered as perfectly solid if their design assumes the ideal slenderness.

b) If the cross-section of the struts is not orthogonally sym- metrical to the plain of deflection, and so flexural-torsion al instability arises, it is no longer possible to make di- rect reference to the European Curves C1-24 and C1-36.

c) The stiffer are the end connections, the better is the per formance of built-up struts.

d) The forces acting on the intermediate fasteners are less than those allowed for by the theory of bifurcation.The de- sign must therefore pay particular attention to the qualita- tive aspects of constructional detailing, stressing stiff- ness rather than strength of the intermediate fasteners.

## 3. Test Equipment

The hydraulic press used for experiments had a pair of fix- tures for the test struts to the machine. These make up a cy- lindrical elastic hinge which allows the end section of the strut to rotate around an axis when loaded, without friction but with a known elastic moment.The test equipment can be used on compressed structural elements of up to 7m in length, and the fixtures have a capacity of 100 metric tons.

These elastic hinges eliminate friction, since the end-hin- ged system (fig.8), adopted by many researchers, has been aban- doned in favour of a continuous beam. In this way the test strut constitues the intermediate element, and the ends always remain within the elastic range thus allowing the end sections of the test strut to rotate, bringing into play an elastic end moment. By using very flexible elements at the ends to transmit the axial load, the elastic end moments can be greatly reduced. In

this way the effective length of the test piece is not much less
than the distance between the intermediate supports and a furth
er advantage is that the transversal reactions of the supports
are quite small compared to the axial loads. Since the members
at the ends never leave the elastic range, the moment applied
at the ends of the test piece can always be measured. The equip
ment is shown in fig.9.

The calculation method for establishing the effective length
of the test piece is given in fig.10. This, as can easily be
seen, is suitable for determining the critical loads correspond
ing to a symmetrical deformation.

The calculation results establish the effective length for
a strut in these test conditions. The diagram in fig.10 shows
the distance L between the axes of the elastic hinges as x-coor
dinate. The y-coordinate gives, for different values of the mo-
ment of inertia I of the test piece, the ratio between its ac-
tual slenderness $\lambda$ and the slenderness $\lambda_E$ it would have if hing
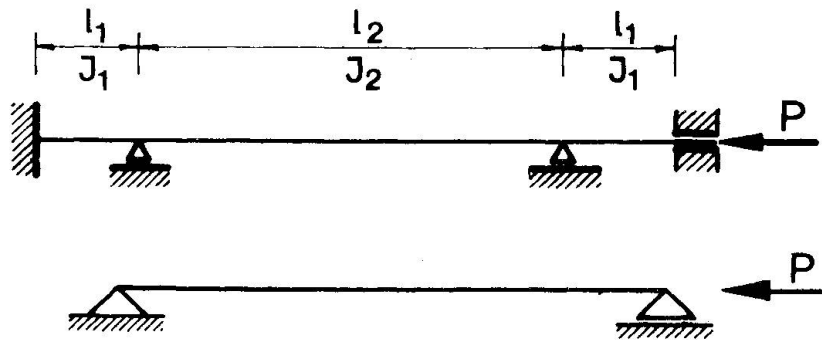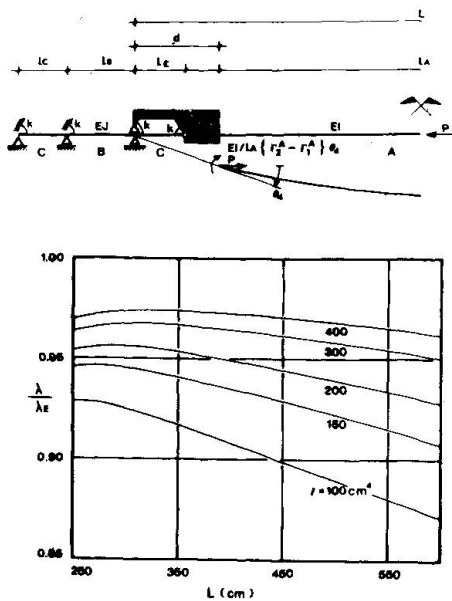ed at the ends of span L.



FIG.8



FIG.10



FIG.11

245
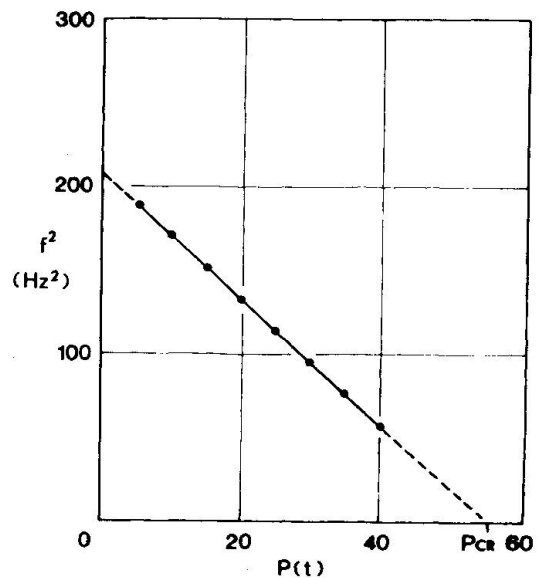
The fixtures were given a series of checks and calibra
tions to verify their static behavior, both when and when
not connected to the test machine. Deflection test were car
ried out in the absence of axial loads. These showed that
the actual position of the axis of rotation coincided with
the theoretical position. They also checked the flexural
stiffness, and calibrated the measuring equipment for bend
ing moments.

The experimental value of the flexural stiffness was
298.6 metric ton cm/rad and agreed very well with the theo
ry based on the model of fig.10: $K_T$ =299.4 metric tons cm/rad.
A further series of tests was carried out to verify the ef
fective lengths of a set of struts with the same moment of
inertia but different lengths. The dynamic method was used
to find Euler critical load experimentally (fig.11).This
was then compared with the theory. The theory turned out to
be only 2% lower than the experimental results, so the cal-
culation criteria may be considered precise enough for all
practical purposes.

## 4. Numerical Approach

A numerical approach for calculating the bearing capaci
ty of a built-up strut should allow for:

a) establishing compatibility of displacements at the inter
   mediate and end connections in order to calculate the
   equilibrium configuration. This is possible, in princi-
   ple, if solution techniques are used which assume that
   the axial load is an indipendent variable.



FIG.12                                    FIG.13

246

FIG.14



FIG.15

247
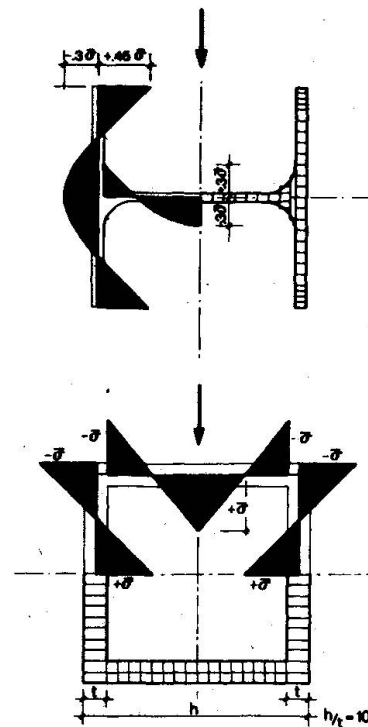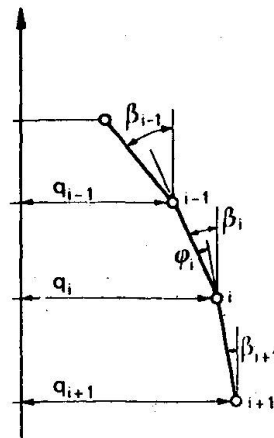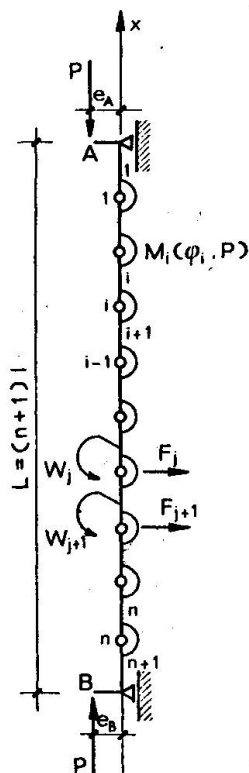
FIG.16
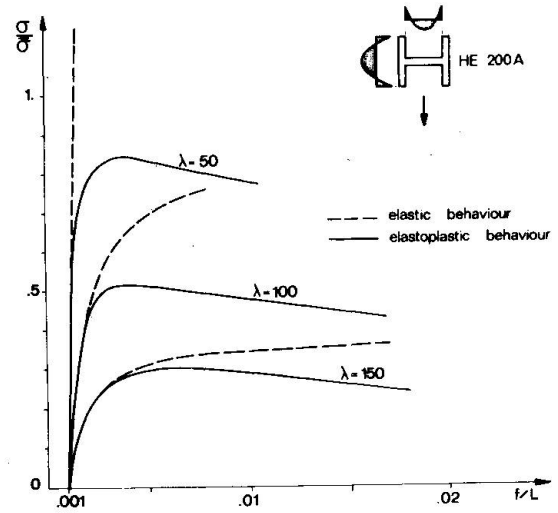


FIG.17
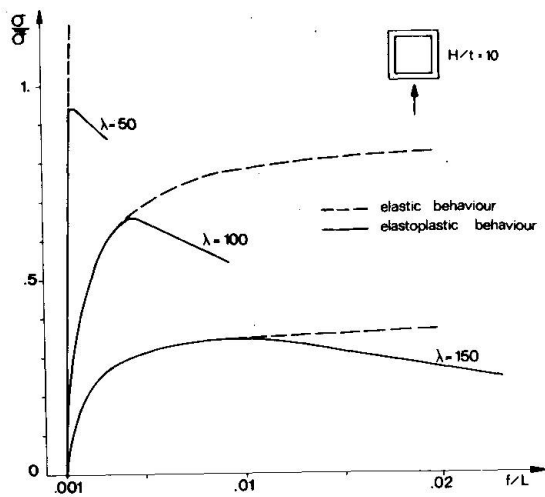


FIG.18



FIG.19

FIG.20



FIG.21

249
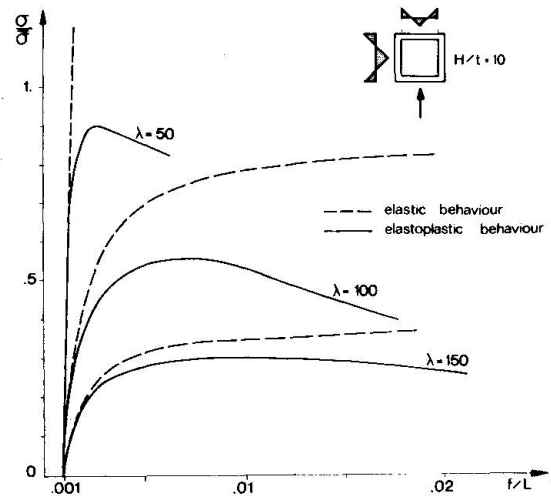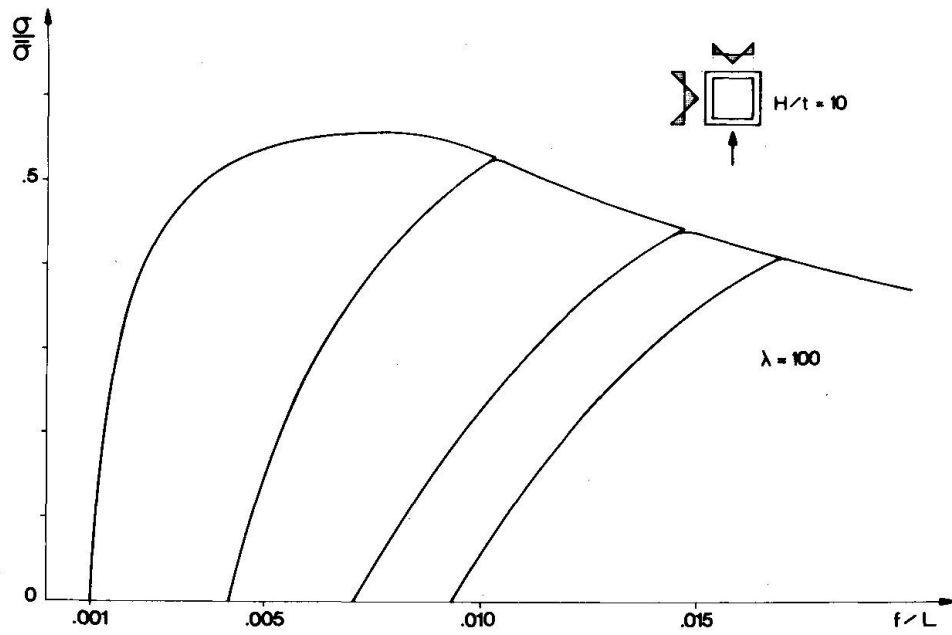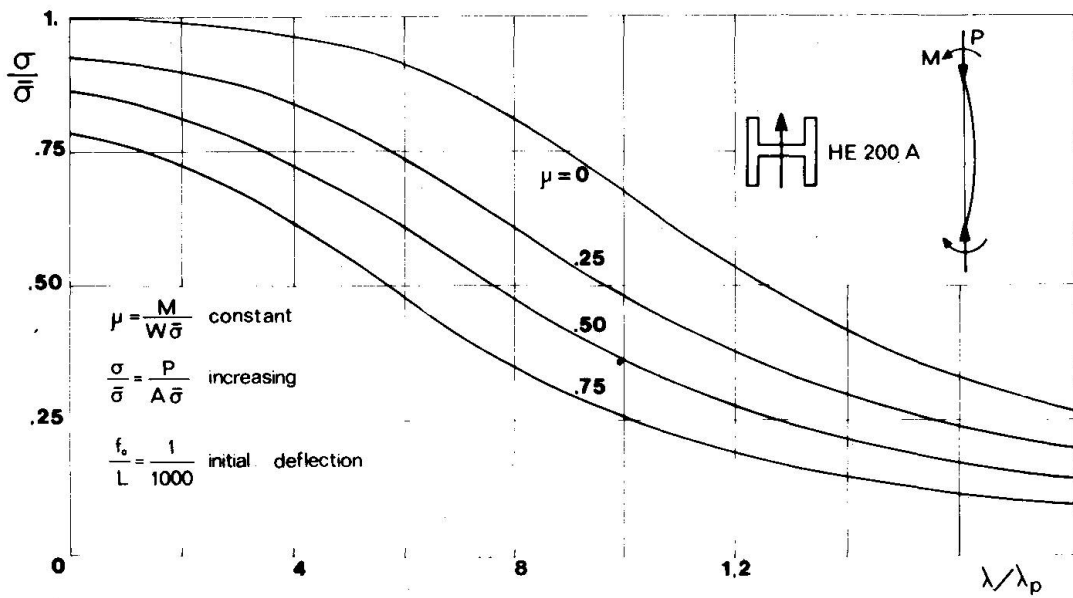
b) global or local elastic unloadings of the chords because as the axial load increases one of the chords might become ten sioned instead compressed. This unloading is possible if the problem is posed in incremental terms, and the equilibrium configuration that corresponds to the load $P+\Delta P$ is calculat ed by starting from the configuration corresponding to $P$ .

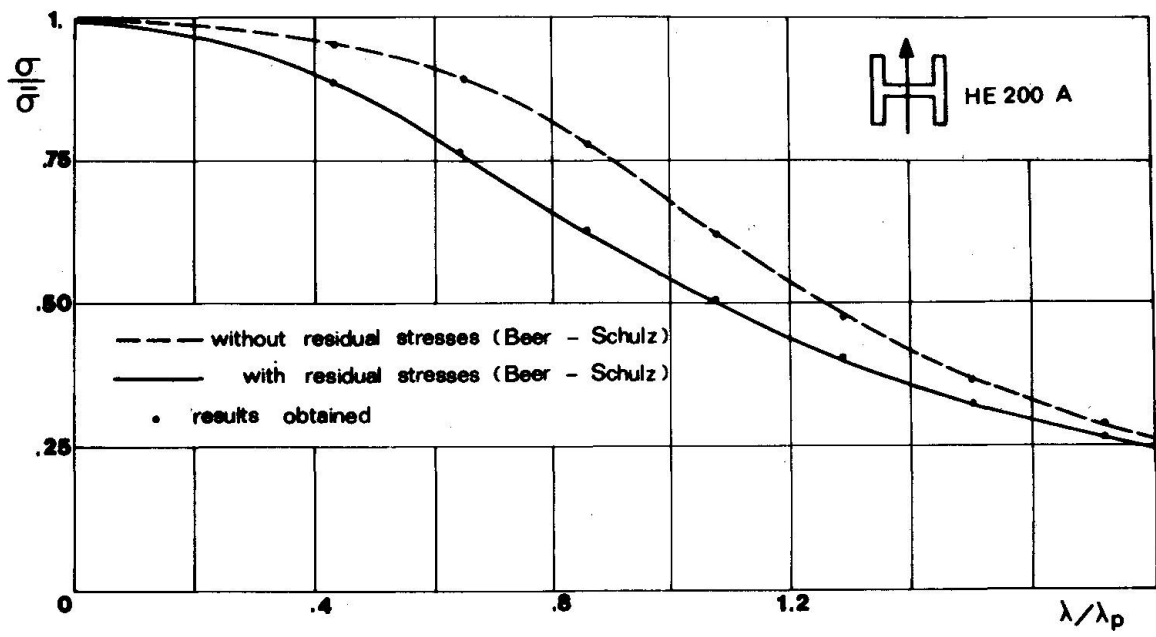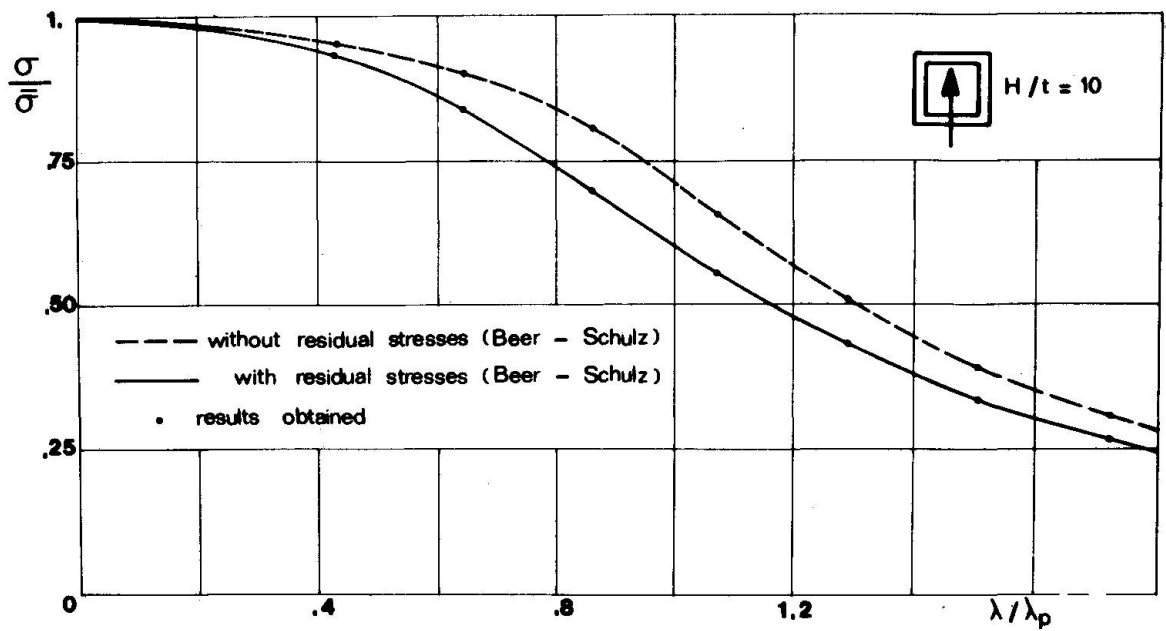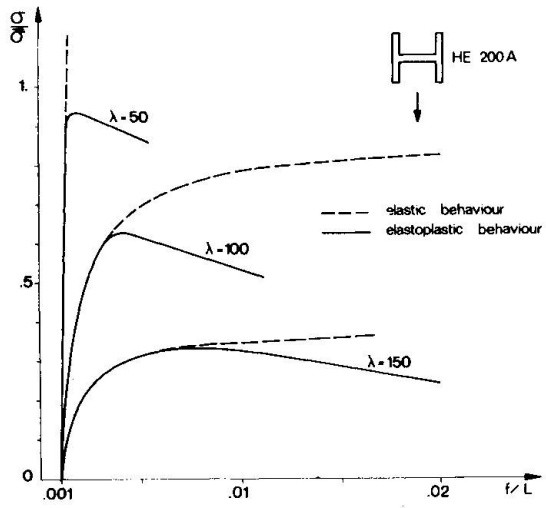Since the non-holonomy of the moment-curvature law cannot be left out, a calculation method was developed that respected points a) and b) in order to study the behaviour of built-up struts. This method has been proved for simple struts, and must now be extended to built-up columns.
The principles of the method are (fig.12):

a) the strut is reduced to a model with a finite number of de grees of freedom and made up of rigide parts and elementary cells in which all the flexibility, both axial and flexural, is concentrated.
b) the equilibrium equations are written in non dimensional form through the equivalence of both the Euler critical load and the limit elastic bending moment of the beam and of the model.
c) the relative rotations $\varphi_i$ of the parts of the model are as sumed as the unknowns depending on the applied load $\sigma_N$: $\varphi_i = \varphi_i(\sigma_N)$
d) the problem is reduced to incremental form by differentiat ing the equilibrium equation with respect to the independent variable $\sigma_N$ .
e) integration of the system of differential equations is ob tained by a technique widely used for dynamic problems bas ed on a modification of Euler-Cauchy method, starting from the initial configuration.

So far, the mathematical program has been checked against some known results. In particular, HE200A and box struts, with or without residual stresses were considered (fig.13)and the results compared with those obtained by Beer and Schulz (see figs. 14 and 15).

The axial load-deflection laws for different slendernesses were computed, also for loads decreasing as the deflection in creases (fig.16,17,18,19).

Overall unloading was also studied (fig.20). Finally the ma ximum axial load carried by struts subject to constant bending moments and increasing axial loads was calculated (fig.21).

## 5. Details of the Calculation Method.

With reference to fig.12 the equilibrium equations are:

1) $\{M\} - P\ell [C]\{\varphi\} = [C](\ell\{F'\} + P\{e\})$

where are:

$M_i$    bending moment,
$P$    axial load,

$\ell$     length of the parts,

$\varphi_i$     relative rotations,

$F_i^x$     generalised external forces,

$e_i$     generalised eccentricities,

$q_i$     transversal displacements,

$[c]$     a matrix defined by the relation: $\{q/\ell\} = [c]\{\varphi\}$.

The following quantities are defined:

$\bar{\sigma}$     yield point,

$A$     area of the cross section,

$\rho$     radius of inertia of the cross section,

$h$     distance of the most compressed fibres from the centroid of the cross section,

$\lambda$     slenderness,

$\lambda_P = \pi \sqrt{E/\bar{\sigma}}$ .

The following non dimensional quantities are defined:

$$\{\mu\} = \left\{\frac{M}{\bar{M}}\right\} \quad , \quad \sigma_N = \frac{P}{\bar{\sigma}A} \quad , \quad \{\Phi\} = \left\{\frac{\varphi}{\bar{\varphi}}\right\} ,$$

$$\{f^*\} = \left\{\frac{F^*\ell}{\bar{M}}\right\} , \qquad \{e^*\} = \left\{\frac{e\,h}{\rho^2}\right\} .$$

The first eigenvalue $\beta_E$ of the problem:

$$\left([I] - \frac{P\ell}{k}[c]\right)\{\varphi\} = 0 ,$$

defines the parameter:

$$\beta = \beta_E \frac{\lambda^2}{\lambda_P^2} .$$

Because of the equivalence of both the limit elastic moment and the Euler critical load of the strut as well as the model equations (1) can be written in the non dimensional form:

2)    $\{\mu\} - \sigma_N \beta [c]\{\Phi\} = [c]\left(\{f^*\} + \sigma_N \{e^*\}\right)$ .

Differentiation with respect to $\sigma_N$ gives:

3)    $\left\{\dfrac{d\Phi}{d\sigma_N}\right\} = \left([D] - \beta\sigma_N[c]\right)^{-1}\left(\beta[c]\{\Phi\} + [c]\{e^*\} - \left\{\dfrac{\partial\mu}{\partial\sigma_N}\right\}\right)$

with:

$$d_{ik} = \begin{cases} 0 & \text{for} \quad i \neq k \\ \dfrac{\partial\mu_i}{\partial\Phi_i} & \text{for} \quad i = k \end{cases}$$

Starting from the configuration A corresponding to $\sigma_N$ the solution is obtained by using the iterative formula:

$$\left\{\Phi_B^{(n+1)}\right\} = \{\Phi_A\} + \frac{1}{2}\Delta\sigma_N\left(\left\{\frac{d\Phi_A}{d\sigma_N}\right\} + \left\{\frac{d\Phi_B^{(n)}}{d\sigma_N}\right\}\right) .$$

The integration step is automatically regulated and becomes smaller and smaller as the number of iterations needed for the required accuracy increases. When the step becomes very small or the derivative (3) is very great the loading process stops. At this point constant axial load is assumed, the relative rotation at the middle is increased and the second equilibrium configuration is found by iteration. After which the integration method is taken up again, making $\Delta \sigma_N < 0$ in formula (3) of the derivatives $\{ \partial \mu / \partial \sigma_N \}$.
If overall unloading is required, $\Delta \phi_i$ must also be negative in formula (3) of the derivatives as well as $\Delta \sigma_N$.

Of course the function $\mu = \mu(\phi, \sigma_N)$ must be calculated at each attempt. This is done by iteration, starting from the characteristics of the cross section. For this purpose in order to speed up the process for ideally elastic-plastic material, the neutral axis can be obtained by a method which take into account the variation of the boundary of the plastic region of the cross section.

## 6. References

F. BLEICH: "Buckling Strength of Metal Structures" Mc. Graw-Hill, New York 1952.
B.G. JOHNSTON: "Design Criteria for Metal Compression Members" John Willey & Sons Inc., New York 1966, pp.76-83.
F. ENGESSER: "Zum Einsturz der Brucke uber den St. Lorenz strom bei Quebeck" Zentralblatt der Bauverwaltung, 27, p. 609, 1907.
E. EMPERGER:"Welchen Querverband bedarf eine Eisensäule?" Beton und Eisen, pp.71,1908.
MULLER-BRESLAU:"Scienza delle Costruzioni",Vol.IV, Hoepli Milano, 1927.
R. KROHN:"Beitrag zur Untersuchung der Knickstigkeit gegliederter Stabe "Zentralblatt der Bauverwaltung, 1908.
E. CHWALLA:"Genaue Theorie der Knickung von Rahmenstaben", HDI Mitt. 1933.
F. JOKISCH:"Zur ebenen Stabilitätstheorie des zweifeldrigen Stokwerkrahmens und des dreiteiligen Druckstabes" Dissertation Technische Hochschule Brunn, 1940.
P. BIJLARD:"Some contributions to the theory of elastic and plastic stability " A.I.P.C. 1943.
L. SANPAOLESI: "Sulla stabilità d'insieme delle aste composte compresse",Atti dell'Istituto di Scienza delle Costruzioni dell'Università di Pisa 1962.
L.T. WYLY:"Brief Review of Steel Column Tests", J. Western Soc. Eng. Vol.45 n.3 (June 1940) p.99.

L. SELTENHAMMER:"Die stabilität des in parallelen Schnei-
den gelagerten und zentrisch gedrückten Rahmenstabes "Si-
tzungsberichte der Akademie der Wissenschaften in Wien,
1933.
R. DELESQUES:"Solidarisation des cornierès jumelées et
des cornières en croix",Construction Métallique, n.2,
1965.
G. BALLIO,L. FINZI, C.URBANO:"Indagine sperimentale sulla
stabilità delle colonne composte con elementi ravvicinati",
Costruzioni Metalliche n.4,1972.
R.L. KETTER,E.L. KAMINSKY and L.S. BEEDLE:"Plastic Defor-
mation of Wide-Flange Beam Columns", Trans.Am.Soc. Civil
Engrs, 120, p.1028 (1955).
R.L. KETTER:"Stability of Beam-Columns Above the Elastic
Limit",Proc.Am.Soc. Civil Engrs, 81 Separate N.692 (May
1955).
R.L. KETTER and T.V. GALAMBOS:"Columns under Combined Ben
ding and Thrust",Trans.Am.Soc. Civil Engrs 126(I)p.1.1961.

R.L. KETTER:"Further Studies on the Strength of Beam-Co-
lumns",Proc.Am.Soc. Civil Engrs, 87 (ST-6) p.135(August
1961).
S. VINNAKOTA - J.C. BADOUX:"Flambage élastoplastique des
poutrescoonnes appuyées sur des ressorts",Construction Mé
tallique n°2 - Juin 1970.
M. OJALVO:"Restrained Columns",Proc.Am.Soc.Civil Engrs.86
(EM-5) p.1 (October 1960).
O. DE DONATO:"Legami forze elongazioni per aste elasto-pla-
stiche compresse ad elongazione crescente",Rendiconti del-
l'Istituto Lombardo Scienze e Lettere (A) Vol.100-1966.
R.H. BATTERMAN, B.G. JOHNSTON:"Behavior and Maximum Stren-
gth of metal columns",Proc. ASCE Vol.93 ST2, pag.205,1967.
F. FREY: "Calcul de flamblement des barres industrielles",
Bulletin Tecnique de la Suisse Romande n°11 Mai 1971.
N. TEBEDGE, P. MAREK, L. TALL:"Méthodes d'essai de flam-
blement des Barres à forte section",Construction Métalli-
que n°4, 1971.
H. BEER et G. SCHULZ:"Die Traglast des plannasig mitting
gedruckten Stabs mit imperfektionen (Charge d'affaissement
théorique des barres avec imperfections, soumises à une com
pression centrée)", Revue VDI-Zeitschrift, vol.III, n°21,23
and 24 (1969) .
G. BALLIO, V. PETRINI,C. URBANO:"Simulazione numerica del
comportamento di elementi strutturali compressi per incre-
menti finiti del carico assiale",Costruzioni Metalliche N°2
1973.

# ULTIMATE STRENGTH OF WIDE FLANGE AND BOX COLUMNS

Fumio Nishino
Associate Professor of Structural Engineering
Asian Institute of Technology, Bangkok, Thailand
On Leave from University of Tokyo, Tokyo, Japan

Tokul Kanchanalai
Engineer
Department of Highways, Bangkok, Thailand

Seng-Lip Lee
Professor and Chairman
Division of Structural Engineering and Mechanics
Asian Institute of Technology, Bangkok, Thailand

## ABSTRACT

The purpose of this study is to investigate the ultimate strength of elastic-plastic steel wide-flange columns subjected to axial load and symmetrical end moments. The presence of residual stresses arising from fabrication processes leads to moment-thrust-curvature relationships which are untractable analytically. The latter is determined numerically. The integration procedure employs a numerical marching technique. The results are presented in the form of critical load-slenderness ratio relationship obtained for welding-type and cooling-type (parabolic) patterns of residual stress distribution. The effects of initial curvature on the strength of the columns are also compared with that of straight columns.

254

# 1. INTRODUCTION

The strength of steel columns is influenced by such unavoidable factors as residual stresses, initial imperfection and eccentricity of loading. Residual stresses are present as the result of uneven cooling after the hot rolling for rolled sections or of welding for built-up sections.

The strength of columns was studied earlier by Karman (10), Chawalla (5), Jezek (9), Shanley (16) and many other investigators. More recently Horne (8) presented a criterion of stability for columns which was utilized later by other investigators (7,11,15) to treat wide flange and box columns with initial imperfection but free of residual stresses. Chen and Santathadaporn (4) studied the strength of eccentrically loaded rectangular columns, formulating the governing equation in term of curvature rather than deflection. The influence of residual stresses on the buckling strength of concentrically loaded steel columns was discussed by Osgood (14) and Beedle and Tall (2). The combined effect of residual stresses and initial imperfection on the strength of concentrically loaded aluminum alloy and steel columns was studied by Batterman and Johnston (1) who employed a numerical incremental scheme to obtain the complete load deflection curves. Recently, Sherman (17) studied the strength of eccentrically loaded straight steel box column with linearly varying residual stresses across the width of the component plates. The latter also made use of Horne's criterion of stability. The reduction of strength due to the presence of residual stresses was found to be as high as 40%. Chen (3) studied the strength of beam-columns using the moment-thrust-curvature relationships of wide flange sections with linearly varying residual stresses.

The purpose of this study is to investigate the influence, on the strength of wide flange and box columns, of the eccentricity of end loading, the initial crookedness and residual stresses arising from the cooling of hot rolled wide flange sections and from the welding of built-up sections. These residual stress patterns as reported in Refs. (2,12) can be idealized more closely by the distributions shown in Fig. 1, where the welding pattern consisting of a series of straight lines represents that encountered in welded built-up shapes while the pattern with parabolic curves represents that in hot-rolled wide flange shapes. The ultimate strength is determined by numerically integrating the governing differential equation and applying Horne's criterion of stability. The moment-thrust-curvature relationships are also determined numerically for the two residual stress patterns considered. Only columns which fail by bending about the strong axis will be considered. It is of interest to mention that the results of this analysis for the special case of the concentrically loaded perfectly straight columns lie in between the values predicted by the tangent modulus theory and the reduced modulus theory.

## 2. MOMENT-THRUST-CURVATURE RELATIONSHIPS

In order to compute the moment-thrust-curvature relationships numerically, a wide flange section is divided into finite grid elements. The coordinate system is chosen to pass through the centroid of the section. Under the action of bending moment and axial thrust, the strain at element i with residual stress can be expressed in the nondimensional form,

$$\frac{e_i}{e_y} = \frac{e_o}{e_y} + \varphi\frac{Y_i}{d} + \frac{e_{ri}}{e_y} \tag{1}$$

where $\epsilon_i$ = total strain at element i, positive for tensile strain; $\epsilon_0$ = strain at the centroid of the section; $\varphi$ = curvature nondimensionalized by the curvature at initial yielding for pure bending moment, $\Phi_y = \epsilon_y/d$; $Y_i$ = distance of the center of element i from the centroidal axis; $\epsilon_{ri}$ = residual strain at element i; $\epsilon_y$ = strain at yield point; and d = half depth of the section.

Assuming an elastic-perfectly plastic stress-strain relationship for the steel, the strain in Eq. 1 is related to the stress by

$$\frac{\sigma_i}{\sigma_y} = \frac{\epsilon_i}{\epsilon_y} \quad \text{for} \quad \left|\frac{\epsilon_i}{\epsilon_y}\right| < 1 \tag{2a}$$

$$\frac{\sigma_i}{\sigma_y} = \pm 1 \quad \text{for} \quad \left|\frac{\epsilon_i}{\epsilon_y}\right| \geq 1 \tag{2b}$$

in which $\sigma_i$ and $\sigma_y$ = normal stress at element i and the yield stress respectively, $\sigma_i$ being positive for tensile stress.

The axial thrust and moment are then determined from the following two equilibrium equations in nondimensionalized form,

$$p = -\frac{1}{A} \sum_{i=1}^{n} \frac{\sigma_i}{\sigma_y} \Delta A_i \tag{3}$$

$$m = \frac{1}{Z} \sum_{i=1}^{n} \frac{\sigma_i}{\sigma_y} Y_i \Delta A_i \tag{4}$$

where p and m = axial thrust and moment nondimensionalized by the yield load, $P_y = \sigma_y A$, and the fully plastic moment, $M_P = \sigma_y Z$, of the section respectively; A and Z = area and plastic modulus of the section respectively; $\Delta A_i$ = area of element i; and n = total number of elements.

The moment-thrust-curvature relationships are obtained from Eqs. 3 and 4, together with Eqs. 1 and 2, by specifying the residual stress distribution, hence the residual strain distribution, and systematically varying $\epsilon_0$ and $\varphi$. For simplicity, it is assumed that the residual stress is constant across the thickness and that equilibrium is maintained within each plate component. Typical curves showing moment-thrust-curvature relationships for different patterns and levels of residual stresses are shown in Fig. 2 for 8 WF 31. The moment-thrust-curvature relationships for a wide flange section is identical with those obtained for a box section provided that the cross sectional shapes of the halves of the wide flange and the box section as well as the residual stress pattern and level are identical.

3. GOVERNING EQUATIONS

The problem of simply supported columns loaded symmetrically at both ends can be represented as a cantilever column loaded as shown in Fig. 3. The free end is subjected to bending moment M and axial thrust P. Initial imperfection can be characterized by initial curvature along the length of the column. The equilibrium of moment and the curvature-displacement relationships, in terms of small deflection theory, are given by

$$M = M_f - PV \tag{5}$$

$$\frac{d^2V}{dX^2} = \Phi + \Phi_0 \tag{6}$$

where M = moment; $M_f$ = fixed end moment; X = distance along the length of column; V = transverse deflection; and $\Phi$ and $\Phi_o$ = bending and initial curvatures, respectively.

Introducing x and v as the nondimensionalized axial distance and transverse deflection defined by

$$x = \frac{X}{r}\sqrt{\epsilon_y} \tag{7a}$$

$$v = \frac{V}{r} \tag{7b}$$

where r = radius of gyration of the cross section, Eqs. 5 and 6 can be written in the nondimensionalized form,

$$m = m_f - \frac{Ar}{z}\,pv \tag{8}$$

$$\frac{d^2v}{dx^2} = (\varphi + \varphi_o)\frac{r}{d} \tag{9}$$

in which $m_f$ = fixed end moment nondimensionalized by the fully plastic moment of the section; $\varphi_o$ = initial curvature nondimensionalized by $\Phi_y$.

With prescribed values of $\varphi_o$, for given values of $m_f$ and p as parameters, the deflected shape of a column can be determined by integrating Eq. 9 in view of Eq. 8 and the moment-thrust-curvature relationship for a particular cross section and residual stress pattern and level. It is noted that, with this formulation, the strength of the steel is not involved and that the results can be applied to columns made of any grade of steel.

4. EQUILIBRIUM CURVES AND ENVELOPE

The integration of Eq. 9 for the general case is analytically untractable and numerical integration is necessary. The procedure is basically as follows:

(1) For a particular value of p, moment m can be determined from Eq. 8, provided displacement v is known. Knowing m, curvature $\varphi$ is determined from Eqs. 3 and 4 in view of Eqs. 1 and 2. From the value of $\varphi$ so obtained, together with the prescribed initial curvature, the right hand side of Eq. 9 is calculated.

(2) Dividing the column into small segments, such that curvature inside each segment may be assumed to be constant, Eq. 9 can be integrated with respect to x within the segment to yield the following relationships among the slope and displacement at both ends of the segment:

$$v'_{i+1} = k_i(\Delta x) + v'_i \tag{10}$$

$$v_{i+1} = \frac{k_i}{2}(\Delta x)^2 + v'_i(\Delta x) + v_i \tag{11}$$

where $k_i$ = quantity on the right hand side of Eq. 9 at segment i; $v_i$ and $v'_i$ = deflection and slope at the left end of segment i; $v_{i+1}$ and $v'_{i+1}$ = deflection and slope at the right end; and $\Delta x$ = length of the segment.

(3) For a specified value of $m_f$, the integration can be started from the fixed end where v and v' are known to be zero until m vanishes.

(4) Repeat the procedure by systematically changing p and $m_f$. In practical computation, the moment-curvature relationship for a particular value of p and pattern and level of residual stress such as shown in Fig. 2 was represented by a series of points and stored in the computer. The curvature corresponding to a particular value of moment was then obtained by interpolating between the points.

The m versus x relationships referred to as the equilibrium curves (7), for particular values of p and $m_f$, can be plotted as shown in Fig. 4. Applying Horne's criterion (8), the envelope of these curves is the boundary of the domain inside which a cantilever column with a combination of end moment, length and thrust is in stable equilibrium. It shows the relationships between the slenderness ratio and the maximum end moment that the column can carry for a given thrust. Fig. 5a illustrates a set of envelopes obtained for various values of p. They are plotted on the m - λ plane in which λ is the normalized slenderness ratio defined by

$$\lambda = \frac{1}{\pi} \frac{L}{r} \sqrt{\epsilon_y} \tag{12}$$

where L = length of simply supported columns, being twice the length X of the corresponding cantilever columns. It should be noted that the integration scheme requires no iteration and is always stable resulting in accurate predictions of the ultimate strength.

For the purpose of discussions, it is convenient to replot the results of the foregoing analysis as shown in Figs. 5b and 5c where the construction of the column curves relating the maximum load to the normalized slenderness ratio and the interaction curves relating the end moment and axial thrust are depicted respectively.

5. NUMERICAL RESULTS AND DISCUSSIONS

Parameters for Numerical Computation

It was reported by Hauck and Lee (7) that, for the study of the strength of wide flange columns, the area ratio, i.e., the ratio of the flange area to the web area, is the most appropriate parameter for describing the sectional properties. The reason for this lies in the fact that, in the non-dimensionalized formulation of the problem, the equilibrium equation and the curvature displacement relationship, Eqs. 8 and 9, involve the parameters Ar/Z and r/d respectively which are primarily functions of the area ratio. For idealized wide flange sections with thin flanges, these two parameters are given in terms of the area ratio by

$$\frac{Ar}{Z} = \frac{\sqrt{(1+R)(\frac{1}{3}+R)}}{\frac{1}{2}+R} \tag{13}$$

$$\frac{r}{d} = \sqrt{\frac{\frac{1}{3}+R}{1+R}} \tag{14}$$

in which $R = A_f/A_w$, $A_f$ being the total flange area and $A_w$ the web area. The moment-thrust-curvature relationship is also primarily a function of the area ratio.

258

The area ratios of all wide flange column sections lie between 2.9 to 3.6, and the ultimate strength analysis is insensitive to the variation of the area ratio. The numerical computations of this study are made for 8 WF 31 of which the area ratio is 3.27.

The magnitudes of the maximum compressive residual stress are varied from 0.1 $\sigma_y$ to 0.5 $\sigma_y$ for both the welding pattern of Fig. 1a and the cooling pattern of Fig. 1b. When initial imperfection is present, the initial shape of the column is assumed to be an arc of a circle in which the initial curvature is constant throughout the length. The degree of initial curvature is included by varying the factor $\varphi_0$ in Eq. 9 in the range 0 to 0.4 for both patterns of residual stresses. The numerical results are presented in Figs. 6 to 12.

In addition to 8 WF 31, two sections which are approximately on the extreme limits of the range of the area ratio for column sections are studied; they are 8 WF 24 and 14 WF 127 whose area ratios are 2.88 and 3.40 respectively. The results, when plotted on the column curves or on the interaction curves, are almost identical to those for 8 WF 31. Therefore the results of this study on 8 WF 31 can be applied for all wide flange columns as well as box columns of similar dimensions.

## Effect of Residual Stresses on Column Curves

Figs. 6 and 7 show the strength of straight columns with residual stresses of the welding and cooling patterns respectively. It can be seen from Fig. 6 that the reduction of column strength is greatest for concentrically loaded columns. Generally speaking, the larger the maximum compressive residual stress, the larger is the reduction in strength. However, in columns with very small eccentricity, higher maximum compressive residual stress results in smaller reduction in strength for the lower range of the slenderness ratio. This can be explained in terms of the penetration of yielding. In the case of low maximum compressive residual stress, when yielding starts, the stiffness decreases faster than the case with high maximum compressive residual stress. It is also noted that the strengths of concentrically loaded columns are constant over a larger range of $\lambda$ for lower maximum compressive residual stresses.

For eccentrically loaded columns, the effect of residual stresses tends to decrease with increasing eccentricity. The presence of residual stresses reduces the strength appreciably for columns of medium length loaded with the same eccentricity, the reductions being smaller for the short and long columns.

Proceeding from Fig. 6 to Fig. 7, the reduction of strength is less severe for the case of cooling type residual stresses. The strength of concentrically loaded columns for the same $\lambda$ is much higher for the latter than that for the welding type with the same maximum compressive residual stress level. The effect of residual stresses diminishes with increasing eccentricity more rapidly for the case of welding type residual stresses.

The different effect of the two residual stress patterns on column strength, together with the fact that the magnitude of compressive residual stresses present in welded sections is larger than those in hot rolled shapes (2,11), suggests that different consideration may be necessary in the design of welded built-up columns and hot rolled wide flange columns.

## Effect of Initial Imperfection

The effect of initial curvature alone and the combined effect of residual stresses and initial curvature for both types of residual stresses can be seen in Figs. 8, 9 and 10. Initial curvature generally decreases the strength of otherwise straight columns. The effect of initial curvature is greatest in the intermediate column range. The same conclusion was reported by Batterman and Johnston (1). Comparing with Figs. 6 and 7, the reduction in strength due to initial curvature covers a wider range of $\lambda$ than that due to residual stresses alone. The behaviour of eccentrically loaded columns with the presence of initial curvature alone or in combination with residual stresses show the same trends. The effect of the difference in residual stress patterns on column strength tends to be diminished by the presence of initial curvature.

## Effect of Residual Stresses on Interaction Curves

The interaction curves shown in Fig. 11 may be more convenient for presenting the ultimate strength of beam-columns. The effect of different patterns and levels of residual stresses is shown in this figure. The parameter $\lambda$ covers the range $0 \leq \lambda \leq 1.5$. It can be seen that the reduction of strength is significant for high p and the effect tends to diminish with increasing $\lambda$. Finally, the cooling type exhibits less effect than the welding type of residual stresses.

## Buckling and Ultimate Strengths

It is well understood that the tangent modulus load is the smallest axial load at which bifurcation of the equilibrium position for a concentrically loaded straight column can occur and that the reduced modulus load is the upper bound of the bifurcation load (6). Fig. 12 shows a comparison between the ultimate strengths of initially straight columns obtained in this study and the buckling loads of concentrically loaded straight columns with welding type residual stresses (13). The effect of maximum compressive residual stresses of 0.2 $\sigma_y$ and 0.4 $\sigma_y$ is shown. For each residual stress level, the ultimate strength curve lies between the two buckling curves, being close to the tangent modulus curve at high p and tend to approach the reduced modulus curve as the load decreases.

## 6.   CONCLUSIONS

The present study supplements the investigation of the influence of residual stresses, initial imperfection and eccentricity of loading on the ultimate strength of steel columns. Two types of residual stress patterns are chosen with varying magnitudes to represent the residual stress distribution present in hot rolled wide flange and welded built-up I and box columns.

It was found that eccentricity, initial imperfection and residual stresses are adverse factors which reduce the strength of columns. For low eccentricity, the reduction of column strength due to initial imperfection and residual stresses is more pronounced in the intermediate column range. However, the reduction diminishes as the eccentricity increases. It was also found that residual stresses and initial curvature exhibit similar trends in the reduction of the strength of practical columns.

The welding type residual stress causes more pronounced reduction in , strength than the cooling type for the same level of maximum compressive residual stress. This fact suggests that different considerations should be given to the design of welded built-up sections and hot rolled wide flange columns.

# APPENDIX I.- REFERENCES

1. Batterman, R.H., and Johnston, B.G., "Behaviour and Maximum Strength of Metal Columns," Journal of the Structural Division, ASCE, Vol. 93, No. ST2, Proceeding Paper 5190, April 1967, pp. 205-230.

2. Beedle, L.S., and Tall, L., "Basic Column Strength," Trans. ASCE, Vol. 127, Part II, 1962, pp. 138-179.

3. Chen, W.F., "Further Studies on Inelastic Beam-Column Problems," Journal of Structural Division, ASCE, Vol. 97, No. ST2, Proceeding Paper 7922, February 1969, pp. 529-544.

4. Chen, W.F. and Santathadaporn, S., "Curvature and the Solution of Eccentrically Loaded Columns," Journal of the Engineering Mechanics Division, ASCE, Vol. 95, No. EM1, Proceeding Paper 6382, February 1969, pp. 21-39.

5. Chwalla, E., "Die Stabilitat zentrisch und exzentrisch gedruckter Stabe aus Baustahl," Sitzungsber. Akad. Wiss. Wien, Abt. IIa, 1928, p. 469.

6. Column Research Council, "Guide to Design Criteria for Metal Compression Members," 2nd ed., B.G. Johnston, ed., John Wiley and Sons, Inc., New York, N.Y., 1967, Chapter 2.

7. Hauck, G.F., and Lee, S.L., "Stability of Elasto-Plastic Wide-Flange Columns," Journal of the Structural Division, ASCE, Vol. 89, No. ST6, Proceeding Paper 3738, December 1963, pp. 297-324.

8. Horne, M.R. "The Elastic-Plastic Theory of Compression Members," Journal of Mechanics and Physics of Solids, Vol. 4, 1956, p. 104.

9. Jezek, K., "Die Tragfahigkeit des Gleichmassig Querbelasteten Druckstabes aus Einem Edeal-Plastischen Stahl," Stahlbau, Vol. 8, 1935, p. 33.

10. Von Karman, T., "Die Knickfestigkeit Gerader Stabe," Phys. Zeitschr, Vol. 9, 1908, p. 136.

11. Lee, S.L., and Hauck, G.F., "Buckling of Steel Columns Under Arbitrary End Loads," Journal of the Structural Division, ASCE, Vol. 90, No. ST2, Proceeding Paper 3782, April 1964, pp. 179-200.

12. Nagaraja Rao, N.R., Estuar, F.R., and Tall, L., "Residual Stresses in Welded Shapes," The Welding Journal, July 1964, pp. 295-306.

13. Nishino, F., and Tall, L., "Numerical Method for Computing Column Curves," Fritz Engineering Laboratory Report No. 290.6, Lehigh University, Bethlehem, Penna., December 1966.

14. Osgood, W.R., "The Effect of Residual Stress on Column Strength," Proceeding of First U.S. National Congress for Applied Mechanics, 1951, p. 415.

15. Rossow, E.C., Barney, G.B., and Lee, S.L., "Eccentrically Loaded Steel Columns with Initial Curvatures," Journal of the Structural Division, ASCE, Vol. 93, No. ST2, Proceeding Paper 5204, April 1967, pp. 339-358.

16. Shanley, F.R., "Inelastic Column Theory," Journal of Aeronautical Science, Vol. 14, No. 5, May 1947, p. 261.

17. Sherman, D., "Residual Stresses and Tubular Compression Members," Journal of the Structural Division, ASCE, Vol. 97, No. ST3, Proceeding Paper 8001, March 1971, pp. 891-905.

The following symbols are used in this paper:

$A$ = area of section;

$A_f, A_w$ = total flange and web areas, respectively;

$d$ = half depth of section;

$E$ = Young's modulus of elasticity;

$i$ = index number;

$k$ = quantity on the right hand side of Eq. 9;

$L$ = length of simply supported column;

$M$ = bending moment;

$M_f$ = fixed-end moment;

$M_p$ = plastic moment;

$m$ = $M/M_p$;

$m_f$ = $M_f/M_p$;

$n$ = total number of area elements;

$P$ = thrust;

$P_y$ = axial yield load;

$p$ = $P/P_y$;

$R$ = area ratio, $A_f/A_w$;

$r$ = radius of gyration;

$V$ = transverse deflection;

$v, v'$ = $V/r$ and $V'/r$, respectively;

$X$ = distance along the length of cantilever column;

$x$ = $\dfrac{X}{r}\sqrt{\epsilon_y}$ ;

$Y$ = vertical coordinate of cross section;

$Z$ = plastic section modulus;

$\Delta A$ = area of sectional element;

$\Delta x$ = length of segment;

$\epsilon$ = total normal strain;

$\epsilon_o$ = strain at the centroid of section;

$\epsilon_r$ = residual strain;

$\epsilon_y$ = strain at yield point;

$\sigma$ = normal stress;

$\sigma_u$ = ultimate strength of columns;

$\sigma_y$ = yield stress;

$\lambda$ = $\dfrac{1}{\pi}\dfrac{L}{r}\sqrt{\epsilon_y}$ ;

$\Phi$ = curvature caused by bending;

$\Phi_o$ = initial curvature;

$\Phi_y$ = curvature at initial yielding for pure bending moment;

$\varphi$ = $\Phi/\Phi_y$; and

$\varphi_o$ = $\Phi_o/\Phi_y$.

+ Tension
− Compression

(a) Welding Pattern      (b) Parabolic Pattern
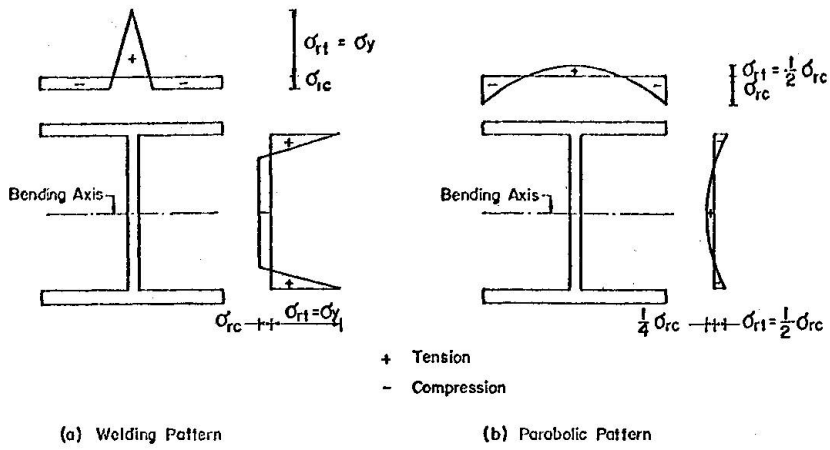
FIG. 1. - IDEALIZED RESIDUAL STRESS PATTERNS



FIG. 3. - CANTILEVER COLUMN
WITH INITIAL IMPERFECTION



FIG. 2. - TYPICAL MOMENT-THRUST-CURVATURE
RELATIONSHIPS
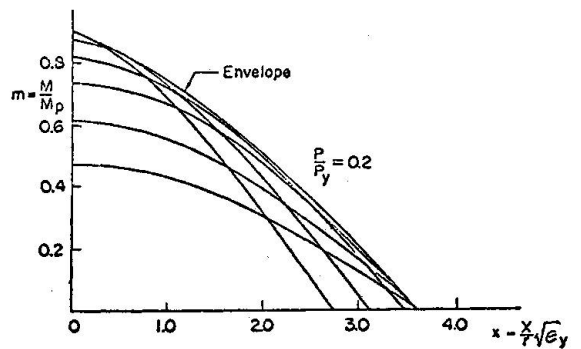


FIG. 4. - EQUILIBRIUM CURVES
AND ENVELOPE
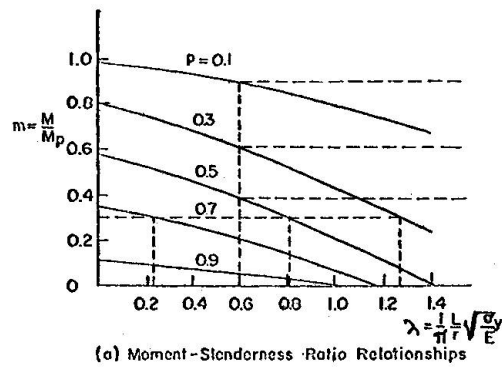


(a) Moment-Slenderness Ratio Relationships

FIG. 5. - CONSTRUCTION OF COLUMN
AND INTERACTION CURVES
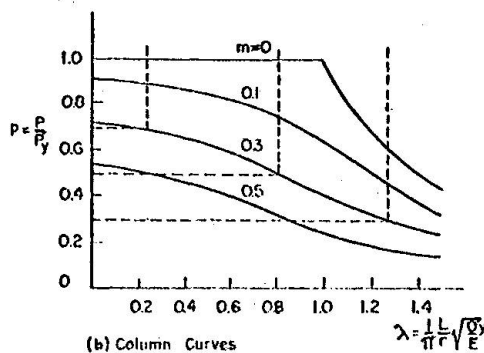
(b) Column Curves

(c) Interaction Curves

263

FIG. 6. - INFLUENCE OF WELDING TYPE RESIDUAL STRESSES



FIG. 7. - INFLUENCE OF COOLING TYPE RESIDUAL STRESSES
ON COLUMN CURVES



FIG. 8. - INFLUENCE OF INITIAL IMPERFECTION
ON COLUMN CURVES
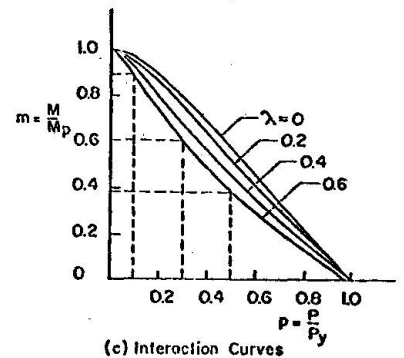


FIG. 9. - INFLUENCE OF INITIAL IMPERFECTION AND
WELDING TYPE RESIDUAL STRESSES ON COLUMN CURVES
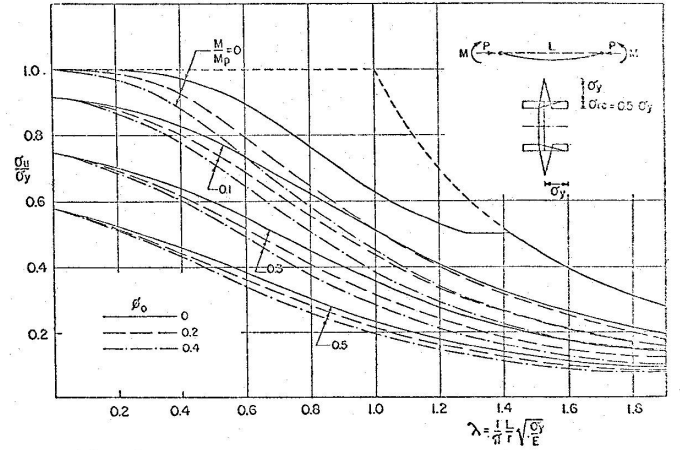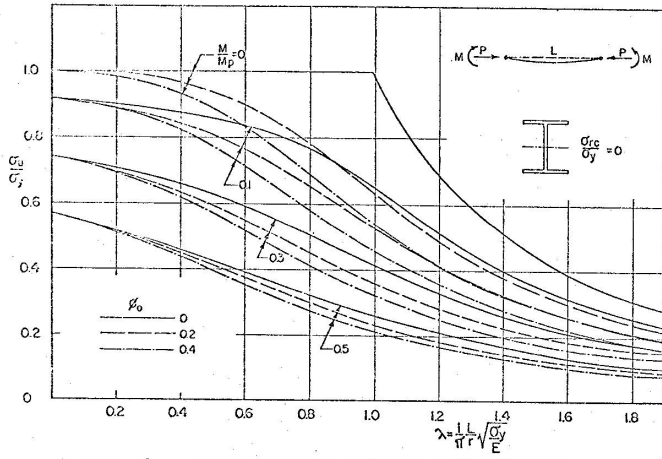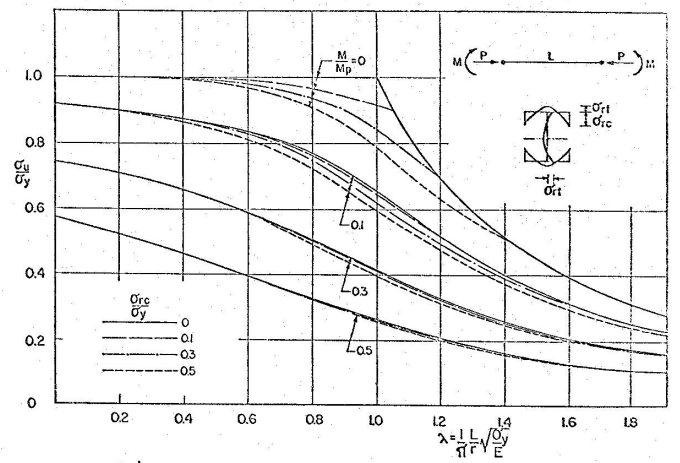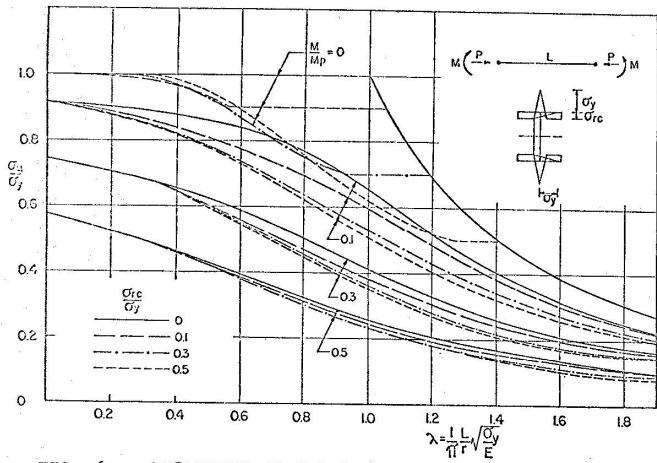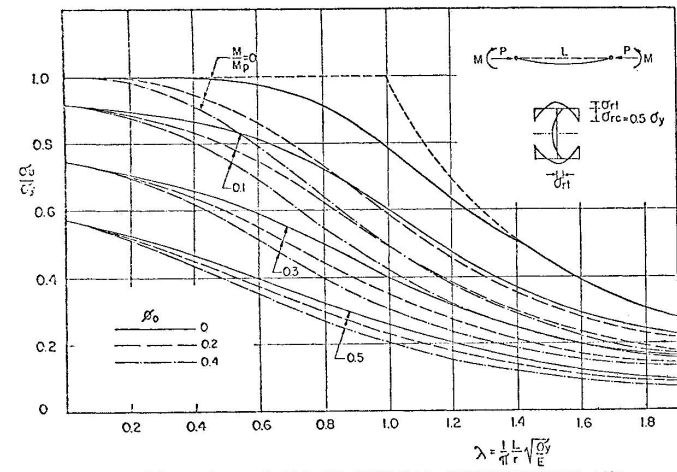
FIG. 10. – INFLUENCE OF INITIAL IMPERFECTION AND
COOLING TYPE RESIDUAL STRESSES ON COLUMN CURVES
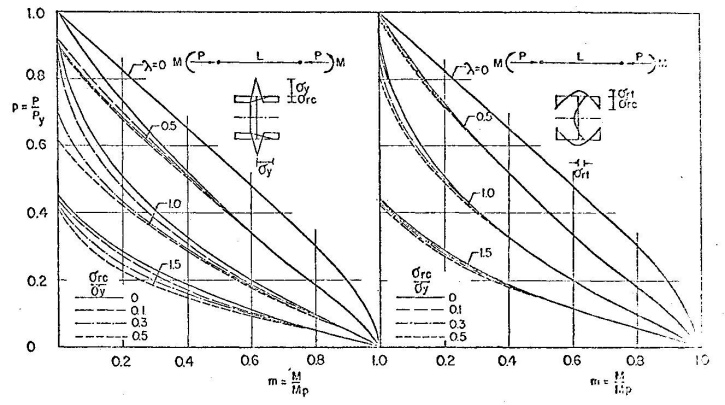
FIG. 11. – INFLUENCE OF RESIDUAL STRESSES ON INTERACTION CURVES
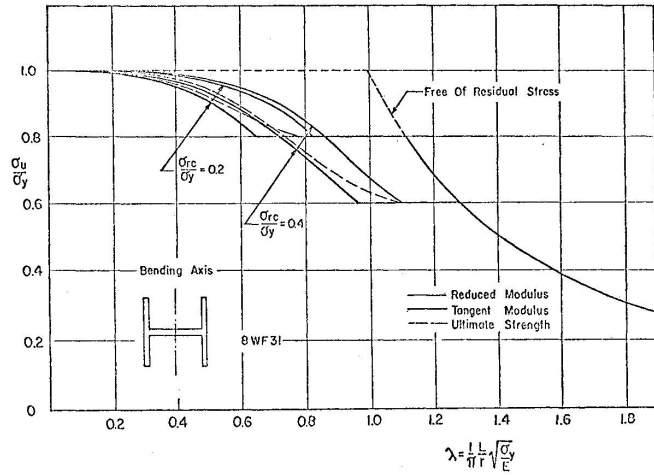


FIG. 12. – COMPARISON OF BUCKLING AND ULTIMATE STRENGTHS

# SOME REMARKS REGARDING BUCKLING CURVES

Miloš Marinček
Professor of Civil Engineering
University of Ljubljana
Yugoslavia

## ABSTRACT

Remarks are given in connection with the buckling resp.instability design curves for pin-ended struts relating the effective stiffness of the cross-section with the influence of residual stresses and of unavoidable geometrical imperfections.

Correlation between buckling and instability design curves is shown. Instability and buckling curves for the struts made of material with Ramberg-Osgood stress-strain diagrams are discussed and the problem of composite struts and of the calculation of load-carrying sistems are mentioned. The need for the typification of the shapes of the stress-strain diagrams for different materials, shapes of the cross-section and the distribution of residual stresses is emphasized.

## INTRODUCTION

Under the guidance of the late Professor Beer there have been determined in Graz, on the basis of extensive analyses, three European curves. Some changes have been done lately for the region of very small slendernesses according to the suggestion of the team from Cambridge. This one parallelly made the British version of curves. Regarding the buckling curves of Graz there is an important addition for the simple consideration of dead and/or wind load of very slender struts. Graz has one more additional proposition, for one higher lying curve for high-strength steel, and lower lying for "jumbo" profiles. Dwight suggests in his present report an interesting simplification of the presentation of curves. Also in the USA an extensive study of multiple curves is going on, both deterministic and probabilistic, as Bjorhovde and Tall will report. We might expect on this colloquium also other important reports regarding strut curves and, of course, possible different views.

In the invitation for this colloquium Professor Beer expressed a very justified wish that there would be reached an unified view about the buckling curves. This would be very important not only for the treatment of pin-ended struts, but especially for struts in a system and so for the determination of the buckling and the instability limit state of the load-carrying system as a whole. It might come very soon to an agreement about the basic curves for compression members made of steel, because an extensive research work has been already done in this field. Or it might not come so soon. There should also be done much more about the composite sections ( steel – concrete ) and regarding struts made of alluminium alloys the finite propositions are still expected. That is why it would be extremely useful to come, at least, to an agreement about the basic assumptions.

In the following some remarks, which should contribute to a better further progress, are given.

## FLEXURAL STIFFNESS, IMPERFECTIONS

For numerical simulation computer programs, which have the decisive part in research of compression instability, the data about the effective flexural stiffness of cross-sections due to the influence of nonelasticity are very important. The effective flexural stiffness depends on the shape of the cross-section, on the shape

of stress-strain diagram of the material, on its cross-section nonhomogenity, and on residual stresses. It would be necessary to make a corresponding selection of the typical cross-sections regarding their geometrical shape and the distribution of residual stresses, taking into account different possible technologies of production ( I-profiles, box sections, tubes, other sections ).

While typifying the sections, only the ratios of dimensions are important. Fig. 1 shows both extreme profiles and a kind of the average section for narrow and wide flange European I-profiles.

The typification of curved stress-strain diagrams ( i.e. of the alluminium alloys ) is possibile when using one single parameter with the dimensionless form of the Osggod- Ramberg's equation, if we omit the classical definition of the yield stress $\sigma_{0,2}$. We replace it with, for example $\sigma_2^0$ , which represents the stress when the plastic strains are equal to the elastic ones ( Fig. 2 ). Fig. 3 shows a choice of the dimensionless curves, the shapes of which are given with only one parameter n. It should not be a problem nowadays to introduce the registration of all necessary parameters, which determine the basic mechanical behaviour of material, into the routine testing. For mild steel also the strain and the tangent modulus at the beginning of strain hardenin should be included. In the stress-strain diagram for concrete we'd better decide, if possible, for only one curve out of different propositions according to Fig. 4. This is important for the treatment of the composite cross-sections.

The determination of typical dimensionless distribution of residual stresses for typical sections would especially help in quicker application of research made till now about the load-carrying capacity of industrially produced compression members. Here team work with metallurgists would be useful. The important thing is, first, to determine the normal technology and then the various possibilities in the technology, and not before this to determine the corresponding distribution of residual stresses. Such a way is, of course, more reliable than that with incidentally taken specimens. The question what should be taken for typical residual stresses, those out of normal technology or those out of irregular processing, but the most unfavourable, is of special consideration.

The use of the load-shortening diagrams obtained by stub column test, will be well exploited, when we analyse them in comparison with computed diagrams at

the consideration of the influence of residual stresses and nonhomogenity. The agreement with computed diagrams should exist also in full tension tests and in tension tests of single strips. For the consideration of the separate influence of nonhomogenity in the strength of the section also the parallel tests in stress-relieved state are useful.

Geometrical imperfections of compression members can be more easily controlled than structural imperfections. Here we have a possibility of variations from the ideal perfect strut regarding the sections and length to those imperfections, which are not permitted according to the definitions of standards of tolerances of measures and shapes.

## BUCKLING AND INSTABILITY CURVES

The possibility that in compression members the most inconvenient structural and geometrical imperfections will appear simultaneously, is of course small. But from the viewpoint of safety we need such curves of instability, which represent the minimum guaranteed instability limit load with the consideration of the most inconvenient state of structural imperfections and the most inconvenient, but still permitted, geometrical imperfections. At the same time, with the help of the appropriate buckling curves ( without geometrical imperfections ), also the determination of the buckling load of compressed members is possible ( with consideration of normal structural imperfections ). In such a way we can have always the survey about the region of the possible actual state ( Fig. 5 ). I do not know if in the present situation there is necessary to think much more about the probability of the appearance of different intermediate possibilities. But it would be very useful to gather sistematically the statistical data about the possible geometrical imperfections of the struts in the systems, where the question of the probability of the simultaneous appearance of the most unfavourable geometrical imperfections is more important.

Previous buckling curves in inelastic region, which at the higher slendernesses pass on to the Euler's curve and are connected with a variable coeficient of safety, are, in fact, principally identical with new instability curves, which take into account the initial crookedness of struts and the constant factor of

safety. The variable coeficient of safety at the buckling curve somehow includes the influence of the initial crookedness. The relations are shown in Fig. 6. In Fig.7 there are shown the present buckling rules for compression members in the USA and West Germany, translated in the instability curves with the constant factor of safety.

There is always and advantage to have a dimensionless presentation of the buckling and instability curves.

To determine the buckling load of the linear systems, we need effective flexural stiffness of the cross-sections ( or the effective modulus of elasticity ), dependent on the axial force in the individual struts. The corresponding relations are given in Fig.8.

We can rely on the fact that in the course of time it will be necessary to have still more dimensionless buckling and instability curves, even interlacing ones. This is to be expected because of the different shapes of cross-sections, stress-strain diagrams and distribution of residual stresses and also because of the different influence of the initial crookedness on the instability limit load at different strength of the material, and smaller effect of residual stresses in high strength material.

STRUTS FROM RAMBERG-OSGOOD MATERIAL

In the following figures from 9 to 12 there is shown how the instability curves for compressed members of rectangular cross-section with initial crookedness 1/1000 depend on the strength degree of the materials at different shapes of stress-strain diagram, expressed by the parameter n. This numerical experimentation with the help of a computer was made with the assumption that there is no strain reversal. Fig.13 shows the comparison of the T curves without strain reversal with the R curves, where strain reversal is taken into account. We can see in Fig.14 the corresponding diagram for the determination of the effective flexural stiffness of the rectangular cross-section, as a function of the dimensionless axial force and bending moment. There is also evident the limited region of R curves, which are computed according to the assumption that the axial force is constant, while the bending moment increases. Fig.15 reminds us of the fact that in materials with the low parameter n of the stress-strain diagram

270

exists considerable difference between the buckling loads according to tangent modulus concept and the buckling loads according to reduced modulus concept for different cross-sections. Although, as it is well known, the actual load-carrying capacity is somewhere in-between, the question is whether it will not be worthwhile, sometimes to take into account the increased carrying capacity because of strain reversal. When n is high ( Fig.16 ), the differences are considerably smaller. However, also here the question exists whether the use of the increased buckling loads above $\overline{N} = 1$, is convenient in the region of very small slenderness, because here the unreversal shortening of the strut becomes substantial. May be we should pay attention sometimes also to a serviceability limit state, defined with an appropriate limit of the unreversal deformation.

## COMPOSITE STRUTS

The suitability of the dimensionless presentation of the bugkling curves, also for the struts with composite cross-sections ( steel - concrete ), can be well seen in Fig.17. The curves for all composite cross-sections are always between the lower curve for plane concrete and the upper one for plane mild steel ( here without influence of residual stresses ). Of course in $\overline{N}$ and $\overline{\lambda}$ there are involved parameters, which take into account the shape of single cross-sections and the properties of single materials. And in Fig.18 there is shown the diagram for the determination of effective flexural stiffness for a concrete filled tube. It is intended for changing compressed axial force and bending moment without strain reversal. According to so many variations regarding possible cross-sections and material properties, the question of the typical composite cross-sections is even more important.

## LOAD CARRYING SYSTEMS

At the end, we might discuss very shortly the question of buckling and instability of the linear systems. We can say in connection with buckling that it is no problem for any multistory plane frame to get automatically the shape of the buckling deformation and the buckling safety factor with the help of computers after Vianello's method, that is with the iteration and the use of the 1st order theory. With given relations of effective flexural stiffness for the given cross-section and with the consideration of structural imperfections, if necessary, we can automatically take into account the influence of inelasticity.

While the buckling calculations of plane frames with the help of computer represent today a routine work ( input of data as in the STRESS program ), the calculation of the elasto-plastic instability of multistory frames, loaded vertically and horizontally, is nowadays possible, but still very unpractical and expensive, because the inelasticity changes in cross-sections, both for the iteration of a given loading and for the increase in loading. That is why this way of computing is intended today before all for research work and especially for the evaluation of different approximate methods like the 2nd order plastic hinge theory, the Merchant's formulae, and interaction formulae for beam-columns. It is evident that the degree of the accuracy of the approximate methods can be well evaluated only with the help of a more precise method.

But the most important basis for the elasto-plastic calculation are the data about the variation of the effective stiffness of the cross-sections. And so we must return to the appeal for the necessity of unification of these data which is even more unavoidable especially at the additional consideration of biaxial bending, torsion and plate buckling. In this way it would be possible to reliably compare the results of the calculation of instability behaviour of complicated structures carried out with different numerical methods in different places. And this would enable considerably quicker progress in the spreading of knowledge in the field of compression instability.


## CONCLUSION

The appropriate unification of stress-strain diagrams, cross-sections and the corresponding distribution of residual stresses give a general value of the data about the effective stiffness, which are the most important basis for the determination of the buckling or instability limit load of any linear load carrying system.

## ACKNOWLEDGEMENT

IPE 330  INP 240  IPB_L 300

IPB_V 340

IPB_V 100

UNP 350

1

1

Fig.1

$\sigma$

$q$

$\varepsilon^\circ$   $2\varepsilon^\circ$   $\varepsilon$

FIg.2

$\bar\sigma$

4
10
30
80

$\bar\varepsilon = \bar\sigma(1 + \bar\sigma^n)$

0   1   2   3   $\bar\varepsilon$

Fig.3

$\bar\sigma$

1   1

1
2
4
3
5
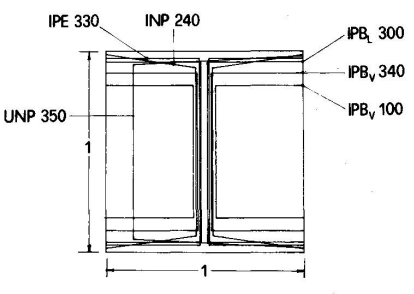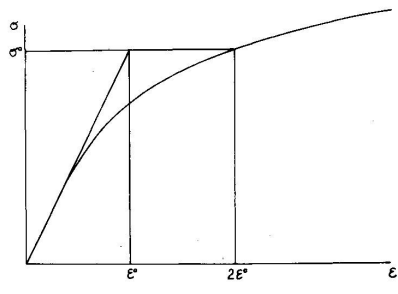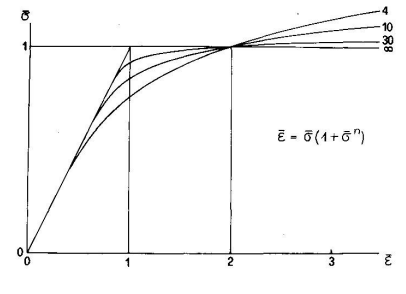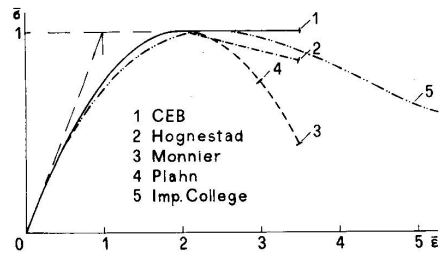
1 CEB
2 Hognestad
3 Monnier
4 Plahn
5 Imp.College

0   1   2   3   4   5   $\bar\varepsilon$

Fig.4

$\bar N$

1

$\frac{1}{\bar\lambda^2}$

only structural

structural
and
geometrical

0   1   2   $\bar\lambda$

Fig.5

$\bar N$

1

$\bar N_b$
$\bar N_i$

$\bar N_i = \bar N_b \dfrac{\nu_o}{\nu} = \dfrac{1}{\omega}$

$\bar N_{allow}$

0   1   2   $\bar\lambda$

$\nu_o$      $\nu = \bar N_b : \bar N_{allow}$
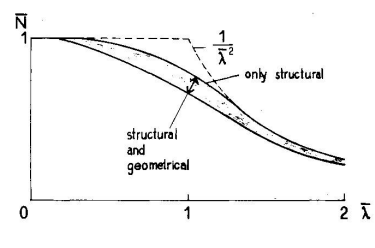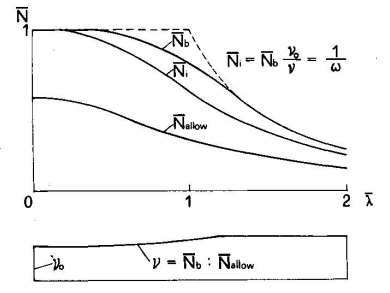
Fig.6
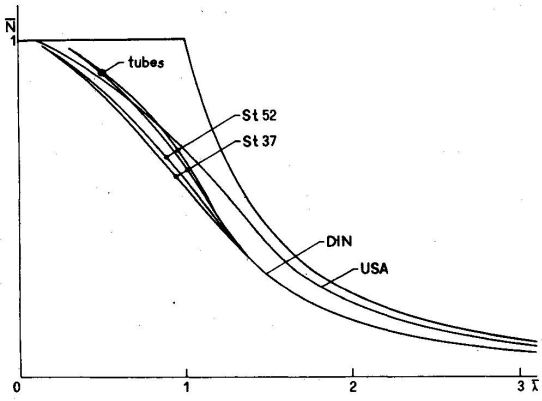
Fig.7
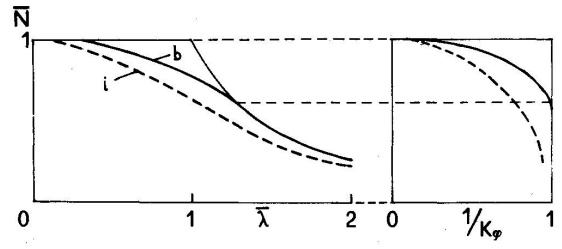
Fig.9

Fig.8

$$\frac{1}{K_\varphi} = \frac{J_{eff}}{J} = \frac{E_{eff}}{E} = \overline{N}_{b,i}\,\overline{\lambda}^2 = f(\overline{N}_{b,i})$$
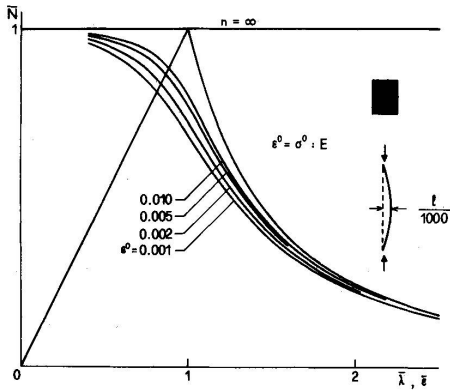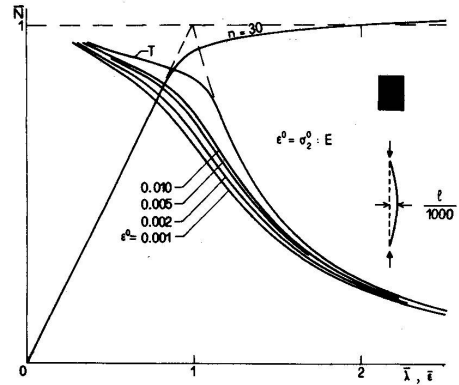
Fig.10
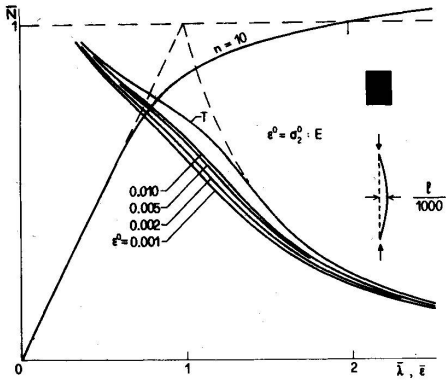
Fig.11
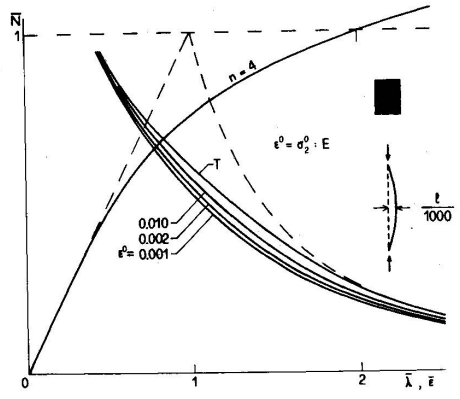


Fig.12
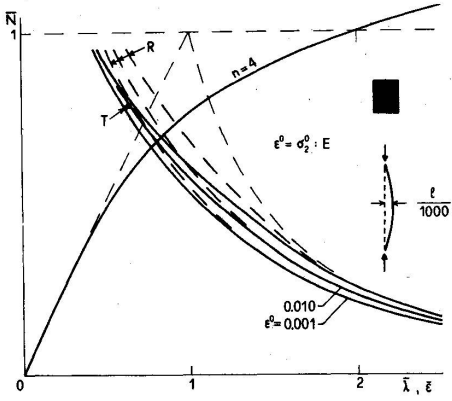


Fig.13
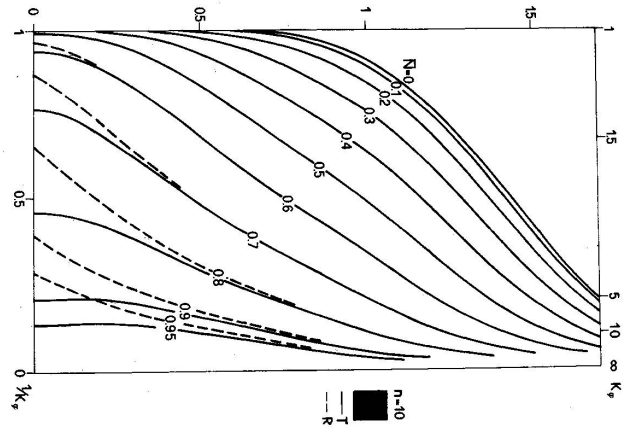


Fig.14
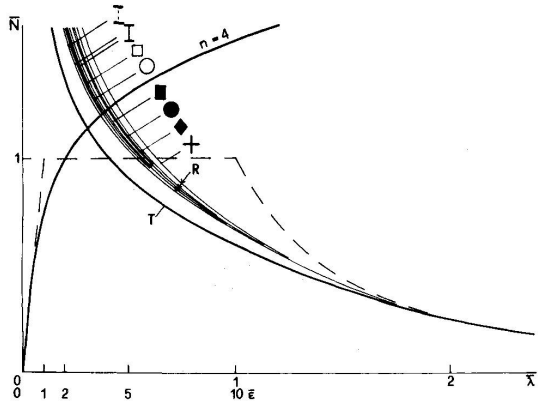
Fig.15
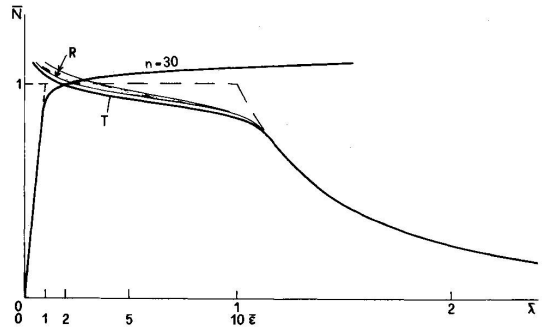


Fig.16
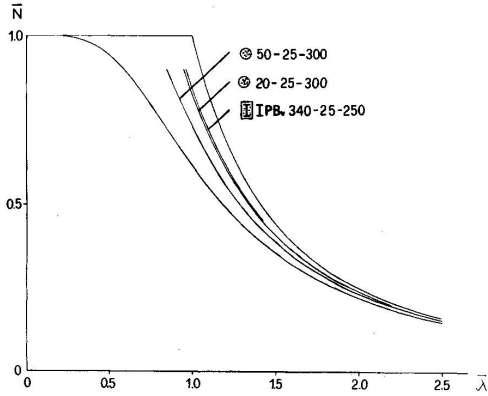


Fig.17
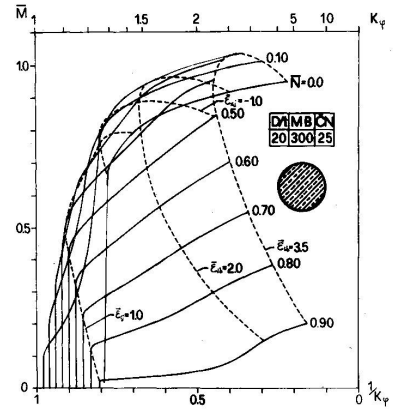


Fig.18

## SOME SIMPLE THOUGHTS ON COLUMN BUCKLING

Thomas A. Barta
Lecturer in Engineering Structures
Department of Civil and Municipal Engineering
University College London

### ABSTRACT

This paper describes briefly the "physical" and "mathematical" models in physics and structural mechanics, leading to the modelling of flexural buckling of pin-ended columns; (this later aspect is presented to a certain extent as a history of ideas). Some simple thoughts on column buckling lead to a modern interpretation and generalisation of Young's formula for the "imperfect" column. A criterion for the definition of the imperfection parameter is established and it's simplest expression proposed. Various possible formulations are shown and a discussion of the "natural parameters" of the problem is followed by an example showing the potential and simplicity of the suggested approach.

The specific contents of this paper are:

1.  Introduction
    1.1 Modelling in Physics
    1.2 Modelling in Structural Mechanics
    1.3 Objective
2.  Column Models
    2.1 Outline
    2.2 The Mechanical Model
    2.3 The Mathematical Model (theory)
    2.4 The Phenomenological Model (analogue)
3.  Some Simple Thoughts on Column Buckling
    3.1 The Interaction Diagram for Column Buckling
    3.2 Young's Formula, Modern Version
    3.3 A Criterion for the Definition of the Non-dimensional Imperfection
    3.4 The Simplest Expression for the Non-dimensional Imperfection
    3.5 Discussion of Other Expressions for the Non-dimensional Imperfection
    3.6 The Buckling Curve and an Alternative Interpretation
    3.7 The Introduction of Alternative Variables
    3.8 On Some Simplified Formulae
    3.9 The "Natural" Column Parameters
    3.10 The European Column Curves and an Example for the Use of the Proposed Formulae.
    3.11 Concluding Remarks

# 1. INTRODUCTION

## 1.1 Modelling in Physics

The real "physical" world is extremely complex. In
order to understand it, at least partially, we restrict our-
selves to a particular system, within certain limits of
practical interest, which we study from a specific point of
view, separating - as far as possible - the major (or primary)
parameters of the system from the minor (or secondary) and
from the negligible ones. (Secondary parameters may be called
"imperfections"). We have thus defined - somehow subjectively
- a "physical model" on which we can make observations and
experiments, (within the limitations of equipment and tech-
niques). In defining the model, the question "how good is
good enough?" has to be asked (and answered as far as possible)
as obviously the importance and value of the expected results,
have to be corelated with the features of the model and with
the cost, complexity and accuracy of its investigation.

The mathematical description of the physical model
(consistent with the general principles of physics) will
involve necessarily idealisations and simplifications; and
further simplifications will be necessary if a specific
mathematical method is to be used. We have now defined -
again somehow subjectively - a "mathematical model" or "theory".
If we consider that the physical model is a reasonably "real"
representation of the actual physical system, then the mathe-
matical model is it's more or less "ideal" representation.
Thus from the physicist's point of view the physical model
is "perfect" and the mathematical model is more or less
"imperfect". From the mathematicians or theoreticians point
of view (assuming that the idealisations of the mathematical
model are fundamental axioms) it is sometimes (wrongly) stated
that he deals with a pure "perfect" model, whereas nature is
"imperfect". However both points of view can be unified by
defining the differences between the physical and the mathe-
matical models as "imperfections". Obviously the question
"how good is good enough?" will govern again the choice of

idealisations and simplifications made in the definition of the "mathematical model".

The exaggeration of certain major parameters of the models can lead to the very useful concepts of upper and lower bounds of the problem.

A better understanding of the phenomena can be achieved through an oversimplification of the mathematical model (which sometimes can be specially constructed physically). Such models are called "Phenomenological models" or "analogues".

The three models are interdependent as they have to be checked against each other; e.g. the simple analogue may lead to the discovery of a major parameter which has been overlooked in the initial physical model, or it might explain some apparently odd behaviour of the physical model.

## 1.2 Modelling in Structural Mechanics

In structural mechanics the limit states of engineering structures interacting with their environment are studied from the point of view of their serviceability. This is the broad definition of the physical or "mechanical model". Various publications on measurements of loading actions and tests of structures, structural elements and structural materials cover this subject. Other publications cover the "theories" or "mathematical models" of these different topics. Phenomenological models of materials are covered in the literature on rheology etc., whereas the most extensive treatment of phenomenological models for structural components is given in a recent book by CROLL and WALKER[11](1972). Unfortunately, there are no textbooks (as far as the author knows) covering all models in equal depth and breadth, and practically no satisfactory attempts have been made to answer the questions of "limitation of validity" and "how good is good enough".

## 1.3 Objective

The main objective of this introduction is to stress that it is necessary again and again to judge and assess assumptions, idealisations, simplifications etc. of the different models, their interrelationship, and to ask - and answer as far as possible - the questions about the range of validity and the question "how good is good enough". In fact every engineer acts, to a certain extent, consciously or unconsciously, in this way.

## 2. COLUMN MODELS

## 2.1 Outline

We will approach this subject (using modern terminology and notation) by following its historical development, as far as it constitutes a history of ideas (not covered in this form elsewhere), and as it will be used in this paper later on.

## 2.2 The Mechanical Model

A straight, axially loaded, slender rod is called a column (strut, or stanchion) and its primary behavioural feature (in the context of this paper) is its flexural deformation. This loose description of flexural buckling goes back to HERON of Alexandria [19] (~A.D. 75) and to LEONARDO da VINCI [21] (1452-1519). The limit state of the column can be defined either through failure MUSSCHENBROEK [24] (1729) or the onset of large deformations EULER [15] (1744) . MUSSCHENBROEK [23] (1726) was the first to define material properties as: "hard, perfectly hard, soft, perfectly soft, flexible, elastic and perfectly elastic", and to design testing machines permitting systematic variations of parameters for the testing of material properties and structural components (1729-op.cit) EULER (1744) (op. cit.) considers elastic deformations and later (1757) [16] inelastic bending "... because it occurs in all bodies that resist flexure, whether they are elastic or not". He suggests to determine the flexural stiffness through bending tests under similar boundary conditions (as for the column). This concept was rediscovered 132 years later by CONSIDÈRE [9] (1889) and ENGESSER [14] (1889) and marked the beginning of modern research into inelastic buckling. THOMAS YOUNG [30] (1807) had an even clearer understanding of inelastic deformations, stating: "... a permanent alteration of form ... limits the strength of materials with regard to practical purposes, almost as much as fracture, since in general the force which is capable of producing this effect, is sufficient, with a small addition, to increase it till fracture takes place". He notices the different behaviour of stocky and slender columns and gives limits for various materials for the two types of behaviour. His understanding of what we call today inhomogeneity of material properties and imperfections is amazing, and has its origin in analyzing experimental results; "... considerable irregularities may be observed in all the experiments ... and there is no doubt but some of them were occasioned by the difficulty of applying the force precisely at the extremities of the axis, and others by the accidental inequalities of the substances, of which the fibres must often have been in such directions as to constitute originally rather bent than straight columns". This concept was rediscovered by several authors, but is usually attributed to AYRTON and PERRY [1] (1886), 79 years later. The importance of "past history of the material" has been demonstrated by B. BAKER [3] (1888) and only since WILSON and BROWN [29] (1935) showed the importance of residual stresses (47 years later), began to be a subject for modern research. R.H. SMITH [27] (1878) (who rediscovered Young's concept of imperfections) recognized that "... the whole question of the strength of struts is one of probability", a concept which gained acceptance only after its rediscovery 72 years later by DUTHEIL [12] (1950).

It can be seen that the physical model of flexural buckling was reasonably well established almost 100 years ago (or even longer) but unfortunately not well known or understood. Rayleigh's remarks about Young as quoted by TIMOSHENKO [28] (1953) that he "... did not succeed in gaining due attention

from his contemporaries. Positions which he had already occupied were in more than one instance reconquered by his successes at great expense of intellectual energy", apply equally well to the 18th and 19th century scientists mentioned above.

## 2.3 The Mathematical Model (theory)

We restrict ourselves to the elementary case of the pin-ended straight column with constant cross-section. In his second memoir EULER (1757) (op.cit), gives his general formula for the "ideal inelastic column", of length $\ell$ :

$$N_B = \frac{\pi^2 B}{\ell^2} \tag{1}$$

where B is termed "stiffness moment", or in todays terminology "flexural stiffness" and includes such more recent concepts as tangent modulus, or deteriorated stiffness etc. In his first memoir (1744) (op.cit) he calls this term the "elastic moment", and in his third memoir (1778)[17] gives it's more precise version, (for the classical "elastic Euler-load")

$$N_E = \frac{\pi^2 EI}{\ell^2} \tag{2}$$

Euler's definition of the elastic modulus E (usually attributed to Young) and of the second moment of area I, are correct, but he ignores JAKOB BERNOULLI's (1695)[7] correct definition of the position of the neutral axis. YOUNG (1807) (op.cit) gives the correct value for I (with the correct position of the neutral axis) and gives also a, clumsy but correct, derivation for the mechanical model of his physical model (see chapter 22). He considers pin-ended elastic columns with an initial sinusoidal curvature of amplitude e , and a straight column with a load N applied with an eccentricity $e_o$. We will transcribe his results for these "imperfect columns" into a more modern form so as to express the second-order moment $M^{II}$ by multiplying the first order moment

$$M^I = Ne_o \tag{3}$$

with an amplification factor $\alpha$ , so that:

$$M^{II} = M^I \alpha \tag{4}$$

For the initially curved column:

$$\alpha = \frac{1}{1-\overline{N}_E} \tag{5}$$

and for the eccentrically loaded column:

$$\alpha = \sec \frac{\pi}{2} \sqrt{\overline{N}_E} \tag{6}$$

with the non-dimensional parameter:

$$\overline{N}_E \equiv N/N_E \tag{7}$$

where $N_E$ is the elastic Euler load, equ.(2). A numerical comparison of (5) and (6), by AYRTON and PERRY (1886) (op.cit) shows that for practical values of $\bar{N}_E$ the algebric expression (5) is a good approximation of (6); so that the initial curvature can be considered as a "generalised imperfection". NAVIER (1826-1833) [25] writes the first modern textbook on engineering mechanics, and gives an elegant mathematical derivation for the eccentrically loaded column, (without indicating the concept of the "imperfect" column). Comparing theoretical results with tests he concludes that the elastic Euler-load $N_E$ and a suitable failure load $N_0$ for the stocky column are upper bounds for the experimental results. Relatively late, MERCHANT (1954) [22] suggested empirically (in the more general context of frame-buckling) that the special form of the well-known Rankine-formula:

$$\bar{N}_0 + \bar{N}_E = 1 \tag{8}$$

with the non-dimensional parameter

$$\bar{N}_0 \equiv N/N_0 \tag{9}$$

is a lower bound. HORNE (1963) [20] has proved theoretically that this is correct under certain conditions (which are satisfied for the pin-ended column). Young did not apply his findings to bridge the gap between the experimental results and his theory. The first best-known attempts in this direction are due to AYRTON and PERRY (1886) (op.cit) who admitted as limit state yield in the extreme fibre; and suggested various expressions for imperfections. This approach was adopted in various codes of practice mainly due to work by ROBERTSON (1925) [26] and DUTHEIL (1950) (op.cit). The development of theories for inelastic buckling including the effect of imperfections, and the extensive study of residual stresses, are well known and will not be discussed here.

## 2.4 The Phenomenological Model (analogue)

JAKOB BERNOULLI, or G. CRAMER (the editor and commentator of his works) (1744) [10] have imagined the two-spring model for the bending of a cross-section, which may be considered as the predecessor of the well-known Shanley-model. EULER (1778) [18] when faced with the problem of self-weight buckling of a column, considers two rigid links connected by a torsional spring. For the modern treatment of such analogues see the book by CROLL and WALKER (1972) (op.cit).

## 3. SOME SIMPLE THOUGHTS ON COLUMN BUCKLING

## 3.1 The Interaction Diagram for Column Behaviour

The mechanical model of the slender column has been defined in (2.2). Obviously a very stocky column (under identical loading and support conditions) has to be represented by a different mechanical model. For a solid cross-section the column degenerates into a block and for a built-up cross-section into a plate-assemblage. For a ductile material like steel, to which we restrict ourselves in this paper, barreling and plate-deformation will be the respective primary behavioural features. For a certain region of slendernesses the behaviour of the slender and

very stocky columns may interact, and for a certain value of slenderness (treating the problem as it has been done tacitly till here, as a deterministic-one) buckling will be predominant. We could thus identify by experiment the practical limit of column behaviour, and will call this limit the "stocky column" with a buckling load $N_E^o$ for which $N \cong N_o$. (The very stocky columns fall outside our present object of study, and as their behaviour depends on different parameters, cannot be included in the same diagrams or tables as the slender columns). When the length of the column tends to zero, the column degenerates into a "sheet", and ends up as a "mathematical fiction" which might be used eventually as a "conventional" value; but could be dangerously misleading in understanding column behaviour. As forces are readily measureable in experiments, we shall call $N_o$, $N_E$ and $N_E^o$ the "primary natural column parameters" which can be studied experimentally and evaluated from a probabilistic point of view. With the non-dimensional parameters $0 \leqslant \overline{N}_o \leqslant 1$ as defined in (9) and $\overline{N}_E^o \leqslant \overline{N}_E \leqslant 1$ as defined in (7), with



**FIG.1**

$$\overline{N}_E^o \cong N_E^o / N_E \qquad (10)$$
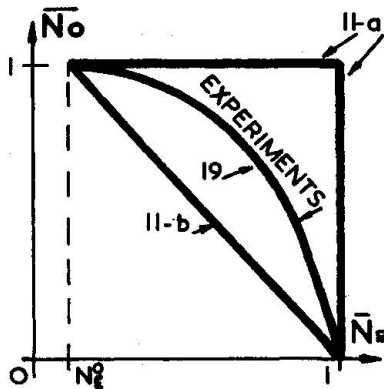
the equations for the bounds can now readily be written:

$$\overline{N}_o + \overline{N}_E - \overline{N}_o \overline{N}_E = 1 \quad \text{(upper bound)} \quad (11\text{-}a)$$

$$\overline{N}_o + \overline{N}_E - \overline{N}_o \overline{N}_E^o = 1 \quad \text{(lower bound)} \quad (11\text{-}b)$$

The equations (11) define a triangle which will contain all experimental results. We will assume that the experimental results can be represented by a curve. (See the interaction diagram in figure 1).

## 3.2. Young's Formula, Modern Version

Young's approach (see 2.2 and 2.3) will be used to find an expression for the experimental curve in fig. 1. Considering the initial curvature $e_o$ as the "generalised imperfection", the second order moment can be written, using equs. (3 to 5):

$$M^{\pi} = \frac{N e_o}{1 - \overline{N}_E} \qquad (12)$$

The interaction diagram in figure 2 shows (as an example for the idealised I-section) the well-known (conventional) elastic and



**FIG.2**

rigid-plastic failure-conditions (limit-states). It can be seen that any failure-condition for any cross-section can be approximated by the linear interaction-formula:
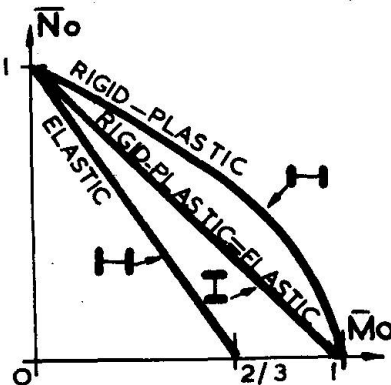
$$\overline{N}_o + c_o \overline{M}_o = 1 \quad (13)$$

where,

$$\overline{M} \cong M / M_o \qquad (14)$$

is the ratio of the actual moment M to the (rigid-plastic) ultimate moment $M_o$ and $c_o$ is a suitable approximation const-

On substituting (12) into (13) we obtain with (14), after some algebric manipulations:

$$(1 - \overline{N}_o)(1 - \overline{N}_E) - \eta \overline{N}_o = 0 \qquad (15)$$

with the "non-dimensional (generalised) imperfection"

$$\eta = \frac{c\, e_o}{M_o / N_o} \qquad (16)$$

Equation (15) with (16) represents the modern version of Young's formula. (In view of the historical account in (2) we consider this name more appropriate than the current name of Perry's formula).

### 3.3 A Criterion for the Definition of the Non-dimensional Imperfection

Young's epigones found it difficult to define a suitable expression for $\eta$. The interaction-diagram in figure 1 is now very useful in providing a necessary criterion for the definition of $\eta$. This criterion is: "Upon specialisation, the expression (16) for $\eta$ and equ. (15) should yield the bounds (11), and so automatically contain the corner points of the interaction diagram (fig. 1)". (There is no proof that this condition is also sufficient).

### 3.4 The Simplest Expression for the Non-dimensional Imperfection

It is obviously possible to define many expressions for $\eta$ which satisfy the criterion given above. The simplest expression will be linear in the three primary natural parameters of the problem (as defined in 3.1):

$$\eta = c\,(\overline{N}_E - \overline{N}_E^o) \qquad (17)$$

with the "imperfection parameter" c, where: $0 \leqslant c \leqslant 1$. The upper bound is obtained for $c \equiv 0$, and the lower bound for $c \equiv 1$. We consider c to be the fourth natural parameter of the problem.

### 3.5 Discussion of Other Expressions for the Non-dimensional Imperfection

The most popular expressions for $\eta$ are due to ROBERTSON (1925) (op.cit.) (although his expression is implied already in the paper by AYRTON and PERRY) and DUTHEIL (1950) (op. cit.) both expressions will be generalised so that they contain the corner point ($\overline{N}_o = 1$, $\overline{N}_E = \overline{N}_E^o$). The ROBERTSON parameter can be written in non-dimensional form (this is a further generalisation of his concept) in our variables

$$\eta_{R1} = c_{R1} \sqrt{\frac{\overline{N}_E - \overline{N}_E^o}{\overline{N}_o}} \qquad (18\text{-}a)$$

or

$$\eta_{R2} = c_{R2}\left(\sqrt{\overline{N}_E/\overline{N}_o} - \sqrt{\overline{N}_E^o/\overline{N}_o}\right) \qquad (18\text{-}b)*$$

---

* An expression of the type (18-b) has been suggested by DWIGHT in his contribution to this colloquium.

Both expressions pass through both corner points; and with c ≡ 0 yield the upper bound, but do not yield upon special-isation the lower bound. DUTHEIL was the first to use non-dimensional parameters, and his generalised parameter is:

$$\eta_D = \zeta_D \frac{\overline{N}_E - \overline{N}_E^o}{\overline{N}_o} \qquad (18\text{-}c)$$

Equation (15) with (18-c) will not pass through the lower corner-point and will not yield upon specialisation the lower bound. A combination of the satisfactory parameter (17) with the Robertson and (or) Dutheil parameters (18) will obviously not satisfy the criterion defined in 3.3.

3.6  The Buckling Curve and an Alternative Interpretation

Substitution of (17) into (15) yields the hyperbola:

$$1 - \overline{N}_E - (1 - c\overline{N}_E^o)\overline{N}_o + (1-c)\overline{N}_E\overline{N}_o = 0 \qquad (19\text{-}a)$$

or

$$\overline{N}_o = \frac{1 - \overline{N}_E}{(1 - c\overline{N}_E^o) - (1-c)\overline{N}_E} \quad (19\text{-}b) \qquad \overline{N}_E = \frac{1 - (1 - c\overline{N}_E^o)\overline{N}_o}{1 - (1-c)\overline{N}_o} \quad (19\text{-}c)$$

An alternative interpretation of $\overline{N}_E$ can be obtained if we consider N to be identical with $N_B$ as defined by equ. (1) Dividing equ. (1) and (2) yields then ·

$$\overline{N}_E \equiv B/EI \qquad (20)$$

i.e. $\overline{N}_E$ can be used to define the ratio of actual and elastic stiffness (or in a more specialised interpretation, the ratio of tangent and elastic moduli).

3.7  The Introduction of Alternative Variables

In our previous formulation both non-dimensional variables $\overline{N}_o$ and $\overline{N}_E$ were load-dependent. By taking the ratio

$$\Psi \equiv \overline{N}_E / \overline{N}_o \qquad (21\text{-}a)$$

or it's equivalent:

$$\Psi \equiv N_o / N_E \qquad (21\text{-}b)$$

we obtain a load-independent, non-dimensional variable which we may call the "strength-stiffness-ratio". Accordingly we will have

$$\Psi^o \equiv \overline{N}_E^o \qquad (22)$$

so that $\Psi^o \leq \Psi \leq \infty$. With (21) and (22) the equations (19) becomes the cubic:

$$1 - (1 - c\Psi^o)\overline{N}_o - \Psi\overline{N}_o + (1-c)\Psi\overline{N}_o^2 = 0 \qquad (23\text{-}a)$$

or, explicitly:

$$\Psi = \frac{1 - (1 - c\Psi^o)\overline{N}_o}{\overline{N}_o[1 - (1-c)\overline{N}_o]} \quad (23\text{-}b) \qquad \overline{N}_o = \frac{[(1 - c\Psi^o) + \Psi] - \sqrt{[(1 - c\Psi^o) + \Psi]^2 - 4(1-c)\Psi}}{2(1-c)}$$

$$(23\text{-}c)$$

An alternative form of (23-c), more suitable for numerical evaluation is:

$$\overline{N}_0 = \frac{2}{[(1-c\Psi^\circ)+\Psi]+\sqrt{[(1-c\Psi^\circ)+\Psi]^2 -4(1-c)\Psi}} \qquad (23\text{-}d)$$
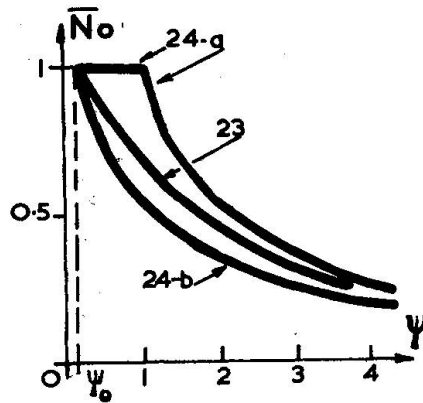


**FIG.3**

A representation of equ. (23) together with the corresponding upper bound:

$$(1-\overline{N}_0)(1-\Psi N) = 0 \qquad (24\text{-}a)$$

and lower bound:

$$1-(1-\Psi^\bullet)\overline{N}_0 -\Psi\overline{N}_0 = 0 \qquad (24\text{-}b)$$

is given in figure 3.
Usually the slenderness-ratio $\lambda = \ell/i$ (i = radius of gyration of the cross-section) is used as parameter for buckling problems. It can be easily shown that the "non-dimensional slenderness-ratio is:

$$\overline{\lambda} \equiv \sqrt{\Psi} \qquad (25\text{-}a)$$

or

$$\overline{\lambda} \equiv N_0 \lambda^2 /\pi^2 EA \qquad (25\text{-}b)$$

and it's corresponding limiting value:

$$\overline{\lambda}^\circ \equiv \sqrt{\Psi^\circ} \qquad (26)$$

Substituting (25) and (26) in (23) we obtain the quartic:

$$1-(1-c\,\overline{\lambda}^{\circ 2})\overline{N}_0 - \overline{\lambda}^2\overline{N}_0 +(1-c)\overline{\lambda}^2\overline{N}_0^2 = 0 \qquad (27\text{-}a)$$

or explicitly:

$$\overline{\lambda} = \sqrt{\frac{1-(1-c\,\overline{\lambda}^{\circ 2})\overline{N}_0}{\overline{N}_0[1-(1-c)\overline{N}_0]}} \qquad (27\text{-}b)$$

$$\overline{N}_0 = \frac{[(1-c\,\overline{\lambda}^{\circ 2})+\overline{\lambda}^2]-\sqrt{[(1-c\,\overline{\lambda}^{\circ 2})+\overline{\lambda}^2] -4(1-c)\overline{\lambda}^2}}{2(1-c)\overline{\lambda}^2} \qquad (27\text{-}c)$$

and the more suitable form:

$$\overline{N}_0 = \frac{2}{[(1-c\,\overline{\lambda}^{\circ 2})+ \overline{\lambda}^2]+\sqrt{[(1-c\,\overline{\lambda}^{\circ 2})+\overline{\lambda}^2] -4(1-c)\overline{\lambda}^2}} \qquad (27.d)$$

Similarly, substituting (25) and (26) in (24) we have the upper bound:

$$(1-\overline{N}_0)(1-\overline{\lambda}^2\overline{N}_0) = 0 \qquad (28\text{-}a)$$

and the lower bound:

$$1-(1-\overline{\lambda}^{\circ 2})\overline{N}_0 -\overline{\lambda}^2\overline{N}_0 = 0 \qquad (28\text{-}b)$$

286
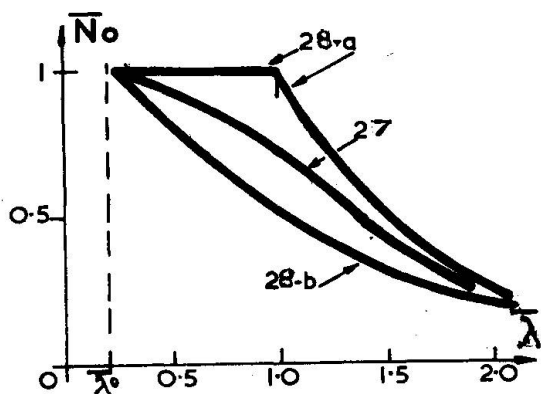
The equations (27) and (28) are shown in figure 4; this is the well known presentation of the buckling curve. It should be noted that the order of the equivalent equations (19)(23) and (27) is increasing by one, and that the corresponding curves in figures (1)(3) and (4) get more complicated.

**FIG. 4**

### 3.8 On Some Simplified Formulae

Considering only relatively small values of $\bar{\lambda}$, (27-d) may be expanded into power series, and retaining only the major terms, we obtain

$$N = 1-c(\bar{\lambda}^2 - \bar{\lambda}^{o2}) \qquad (29\text{-}a)$$

or

$$N = \frac{1}{1+c(\bar{\lambda}^2 - \bar{\lambda}^{o2})} \qquad (29\text{-}b)$$

Equ. (29-a) is a generalised form of the JOHNSON-parabola (as used in the USA with $\bar{\lambda}^o \equiv 0$) and equ. (29-b) is the generalised form of the well known RANKINE-formula.

### 3.9 The "Natural" Column Parameters

The natural column parameters, defined earlier will be discussed again. The "elastic" Euler load $N_E$ (equ. 2) is well understood and reasonably well known experimentally. For the coupled parameters $N_0$ and $N_E^o$ of the "stocky column" (chapter 3.1) there is little experimental evidence and few theoretical studies available, and values are adopted at present through some kind of intuitive extrapolation. The imperfection parameter c should be studied in the region of highest "imperfection sensitivity". The scatter of experimental results, and column behaviour in this region has been explained, on an analogue, by CHILVER and BRITVEC (1963)[8], and there is sufficient experimental evidence available. It seems that a single imperfection parameter c is good enough for the description of column behaviour. Obviously a probabilistic study of all these parameters is desirable for design purposes. As the number of parameters is small, such an approach is feasible.

### 3.10 The European Column Curves and an Example for the Use of the Proposed Formulae

The late Professor H. BEER chaired and inspired Commission 8 (Buckling) of the European Convention for Structural Steelwork. The main results on column buckling obtained by this commission are reported in several papers in the September 1970 issue of "Construction Métallique". The theoretical foundations for the European Column Curves are given in a paper by BEER and SCHULZ (1970)[5]. At a meeting of Commission 8 in London (April 1971) J.B. DWIGHT and B.W. YOUNG (1971)[13] summarized their work, on

similar lines but adopting the concept of $N_E^o \neq 0$*). At the
discussions at this meeting BARTA (1971)[4] proposed the use of
Young's formulae (equs. 15 and 16) suggesting as generalised
imperfection the sum of the Dutheil term (equ. 18-c) and of his
term (17), both with the assumption $N_E^o \equiv 0$. Barta's final
formula is practically identical with an algebric approximation
formula reported by BEER and SCHULZ (1971)[6] at the same
meeting and due to BAAR (1970)[2], and unknown to the author
at that time. (Baar investigated four algebric approximation
formulae, without any attempt of a theoretical justification).
In the search for a generally accepted approach, the concept
$N_E^o \neq 0$ has been adopted, but (to the authors knowledge) the
final curves are still subject to discussions. In order to
show the potential of the proposed simple approach, we repro-
duce in figure (5) the European curves ($N_E^o \equiv 0$) from a paper
by BEER and SCHULZ (1971)[6] to which we have ($N_E^o \equiv 0$) added the
Merchant lower-bound curve. For the present purpose it is
"good enough" to use equ. (27-d) with $\bar{\lambda}^o \equiv 0$, and to determine
the imperfection parameter c for the most imperfection-sensitive
value of $\bar{\lambda}$ ; (i.e. $\bar{\lambda} \equiv 1$); This results in the following values
for the three curves

$$c_a = 0.232 \ ; \qquad c_b = 0.444 \ ; \qquad c_c = 0.743$$

---

*) Dwight's and Young's contribution to this colloquim represent
   a more detailed version of this report.
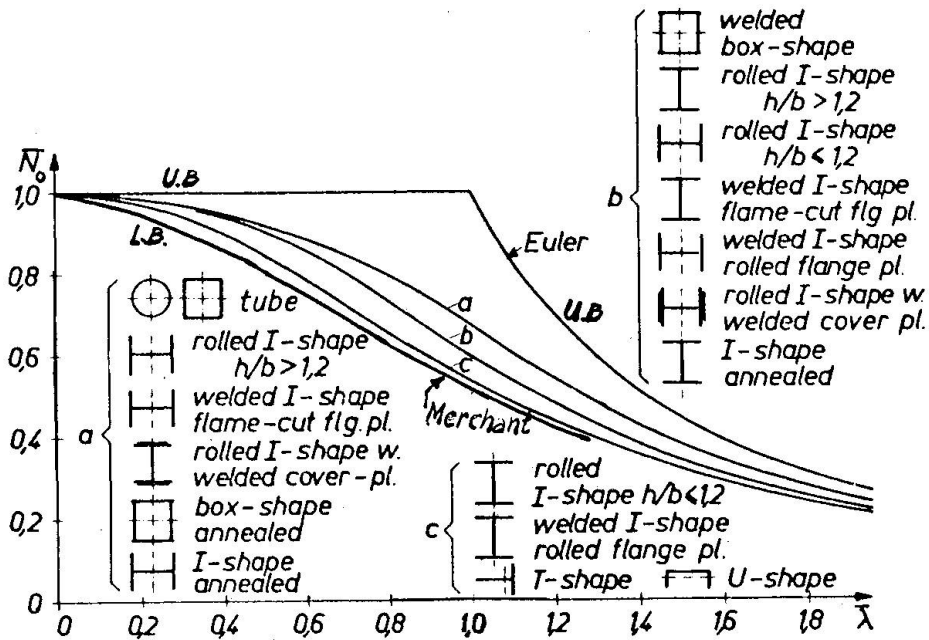


FIG.5

The results differ so little from those of Beer and Schulz that
the curves could not be clearly traced together. We give
therefore a numerical table of comparison:

Values of $\overline{N}_0$

| curve \ $\overline{\lambda}$ | | 0 | 0.25 | 0.50 | 0.75 | 1.00 | 1.50 | 2.00 |
|---|---|---|---|---|---|---|---|---|
| U.B. | | 1 | 1 | 1 | 1 | 1 | 0.444 | 0.250 |
| a | B-S | 1 | 0.990 | 0.923 | 0.821 | 0.675 | 0.381 | 0.228 |
| | B | 1 | 0.985 | 0.934 | 0.831 | 0.675 | 0.388 | 0.234 |
| b | B-S | 1 | 0.983 | 0.885 | 0.757 | 0.600 | 0.343 | 0.207 |
| | B | 1 | 0.972 | 0.887 | 0.754 | 0.600 | 0.357 | 0.222 |
| c | B-S | 1 | 0.975 | 0.884 | 0.687 | 0.537 | 0.323 | 0.202 |
| | B | 1 | 0.955 | 0.836 | 0.683 | 0.537 | 0.327 | 0.209 |
| L.B. | | 1 | 0.941 | 0.800 | 0.640 | 0.500 | 0.308 | 0.200 |

U.B. = upper bound; L.B. = lower bound  
B-S = results by Beer and Schulz*)  
B = present paper

## 3.11 Concluding Remarks

The approach shown in this paper will be extended in
further publications to other materials, boundary conditions
and loading cases. It's extension to post-buckling of structures
will be given in joint paper with Dr. A.C. Walker.

*) The numerical values have been obtained in a private commun-
ication from Professor H. Beer.

## References

1. AYRTON, W.E. and PERRY, J.
   On Struts
   The Engineer, 1886, p. 464-465; and 573-515.

2. BAAR, S.
   Courbes de flambement de la CECM. - Recherche d'une
   équation simple représentant au mieux les points
   donnés. Rapport to Committee 8 of CECM - SERCOM
   No. SB/1W st 26, 1970.

3. BAKER, B.
   Discussion on Open-hearth Steel for Boilers.
   Proc. Inst. Civ. Eng. London, Vol. XCII p. 44 (1888).

4. BARTA, T.A.
   A simple equation for the buckling curve.
   U.C.L. Communication (unpublished) to Committee 8
   CECM - London Meeting 1971.

5. BEER, H. and SCHULZ, G.
   Bases théoriques des courbes européennes de flambe-
   ment. Construction Métallique 7, (1970) p. 37-57.

6. BEER, H. and SCHULZ, G.
   Die neuen Knickspannungslinien der Europäischen Konven-
   tion der Stahlbauverbände.
   Wiss. Zeitschr. T.U. Dresden, Vol. 20 (1971) p. 817-821.

7.  BERNOULLI, J.
    Expliciationes, annotationes et additiones ad ea, quae
    in actis sup. anni de curva elastica ...
    Acta Erud. Dec. 1695 p. 537-553.

8.  CHILVER, A.H. and BRITVEC, S.J.
    The plastic buckling of aluminium columns.
    Proc. Symposium on Aluminium in Structural Engineering,
    Published by the Aluminium Federation London, 1963. .

9.  CONSIDÈRE, A.
    Résistance des pièces comprimées.
    Congrès international de procedés de construction, 1889.

10. CRAMER, G.
    Jakob Bernoulli: Opera
    Geneva 1744.

11. CROLL, J.A. and WALKER, A.C.
    Elements of structural stability
    Macmillan, London, 1972.

12. DUTHEIL, J.
    Le flambement des éléments comprimès dans la construction
    métallique; le flambement et le deversement.
    Bull. Soc. Roy. Belge des Ingénieurs et des Industriels
    No. 3, 1950.

13. DWIGHT, J.B. and YOUNG, B.W.
    Comparison of European and British Column Curves.
    Report (unpublished) at meeting of Committee 8 of
    the European Convention for Structural Steelwork,
    London 1971.

14. ENGESSER, F.
    Über die Knickfestigkeit gerader Stäbe
    Zeitschr. des Arch. u. Ing. Vereins, Hannover, 1889,
    p. 455.

15. EULER, L.
    Methodus Inveniendi Lineas Curvas Maximi Minimive
    Proprietate Gaudentes. Additamentum I: De Curvis
    Elasticis.
    M.M. Bousquet, Lausanne & Geneve 1744.

16. EULER, L.
    Sur la force des colonnes,
    Mem. Acad. Berlin. Vol. 13 1759 p. 252-282 (presented
    in 1757).

17. EULER, L.
    Determinatio onerum, quae columnae gestare valent.
    Acta Acad. Sci. Petrop. 2 (1778) p.121-145 (1780).

18. EULER, L.
    De altitudine columnarum sub proprio pondere curruentium.
    Acta Acad. Sci. Petrop. 2 (1778) p. 163-193 (1780).

19. HERON of ALEXANDRIA ( A.D. 75?)
    Mechanics II (34-h) in Arabic, ed. with german translation
    by L. Nix and W. Schmidt Leipzig 1900.

20. HORNE, M.R.
    Elastic-plastic Failure Loads of Plane Frames.
    Proc. Roy. Soc. A 274, (1963) p. 343.

21. LEONARDO DA VINCI (1452-1519).
    Inst. France Ms. A. f 45v.

22. MERCHANT, W.
    The failure load of rigidly jointed frameworks as
    influenced by stability.
    Structural Engineer, Vol. 32, 1954, p. 185.

23. MUSSCHENBROEK, P.
    Epitome elementorum physico-mathematicorum conscripta
    in usus academicos, S. Lugtmans, Lugdumi Batavorum,
    1726 ( p. 380-395).

24. MUSSCHENBROEK, P.
    Phisicae Experimentales et Geometricae Dissertationes.
    Introductio ad coherentiam corporum firmorum. p.466-662.
    S. Luchtmans, Lugduni Batavorum (Leyden) 1729.

25. NAVIER, L.
    Résumé des Leçons données a l'École des Ponts et
    Chaussées sur l'Application de la Mecanique.Part I,
    second, corrected and augmented edition. Carillan-
    Goeury - Paris 1833 (first ed. 1826).

26. ROBERTSON, A.
    The strength of struts
    Selected Engineering Paper No. 28 Inst. of Civ. Eng.
    London, 1925.

27. SMITH, R.H.
    The Strength of Struts.
    Proceedings Edinburgh and Leith Engineering Society,
    Vol. 4, 1878, p. 42-67.

28. TIMOSHENKO, S.P.
    History of strength of materials.
    McGraw-Hill Publishing Co. Ltd., New York 1953.

29. WILSON, W.M. and BROWN, R.L.
    The effect of residual longitudinal stresses upon the
    load-carrying capacity of steel columns.
    Univ. of Illinois Bull. No. 280 1935.

30. YOUNG, Th.
    A course of lectures on natural philosophy and the
    mechanical arts. (Vol. I and II).
    J. Johnson, London 1807.

# DETERMINATION OF THE ELASTIC LIMITS FOR BUCKLING ANALYSIS

A. Carpena
Senior Development Engineer
Società Anonima Elettrificazione S.p.A.
Milan, Italy

## ABSTRACT

This paper presents the results of a statistical research on the yield points to introduce in the buckling curves. If an even degree of safety should be obtained for all the components of a structure, whether in tension or in compression, a higher yield point than the minimum guaranteed tensile limit must be adopted for the buckling curves.

This conclusion was accepted by the "Convention Européenne" for its column strength curves.


## RESUME

Ce rapport présente les résultats d'une recherche statistique sur les limites élastiques à introduire dans les courbes de flambement. Si l'on veut obtenir une sécurité homogène pour toutes les pièces d'une structure, tant tendues que comprimées, une limite élastique plus élevée que celle minima garantie en traction, doit être adopté pour les courbes de flambement.

Cette conclusion a été acceptée par la "Convention Européenne" dans ses courbes de flambement.

The buckling curves recommended by Commission No. 8 of the "Convention Européenne de la Construction Métallique" (CECM) represent a substantial achievement by that organization, illustrated by the fact that the failure stresses given thereon are some 20% higher than those of the German Standard DIN 4114 for the majority of ordinary sections over the range of slenderness with which constructors are mainly concerned.

This outcome is based on:

- a very extensive programme of experimental research into the mechanical properties of the steel and the buckling strength of columns with varying cross section and slenderness ratio;

- an equally comprehensive programme of theoretical research into buckling of columns with or without geometrical and structural imperfections, undertaken on computers on which the buckling phenomenon has been simulated in a certain way to reproduce the loading tests;

- the "statistical-probabilistic" philosophy of safety adopted by the CECM, which not only led to a rational interpretation of the theoretical and experimental results but was used to specify the research programmes themselves.


## DEFINITION OF PROBLEM

A significant aspect of the buckling curves, related in part to the probabilistic theory of safety, is their termination, for slenderness ratio 0, at points sometimes higher than the allowable elastic limits of 24 and 36 kg/mm$^2$ for steels E24 and E36 (previously designated as A37 and A52).

It is perhaps without precedent that values higher than the guaranteed minimum elastic limits should be adopted for standards, or recommendations, as allowable structural failure stresses.

There are three reasons for this conclusion:

a) the experimental curve, connecting points situated at two Standard Deviations SD below the mean values curve, ends at 26 kg/mm$^2$;

b) the elastic limit of open walled sections is higher in overall compression than in tension, the compression limit being the failure stress at slenderness ratio 0. Both the mean value derived from these tests and that value minus two SD are higher in overall compression than in tension - as per EURONORM (1) - this latter value (mean M - 2 SD) being the failure stress according to the failure criterion of Commission No. 1 of the "Convention Européenne". If this guaranteed tensile level is 24 for A37 and 36 kg/mm$^2$ for A52, it is logical to adopt higher values for the buckling curves at slenderness ratio 0, since these are directly affected by the overall elastic limit in compression and not by that in tension;

c) an even degree of safety should be maintained for all components, whether in tension or in compression, constituting a structure.

This last point, however, requires a much longer explanation.


## HOMOGENEOUS SAFETY AND FAILURE CRITERION

The failure criterion adopted by Commission No. 1 of the "Convention Européenne" is the following: the stress or failure load of a member is the measured mean value for a series of specimens minus two SD. If the sta

tistical distribution is a normal one of the "Gauss-Laplace" type (as is the case for the CECM measurements), there is a 97.7% probability that the value question will be under the member's strength and a 2.3% one that it will be over.

The CECM experimental programme has been precisely elaborated so that members were tested under conditions very close to those found in actual structures, and in sufficient number to obtain mean ultimate loads and Standard Deviations possessing statistical validity for the whole European production.

The designer wishing to maintain an even degree of safety in the various elements of a structure must base his calculations on the failure loads of the various component parts, all such loads having the same probability of being exceeded (or of not being reached) irrespective of whether the loading is in tension, compression or bending.

According to the failure criterion of Commission No. 1 - buckling load equal to the mean minus two SD - the probability of not reaching this value is 2.3% and must be the same for all components so as to avoid wasting material in some part of the structure without rationally adding to its general safety.

Under these conditions, it is fairly easy to check that the elastic limit used for the buckling curves must be higher than that of the tensile specimens (and also higher than that adopted for designing parts in simple tension); in other words, if 24 kg/mm$^2$ is guaranteed as mean minus two SD, the elastic limit to be used for establishing the buckling curves must be higher than 24 kg/mm$^2$ in order to preserve the failure probability of 2.3% for compressed members.

## INVESTIGATION OF STATISTICAL VALUES FOR ULTIMATE BUCKLING LOADS

The ultimate buckling load P of a member is given to the structural designer by functions of the type:

$$P = P (R, T, F, A, \lambda) \tag{1}$$

where:

R = elastic limit in kg/mm$^2$

T = residual stress at a given point (at the edges of the flanges, for example) in kg/mm$^2$

F = initial deflection of the member per $^o/oo$ of its length

A = section area in mm$^2$

$\lambda$ = slenderness ratio

Functions (1) can be determined either experimentally or more rapidly by means of a computer by simulating load tests under various initial conditions [2].

R, T, F, A are not exactly known, though their probable distribution can be found, and a normal distribution of the Gauss-Laplace type can be assumed with average values $\bar{R}$, $\bar{T}$, $\bar{F}$, $\bar{A}$ and Standard Deviations r, t, f, a. The slenderness ratio $\lambda$, on the other hand, can be assumed, at least at its first approximation, exactly known, since any variation of A (due in gene-

ral, more to wall thickness differences than to wall dimensions) has negligible effect on the radius of gyration. The member's length is an obviously known factor.

The mean value $\overline{P}$ of the buckling load, its Standard Deviation and the value $\overline{\overline{P}}$ of this load, to which reference is made after the adopted failure criterion, will be:

$$\overline{P} = P\ (\overline{R},\ \overline{T},\ \overline{F},\ \overline{A},\ \lambda) \tag{2}$$

$$p^2 = (\frac{\partial P}{\partial R}\ r)^2 + (\frac{\partial P}{\partial T}\ t)^2 + (\frac{\partial P}{\partial F}\ f)^2 + (\frac{\partial P}{\partial A}\ a)^2 \tag{3}$$

$$\overline{\overline{P}} = \overline{P} - 2p = P\ (\overline{R},\ \overline{T},\ \overline{F},\ \overline{A},\ \lambda)\ -$$

$$-\ 2\sqrt{(\frac{\partial P}{\partial P}\ r)^2 + (\frac{\partial P}{\partial T}\ t)^2 + (\frac{\partial P}{\partial F}\ f)^2 + (\frac{\partial P}{\partial A}\ a)^2} \tag{4}$$

We would be tempted, knowing (1), to calculate (4) as follows:

$$\overline{\overline{P}}_1 = P\ (\overline{R} - 2r,\ \overline{T} + 2t,\ \overline{F} + 2f,\ \overline{A} - 2a,\ \lambda) \tag{5}$$

but we would find: $\overline{\overline{P}}_1 < \overline{\overline{P}}$.

This appears evident when we reflect that the 2.3% probability of having a column with a failure load below $\overline{\overline{P}}$ (4) is equal to that of having a column with an elastic limit below $(\overline{R} - 2r)$, with any T, F and A, or a column with $T > (\overline{T} + 2t)$ and any R, F, A, or else $F > (\overline{F} + 2f)$ and any R, T, A, or, finally, $A < (\overline{A} - 2a)$ and any R, T, F.

The "composite" probability of having simultaneously $R < \overline{R} - 2r$, $T > \overline{T} + 2t$, $F > \overline{F} + 2f$, $A < \overline{A} - 2a$ is the product of four 2.3% degrees of probability that each event should occur independently of the three others, this is equal to: $(2.3 \times 10^{-2})^4 = 28 \times 10^{-8}$ which is well below the 2.3% probability that $\overline{\overline{P}}$ (4) be smaller than the member's buckling load, assuming fairly reasonably that the variables R, T, F, A are statistically independent.

It follows that, in order to obtain $\overline{\overline{P}}$, it will be necessary to introduce at (1) the values $R_1$, $T_1$, $F_1$, $A_1$ so that:

$$\overline{\overline{P}} = P\ (R_1,\ T_1,\ F_1,\ A_1,\ \lambda) = \overline{P} - 2p \tag{6}$$

with

$$R_1 = \overline{R} - \alpha r,\ T_1 = \overline{T} + \alpha t,\ F_1 = \overline{F} + \alpha f,\ A_1 = \overline{A} - \alpha a \tag{7}$$

where $\alpha < 2$.

This coefficient $\alpha$ has been determined with sufficient accuracy in various conditions as follows. $\overline{\overline{P}}$ can be calculated by means of (4) or by developing in series (6), we can write (the terms in the bracket are all positive, taking into account the signs r, t, f, a and the partial derivates - see Table II):

$$\overline{\overline{P}} = P\ (R_1,\ T_1,\ F_1,\ A_1,\ \lambda) = P\ (\overline{R},\ \overline{T},\ \overline{F},\ \overline{A},\ \lambda)\ -$$

$$-\ \alpha(\frac{\partial P}{\partial R}\ r + \frac{\partial P}{\partial T}\ t + \frac{\partial P}{\partial F}\ f + \frac{\partial P}{\partial A}\ a) \tag{8}$$

and by comparing (4) and (8):

$$2p = \alpha \left( \frac{\partial P}{\partial R} r + \frac{\partial P}{\partial T} t + \frac{\partial P}{\partial F} f + \frac{\partial P}{\partial A} a \right) \tag{9}$$

By squaring and taking account of (3):

$$4p^2 = 4 \left\{ \left(\frac{\partial P}{\partial R} r\right)^2 + \left(\frac{\partial P}{\partial T} t\right)^2 + \left(\frac{\partial P}{\partial F} f\right)^2 + \left(\frac{\partial P}{\partial A} a\right)^2 \right\} =$$

$$= \alpha^2 \left( \frac{\partial P}{\partial R} r + \frac{\partial P}{\partial T} t + \frac{\partial P}{\partial F} f + \frac{\partial P}{\partial A} a \right)^2 =$$

$$= \alpha^2 \left\{ \left(\frac{\partial P}{\partial R} r\right)^2 + \left(\frac{\partial P}{\partial T} t\right)^2 + \left(\frac{\partial P}{\partial F} f\right)^2 + \left(\frac{\partial P}{\partial A} a\right)^2 \right\} +$$

$$+ \alpha^2 \left\{ 2 \frac{\partial P}{\partial R} \frac{\partial P}{\partial T} rt + 2 \frac{\partial P}{\partial R} \frac{\partial P}{\partial F} rf + 2 \frac{\partial P}{\partial R} \frac{\partial P}{\partial A} ra + \right.$$

$$\left. + 2 \frac{\partial P}{\partial T} \frac{\partial P}{\partial F} tf + 2 \frac{\partial P}{\partial T} \frac{\partial P}{\partial A} ta + 2 \frac{\partial P}{\partial F} \frac{\partial P}{\partial A} fa \right\} \tag{10}$$

All the terms of (10) being positive or equal to zero, we obtain additional confirmation of the fact that $\alpha < 2$. Indeed, in the last of the expressions for $4p^2$ set down in (10) above, we recognize the value of $p^2$ in the first quantity between the braces; let us designate the second quantity between the braces $\gamma^2$. We thus have:

$$4p^2 = \alpha^2(p^2 + \gamma^2) \quad \text{then} \quad \alpha = 2\left(\frac{1}{1 + \gamma^2/p^2}\right)^{1/2} \tag{11}$$

TABLE I – Mean values $\overline{R}$, $\overline{T}$, $\overline{F}$, $\overline{A}$ and their SD r, t, f, a
in % and in absolute values for calculating $\alpha$
($\overline{\overline{R}} = \overline{R} - 2r = 24$ kg/mm²)

| $\overline{R}$ kg/mm² | r % | r kg/mm² | $\overline{T}$ kg/mm² | t % | t kg/mm² | $\overline{F}$ | f % | f | $\overline{A}$ mm² | a % | a mm² |
|---|---|---|---|---|---|---|---|---|---|---|---|
| 26,70 | 5 | 1,35 | 3,33 | 10 | 0,33 | 10⁻³ | 10 | 10⁻⁴ | 2 010 | 2 | 40 |
| 26,70 | 5 | 1,35 | 3,33 | 15 | 0,50 | 10⁻³ | 15 | 1,5 × 10⁻¹ | 2 010 | 2 | 40 |
| 26,70 | 5 | 1,35 | 3,33 | 15 | 0,50 | 10⁻³ | 15 | 1,5 × 10⁻⁴ | 2 010 | 3 | 60 |
| 26,70 | 5 | 1,35 | 3,33 | 20 | 0,66 | 10⁻³ | 20 | 2 × 10⁻⁴ | 2 010 | 3 | 60 |
| 26,70 | 5 | 1,35 | 3,33 | 20 | 0,66 | 10⁻³ | 20 | 2 × 10⁻⁴ | 2 010 | 4 | 80 |
| 28,25 | 7,5 | 2,12 | 3,53 | 10 | 0,35 | 10⁻³ | 10 | 10⁻⁴ | 2 010 | 2 | 40 |
| 28,25 | 7,5 | 2,12 | 3,53 | 15 | 0,53 | 10⁻³ | 15 | 1,5 × 10⁻⁴ | 2 010 | 2 | 40 |
| 28,25 | 7,5 | 2,12 | 3,53 | 15 | 0,53 | 10⁻³ | 15 | 1,5 × 10⁻⁴ | 2 010 | 3 | 60 |
| 28,25 | 7,5 | 2,12 | 3,53 | 20 | 0,70 | 10⁻³ | 20 | 2 × 10⁻⁴ | 2 010 | 3 | 60 |
| 28,25 | 7,5 | 2,12 | 3,53 | 20 | 0,70 | 10⁻³ | 20 | 2 × 10⁻⁴ | 2 010 | 4 | 80 |
| 30,00 | 10 | 3,00 | 3,75 | 10 | 0,375 | 10⁻³ | 10 | 10⁻⁴ | 2 010 | 2 | 40 |
| 30,00 | 10 | 3,00 | 3,75 | 15 | 0,56 | 10⁻³ | 15 | 1,5 × 10⁻⁴ | 2 010 | 2 | 40 |
| 30,00 | 10 | 3,00 | 3,75 | 15 | 0,56 | 10⁻³ | 15 | 1,5 × 10⁻¹ | 2 010 | 3 | 60 |
| 30,00 | 10 | 3,00 | 3,75 | 20 | 0,75 | 10⁻⁴ | 20 | 2 × 10⁻⁴ | 2 010 | 3 | 60 |
| 30,00 | 10 | 3,00 | 3,75 | 20 | 0,75 | 10⁻³ | 20 | 2 × 10⁻⁴ | 2 010 | 4 | 80 |

EXPERIMENTAL DATA

We have adopted in the Table I values of r, t, f, a and $\overline{R}$, $\overline{T}$, $\overline{F}$, $\overline{A}$.
Those of $\overline{R}$ have been selected so that, for deviations of 5%, 7.5% and 10%

of $\bar{R}$, the elastic limit $\bar{\bar{R}} = \bar{R} - 2r$ amounts to 24 kg/mm$^2$. The actual value of $r$, derived from CECM stub column tests 1 was 7.5% of $\bar{R}$, thus giving an $\bar{\bar{R}}$ value always above 24 kg/mm$^2$. A Standard Deviation of about 10% would seem to result from a Belgian statistical investigation [4].

For $\bar{T}$ and $\bar{F}$ and their Standard Deviations t, f (10%, 15% and 20%), we have adopted values equal to or below those experimentally ascertained by the "Convention Européenne" or other research workers. A SD smaller than that actually found has been adopted, since the resulting value of $\alpha$ is then greater and this would further penalise the mean values $\bar{R}$ as can be seen in Table III. We have even found values of t above 30% of $\bar{T}$ (figure 3, reproduced after [3], figure 2a).

The nominal section IPE 160 has been used for $\bar{A}$. The deviation a% of 4% has been experimentally obtained but the deviations of 2% and 3% have also been adopted for this investigation.

The partial derivatives have been extracted, for different slenderness ratios, from figures in report [2] and more precisely:

$\dfrac{\partial P}{\partial R}$ from the curve with initial deflection F = 1/1,000 (fig. 2)

$\dfrac{\partial P}{\partial T}$ by comparing the curves for F = 1/1,000 of both figures with and without residual stresses T (fig. 1 and 2)

$\dfrac{\partial P}{\partial F}$ by comparing the curves for F = 1/1,000 and F = 1/500 (fig. 2)

$\dfrac{\partial P}{\partial A}$ limit buckling stresses obtained from the curve with F = 1/1,000 (fig. 2)

These derivates are recorded in Table II.

TABLE II - Partial derivates of buckling load P of the column in relation to: elastic limit R, residual stress T, initial deflection F, section area A

| $\lambda$ | $\dfrac{\partial P}{\partial R}$ mm$^2$ | $\dfrac{\partial P}{\partial T}$ mm$^2$ | $\dfrac{\partial P}{\partial F}$ kg | $\dfrac{\partial P}{\partial A}$ kg/mm$^2$ |
|---|---|---|---|---|
| | $\bar{R} = 26,70$ kg/mm$^2$ | | | |
| 0 | + 2 010 | 0 | 0 | + 26,70 |
| 55 | + 1 350 | — 580 | — 2 950 × 10$^3$ | + 23,20 |
| 75 | + 905 | — 580 | — 4 850 × 10$^3$ | + 19,75 |
| 95 | + 455 | — 330 | — 4 300 × 10$^3$ | + 15,90 |
| 105 | + 135 | — 83 | — 3 750 × 14$^3$ | + 14,15 |
| | $\bar{R} = 28,25$ kg/mm$^2$ | | | |
| 0 | + 2 010 | 0 | 0 | + 28,25 |
| 55 | + 1 350 | — 562 | — 3 400 × 10$^3$ | + 24,30 |
| 75 | + 905 | — 482 | — 5 100 × 10$^3$ | + 20,50 |
| 95 | + 455 | —241 | — 4 300 × 10$^3$ | + 16,25 |
| 105 | + 135 | — 83 | — 3 700 × 10$^3$ | + 14,30 |
| | $\bar{R} = 30$ kg/mm$^2$ | | | |
| 0 | + 2 100 | 0 | 0 | + 30,00 |
| 55 | + 1 430 | — 652 | — 3 900 × 10$^3$ | + 25,50 |
| 75 | + 975 | — 650 | — 5 450 × 10$^3$ | + 21,30 |
| 95 | + 460 | — 190 | — 4 550 × 10$^3$ | + 16,55 |
| 105 | + 150 | — 93 | — 3 650 × 10$^3$ | + 14,40 |

## CALCULATIONS AND RESULTS ANALYSIS

The values of $\alpha$ and $R_1 = \bar{R} - \alpha r$ have been calculated for various slenderness ratios, for different combinations of the Standard Deviations r, t, f, a and for three values of $\bar{R}$ (26.70 - 28.25 - 30 kg/mm$^2$). The results, given in Table III, indicate that:

a) $\alpha$ increases when the SD t% and f% are reduced and the value of $R_1 = \bar{R} -$
   $- \alpha r$ to be adopted for the buckling curves is thus also reduced; this is
   the reason for chosing t and f smaller than the actual values.

b) $\alpha$ increases with r% and $R_1 = \bar{R} - \alpha r$ decreases to equality with $\bar{R}$; for
   the cases referred to in Table III, however, $\bar{\bar{R}} = \bar{R} - 2r$ being fixed at
   24 kg/mm$^2$, r% increases with $\bar{R}$ and $R_1$ follows suit (see column 6 of Table III).
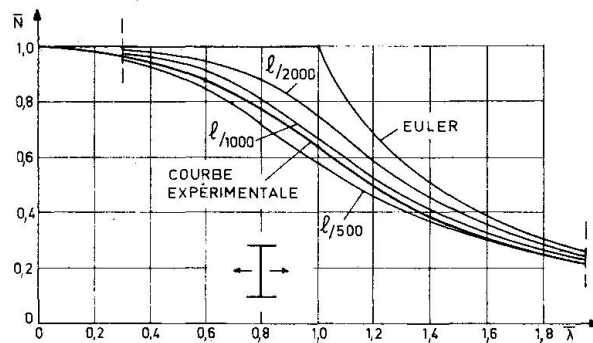


Fig. 1 - Theoretical curves, non-dimensional,
         for IPE 160, without residual stresses.
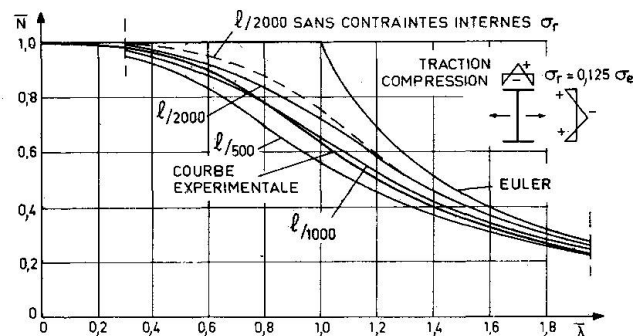         Buckling about the minor axis



Fig. 2 - Theoretical curves, non-dimensional,
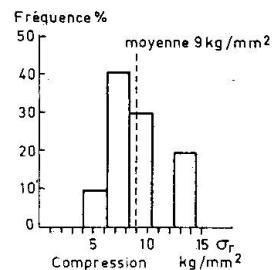         for IPE 160, with residual stresses.



Fig. 3 - Diagram of distribution of residual stresses $\sigma_r$ measured in flanges of sections.

TABLE III

| $\lambda$ (1) | r/t/f/a $\neq$ (2) | $\alpha$ (3) | $\bar{R}$ kg/mm² (4) | $\bar{\bar{R}} = \bar{R} - 2r$ kg/mm² (5) | $R_1 = \bar{R} - \alpha r$ kg/mm² (6) |
|---|---|---|---|---|---|
| 0 | 5/10/10/2 | 1,54 | 26,70 | 24 | 24,62 |
| 0 | 5/15/15/2 | 1,54 | 26,70 | 24 | 24,62 |
| 0 | 5/15/15/3 | 1,46 | 26,70 | 24 | 24,73 |
| 0 | 5/20/20/3 | 1,46 | 26,70 | 24 | 24,73 |
| 0 | 5/20/20/4 | 1,42 | 26,70 | 24 | 24,78 |
| 0 | 7,5/10/10/2 | 1,64 | 28,25 | 24 | 24,78 |
| 0 | 7,5/15/15/2 | 1,64 | 28,25 | 24 | 24,78 |
| 0 | 7,5/15/15/3 | 1,54 | 28,25 | 24 | 25,-- |
| 0 | 7,5/20/20/3 | 1,54 | 28,25 | 24 | 25,-- |
| 0 | 7,5/20/20/4 | 1,48 | 28,25 | 24 | 25,11 |
| 0 | 10/10/10/2 | 1,70 | 30,-- | 24 | 24,9 |
| 0 | 10/15/15/2 | 1,70 | 30,-- | 24 | 24,9 |
| 0 | 10/15/15/3 | 1,61 | 30,-- | 24 | 25,18 |
| 0 | 10/20/20/3 | 1,61 | 30,-- | 24 | 25,18 |
| 0 | 10/20/20/4 | 1,54 | 30,-- | 24 | 25,38 |
| 55 | 5/10/10/2 | 1,28 | 26,70 | 24 | 24,97 |
| 55 | 5/15/15/2 | 1,21 | 26,70 | 24 | 25,06 |
| 55 | 5/15/15/3 | 1,19 | 26,70 | 24 | 25,09 |
| 55 | 5/20/20/3 | 1,15 | 26,70 | 24 | 25,15 |
| 55 | 5/20/20/4 | 1,16 | 26,70 | 24 | 25,14 |
| 55 | 7,5/10/10/2 | 1,39 | 28,25 | 24 | 25,29 |
| 55 | 7,5/15/15/2 | 1,33 | 28,25 | 24 | 25,44 |
| 55 | 7,5/15/15/3 | 1,27 | 28,25 | 24 | 25,55 |
| 55 | 7,5/20/20/3 | 1,23 | 28,25 | 24 | 25,65 |
| 55 | 7,5/20/20/4 | 1,21 | 28,25 | 24 | 25,69 |
| 55 | 10/10/10/2 | 1,49 | 30,-- | 24 | 25,53 |
| 55 | 10/15/15/2 | 1,43 | 30,-- | 24 | 25,72 |
| 55 | 10/15/15/3 | 1,36 | 30,-- | 24 | 25,92 |
| 55 | 10/20/20/3 | 1,31 | 30,-- | 24 | 26,07 |
| 55 | 10/20/20/4 | 1,27 | 30,-- | 24 | 26,20 |
| 75 | 5/10/10/2 | 1,15 | 26,70 | 24 | 25,15 |
| 75 | 5/15/15/2 | 1,09 | 26,70 | 24 | 25,23 |
| 75 | 5/15/15/3 | 1,09 | 26,70 | 24 | 25,22 |
| 75 | 5/20/20/3 | 1,06 | 26,70 | 24 | 25,27 |
| 75 | 5/20/20/4 | 1,08 | 26,70 | 24 | 25,24 |
| 75 | 7,5/10/10/2 | 1,26 | 28,25 | 24 | 25,58 |
| 75 | 7,5/15/15/2 | 1,19 | 28,25 | 24 | 25,73 |
| 75 | 7,5/15/15/3 | 1,16 | 28,25 | 24 | 25,79 |
| 75 | 7,5/20/20/3 | 1,12 | 28,25 | 24 | 25,88 |
| 75 | 7,5/20/20/4 | 1,12 | 28,25 | 24 | 25,88 |
| 75 | 10/10/10/2 | 1,36 | 30,-- | 24 | 25,92 |
| 75 | 10/15/15/2 | 1,28 | 30,-- | 24 | 26,16 |
| 75 | 10/15/15/3 | 1,23 | 30,-- | 24 | 26,31 |
| 75 | 10/20/20/3 | 1,18 | 30,-- | 24 | 26,46 |
| 75 | 10/20/20/4 | 1,16 | 30,-- | 24 | 26,53 |
| 95 | 5/10/10/2 | 1,11 | 26,70 | 24 | 25,21 |
| 95 | 5/15/15/2 | 1,07 | 26,70 | 24 | 25,25 |
| 95 | 5/15/15/3 | 1,11 | 26,70 | 24 | 25,21 |
| 95 | 5/20/20/3 | 1,09 | 26,70 | 24 | 25,23 |
| 95 | 5/20/20/4 | 1,13 | 26,70 | 24 | 25,18 |
| 95 | 7,5/10/10/2 | 1,17 | 28,25 | 24 | 25,77 |
| 95 | 7,5/15/15/2 | 1,12 | 28,25 | 24 | 25,88 |
| 95 | 7,5/15/15/3 | 1,12 | 28,25 | 24 | 25,87 |
| 95 | 7,5/20/20/3 | 1,10 | 28,25 | 24 | 25,93 |
| 95 | 7,5/20/20/4 | 1,12 | 28,25 | 24 | 25,88 |
| 95 | 10/10/10/2 | 1,24 | 30,-- | 24 | 26,27 |
| 95 | 10/15/15/2 | 1,29 | 30,-- | 24 | 26,44 |
| 95 | 10/15/15/3 | 1,16 | 30,-- | 24 | 26,52 |
| 95 | 10/20/20/3 | 1,13 | 30,-- | 24 | 26,61 |
| 95 | 10/20/20/4 | 1,13 | 30,-- | 24 | 26,61 |
| 105 | 5/10/10/2 | 1,22 | 26,70 | 24 | 25,05 |
| 105 | 5/15/15/2 | 1,21 | 26,70 | 24 | 25,06 |
| 105 | 5/15/15/3 | 1,27 | 26,70 | 24 | 25,-- |
| 105 | 5/20/20/3 | 1,25 | 26,70 | 24 | 25,-- |
| 105 | 5/20/20/4 | 1,29 | 26,70 | 24 | 24,95 |
| 105 | 7,5/10/10/2 | 1,18 | 28,25 | 24 | 25,76 |
| 105 | 7,5/15/15/2 | 1,16 | 28,25 | 24 | 25,78 |
| 105 | 7,5/15/15/3 | 1,22 | 28,35 | 24 | 25,67 |
| 105 | 7,5/20/20/3 | 1,20 | 28,25 | 24 | 25,70 |
| 105 | 7,5/20/20/4 | 1,25 | 28,25 | 24 | 25,60 |
| 105 | 10/10/10/2 | 1,15 | 30,-- | 24 | 26,56 |
| 105 | 10/15/15/2 | 1,13 | 30,-- | 24 | 26,62 |
| 105 | 10/15/15/3 | 1,17 | 30,-- | 24 | 26,49 |
| 105 | 10/20/20/3 | 1,15 | 30,-- | 24 | 26,54 |
| 105 | 10/20/20/4 | 1,20 | 30,-- | 24 | 26,41 |

c) when a% increases, $\alpha$ can either increase or decrease.

d) the $R_1$ values, in the last column of Table III, are the elastic limits to be used for the buckling curves which give loads with a 2.3% probability of not being reached. $R_1$ varies with the slenderness ratio, but this variation is fairly small, especially in the slenderness ratio range between 50 and 90 which concerns the constructor.

For steel with r% = 7.5%, i.e. with the most probable value of the SD (according to 4 , fig. 8, 9, 10, etc.) $R_1$ is almost consistently higher than 25.5 kg/mm² for $\lambda > 55$. For r% = 5% we have $R_1 > 25$ kg/mm² and for steel with r% = 10% we then have $25.5 < R_1 < 26.5$ kg/mm² for $\lambda > 55$.

There results an $R_1$ value systematically and clearly above $\bar{\bar{R}} = \bar{R} - 2r = 24$ kg/mm .

If $\bar{R}$ is above 24 kg/mm², as the tests of the "Convention Européenne" have confirmed, $R_1$ will be even higher and be above the values given in Table III for the equality between r%, t%, f% and a%.

The values of $R_1$ adopted by the "Convention Européenne" for establishing the buckling curves are sufficiently near the values of Table III, in particular those found for steel with $\bar{R} = 28.25$ kg/mm² and r% = 7.5%.

It is worth recalling that the overall compression values of $\bar{R}$ found experimentally have been consistently higher than those measured in tension for open sections.

## CONCLUSIONS

For the reasons given above, and in particular for preserving an even degree of safety over the various parts of a structure, whatever the type of loading, the "Convention Européenne" has deemed it appropriate to adopt, for relatively thin sections (thickness < 20 mm), elastic limits higher than the minimum values guaranteed by conventional tensile tests.

This decision, which may appear audacious and strange at first sight, does not introduce an entirely new principle in structural design. Indeed, this same principle has been applied for a long time, if not from the inception, when we are dealing with applied loads, and there seems to be no valid reason for not accepting it for strength of materials.

When loads act separately, we take from each the maximum value that can be anticipated. When several statistically independent loads work in unison, we apply reduction coefficients to the maximum loads adopted when each was acting on its own. In the same way, it is fairly logical in a complex phenomenon depending on several independent variables (R, T, F and A) such as buckling to admit that these variables do not all possess simultaneously the most unfavourable values amounting to the minimum or maximum values imposed by inspection regulations, or adopted for investigating less complex phenomena. For phenomenon less complex than buckling, it does, however, appear that a single variable can play a determining role which must be counteracted by taking a mean value less 2 Standard Deviations and not merely less $\alpha < 2$.

## BIBLIOGRAPHY

[1] Annales de l'Institut Technique du Bâtiment et des Travaux Publics, No. 210, June 1965, p. 764.

[2] CECM: "Bericht über die elektronische Berechnung der Traglast von planmässig geraden Druckstäben mit Imperfektionen", Graz, March 2, 1967 (fig. 1 and 2). Interim report presented to CECM Committee 8.

[3] Lynn S. Beedle and Lambert Tall: "Basic Column Strength", ASCE Journal of the Structural Division, Proceeding Paper 2555.

[4] "Résultats actuels de l'étude statistique des caractéristiques mécaniques des aciers A 37 et A 42", l'Ossature Métallique, No. 2 and 3, 1954.